

# **Development and Characterization of Doxycycline hydiate loaded halloysite nanotube in-situ gel for the treatment of periodontitis**

Thesis submitted in partial fulfillment for the requirement of the

**Degree of Master of Pharmacy**

By

**Kaushiki Priya**

M.Pharm, 2<sup>nd</sup>Year, 2<sup>nd</sup>Sem.

Class Roll No: **002211402031**

Examination Roll No:**MP4PHL24005**

Registration No: **163673 of 2022-2023**

Under the Guidance and co-guidance of

**Prof. (Dr.) Amalesh Samanta**

**Dr. Kajal Ghosal**

Division of Microbiology & Pharmaceutical Biotechnology

Division of Industrial Pharmacy

**DEPARTMENT OF PHARMACEUTICAL TECHNOLOGY**

Faculty Council of Engineering & Technology

**Jadavpur University**

Kolkata- 700032

**NAME: Kaushiki Priya**

**M.Pharm; 2<sup>nd</sup>Year, 2<sup>nd</sup>Sem.**

**DEPARTMENT OF PHARMACEUTICAL TECHNOLOGY**

**JADAVPUR UNIVERSITY**

**Classroll no.:002211402031**

**Examination Roll No:MP4PHL24005**

**Registration No:163673 of 2022-2023**

**Batch: 2022-2024**

.....  
**Signature of external examiner with date**

### CERTIFICATE OF APPROVAL

This is to certify that the thesis entitled "Development and Characterization of Doxycycline hydride loaded halloysite nanotube in-situ gel for the treatment of periodontitis" submitted to Jadavpur University, Kolkata for the partial fulfillment of the Master Degree in Pharmacy, is a faithful record of bona fide and original research work carried out by Ms. Kaushiki Priya bearing Class Roll no. 002211402031 and Registration no. 163673 of 2022-2023 under my supervision and guidance.

29.8.24.

Prof. (Dr.) Amalesh Samanta  
Prof. Amalesh Samanta, Ph.D.  
Head  
Dept. of Pharmaceutical Technology  
Head of the Department  
Jadavpur University, Kolkata, India

Department of Pharmaceutical Technology  
Jadavpur University  
Kolkata - 700032

29.8.24.

Prof. (Dr.) Amalesh Samanta  
Prof. Amalesh Samanta  
Dept. of Microbiology & Biotechnology  
Jadavpur University  
(Supervisor) 0032, India

Division of Microbiology and  
Pharmaceutical Biotechnology

Department of Pharmaceutical  
Technology  
Jadavpur University  
Kolkata - 700032

Dipan Laha 29.8.24

Prof. Dipak Laha  
(Dean)  
Faculty Council of Engineering and Technology

Kajal Ghosal 29.8.24

Assistant Professor  
Dr. Kajal Ghosal of Ph. Tech  
Jadavpur University  
(Co-supervisor) 0032

Division of Industrial  
Pharmacy

Jadavpur University  
Kolkata

DEAN  
Faculty of Engineering & Technology  
JADAVPUR UNIVERSITY  
KOLKATA-700 032

Department of  
Pharmaceutical Technology

Jadavpur University  
Kolkata

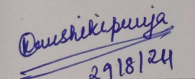
**Declaration of the Originality and Compliance of Academic Ethics**

I, Kaushiki Priya, a student of M.Pharm, 2<sup>nd</sup> year, bearing Class Roll No: 002211402031, Registration No. 163673 of 2022-2023 studying in Department of Pharmaceutical Technology, Jadavpur University, Kolkata-32, hereby declare that my thesis work titled – “Development and Characterization of Doxycycline hydiate loaded halloysite nanotube in-situ gel for the treatment of periodontitis”, is original and presented in accordance with academic rules and ethical conduct and no part of this project work has been submitted for any other degree of mine. All the information and works are true to the best of my sense and knowledge.

**Name:** Kaushiki Priya

**Class Roll No.: 002211402031**

**Registration No.: 163673, 2022-2023**

  
29/8/24

**Signature with date**

**Place:** Jadavpur, Kolkata.

**DEDICATED TO MY  
GUIDE, CO-GUIDE AND  
PARENTS**

### **ACKNOWLEDGEMENT**

I deem it to be a privilege to work under the guidance of Prof. (Dr.) Amalesh Samanta, Division of Microbiology & Pharmaceutical Biotechnology, Jadavpur University on the very current and innovative topic “Development and Characterization of Doxycycline hydride loaded halloysite nanotube in-situ gel for the treatment of periodontitis” I am blessed to work under his constructive and suggestive guidance throughout my work. His expert supervision with undue patience throughout my work at every stage helped me complete this work effortlessly.

I also express my sincere gratitude to our H.O.D., Department of Pharmaceutical Technology, Jadavpur University, Prof. (Dr.) Amalesh Samanta for providing me an opportunity to do my thesis work successfully.

I am grateful to All India Council for Technical Education (AICTE), Government of India for providing financial support.

I express my heartfelt gratitude to Ph.D. scholars – Sohini Chatterjee, Mousumi Tudu, Abhishek Mohanta, Ahana Hazra, Suparna Garai, Shreya Chatterjee; PG senior Pankaj Paul & Amrita Das; my classmate; Md. Ahsan Ansari, Riya Hazra, Ankit Tiwari, Khubaib Akhtar Khan, Souvik Singha and Samrat Chowdhury. PG juniors: Md. Nahid Zaman, Pijush Kanti Shit, Sahanaz Khatun, Somnath Singha & Puspender Singha.

I also want to extend my gratitude to my friends who mentally supported in my thesis work, Shivam Kumar, Jeslin Jacob, Jigyasa Shankar, Harsha Balledina Bideshi, Khubaib Akhtar Khan, Anirbita Ghosh & Sonali Mandal.

I will remain forever grateful to The Almighty and my parents and siblings Rama Priya and Shashank Mishra, whose dedication and untiring efforts towards me has brought me at this stage of life.

*Kaushiki Priya*  
29/8/24

**(Kaushiki Priya)**

# Contents

<b>Chapter 1: Introduction.....</b>	<b>11</b>
<b>Chapter 2:Literature Review .....</b>	<b>30</b>
<b>Chapter 3: Aims and Objectives .....</b>	<b>38</b>
<b>Chapter 4:Materials and Reagents .....</b>	<b>40</b>
<b>Chapter 5: Materials and methods .....</b>	<b>49</b>
<b>Chapter 6: Results and Discussion.....</b>	<b>62</b>
<b>Chapter 7: Conclusion .....</b>	<b>102</b>
<b>Chapter 8:References.....</b>	<b>105</b>
<b>Chapter 9: Certificate and Conferences.....</b>	<b>110</b>

# List of Figures

<b>Figure 1 Types of NDDS.....</b>	<b>12</b>
<b>Figure 2:Types of in-situ gel.....</b>	<b>17</b>
<b>Figure 3 Tooth decay and gum swelling .....</b>	<b>23</b>
<b>Figure 4 Prepatation of DOH loaded HNT in-situ gel .....</b>	<b>53</b>
<b>Figure 5 Calibration graph of DOH .....</b>	<b>64</b>
<b>Figure 6 Zone of Inhibition of F1, F2, and F3 .....</b>	<b>70</b>
<b>Figure 7 Graph of zone of inhibition of F1, F2, and F3 .....</b>	<b>71</b>
<b>Figure 8 Graph of Spreadability of F1, F2, and F3.....</b>	<b>73</b>
<b>Figure 9 Graph of Swelling degree of F1, F2, and F3 .....</b>	<b>75</b>
<b>Figure 10 Syringibility of in-situ gel .....</b>	<b>76</b>
<b>Figure 11 Optical microscopy images of the a. HNT b. F2 and c. F2G .....</b>	<b>77</b>
<b>Figure 12 Stability testing of a. sample kept in refrigerated condition &amp; b. sample kept at room temperature .....</b>	<b>78</b>
<b>Figure 13 FTIR graph of Blank, F2, HNT and F2G .....</b>	<b>81</b>
<b>Figure 14 XRD graph of DOH, Blank, F2G.....</b>	<b>84</b>
<b>Figure 15 Resazurin assay .....</b>	<b>85</b>
<b>Figure 16 TGA and DTA graph of drug, Blank and F2G .....</b>	<b>88</b>
<b>Figure 17 Graph of Antioxidant assay.....</b>	<b>91</b>
<b>Figure 18 SEM images of A. HNT, B. F2, C. Blank, and D. F2G .....</b>	<b>92</b>
<b>Figure 19 TEM images of A. HNT, B. F2, C. F2G.....</b>	<b>93</b>
<b>Figure 20 In-vitro drug release Graph .....</b>	<b>96</b>
<b>Figure 21 Zero order drug release graph .....</b>	<b>98</b>
<b>Figure 22 First order drug release graph .....</b>	<b>99</b>
<b>Figure 23Hixon Crowell drug release graph .....</b>	<b>99</b>
<b>Figure 24 Higuchi model drug release graph .....</b>	<b>100</b>
<b>Figure 25 Korsmeyer Peppas drug release graph.....</b>	<b>101</b>

# List of Tables

<b>Table 1 Preparation of Drug solution and PBS for standard curve of DOH .....</b>	<b>51</b>
<b>Table 2 Formulation Chart of DOH loaded HNT .....</b>	<b>51</b>
<b>Table 3 Formulation table for bacterial assay.....</b>	<b>55</b>
<b>Table 4 Initial and final melting point .....</b>	<b>63</b>
<b>Table 5 Calibration curve of DOH .....</b>	<b>63</b>
<b>Table 6 Zone of inhibition of F1 for E. coli K-88.....</b>	<b>65</b>
<b>Table 7 Zone of inhibition of F1 for L. acidophilus NCIM 2056 .....</b>	<b>66</b>
<b>Table 8 Zone of inhibition of F1 for L.casei 2586.....</b>	<b>66</b>
<b>Table 9 Zone of inhibition of F2 E. coli K-88 .....</b>	<b>67</b>
<b>Table 10 Zone of inhibition of F2 L. acidophilus NCIM 2056 .....</b>	<b>67</b>
<b>Table 11 Zone of inhibition of F2 L.casei NCIM 2586 .....</b>	<b>68</b>
<b>Table 12 Zone of inhibition of F3 for E. coli.....</b>	<b>68</b>
<b>Table 13 Zone of inhibition of F2 L. acidophilus NCIM 2056 .....</b>	<b>69</b>
<b>Table 14 Spreadability (cm) of F1, F2 and F3 samples .....</b>	<b>72</b>
<b>Table 15 Swelling Weight of F1G, F2G and F3G sample for 1-5 days .....</b>	<b>74</b>
<b>Table 16 Swelling degree of F1G, F2G and F3G samples.....</b>	<b>74</b>
<b>Table 17 Antioxidant % of F2 sample .....</b>	<b>89</b>
<b>Table 18 Antioxidant % of F1G sample.....</b>	<b>90</b>
<b>Table 19 Antioxidant % of F2G sample.....</b>	<b>90</b>
<b>Table 20 Antioxidant % of F3G sample.....</b>	<b>90</b>
<b>Table 21 %CDR calculation for F1 formulation (n=3) .....</b>	<b>94</b>
<b>Table 22 %CDR calculation for F2 formulation (n=3) .....</b>	<b>95</b>
<b>Table 23 %CDR calculation for F3 formulation (n=3) .....</b>	<b>95</b>
<b>Table 24 Calculation of Zero order kinetics .....</b>	<b>98</b>
<b>Table 25 Calculation of First order kinetics .....</b>	<b>98</b>
<b>Table 26 Calculation of Hixon Crowell model kinetics.....</b>	<b>99</b>
<b>Table 27 Calculation of Higuchi model kinetics.....</b>	<b>100</b>
<b>Table 28 Calculation of Korsmeyer Peppas kinetics.....</b>	<b>101</b>

# List of Abbreviation

<b>Symbols</b>	<b>Abbreviations</b>
<b>UV</b>	Ultra Violet
<b>DPPH</b>	2,2-diphenyl-1-picrylhydrazyl
<b>PBS</b>	Phosphate Buffer Solution
<b>FTIR</b>	Fourier Transformed Infrared
<b>UV-Vis</b>	Ultra violet visible spectrometer
<b>XRD</b>	X-Ray Diffraction
<b>SEM</b>	Scanning Electron Microscope
<b>TEM</b>	Transmission electron microscopy
<b>TGA</b>	Thermogravimetric analysis
<b>DTA</b>	Differential thermal analysis
<b>%</b>	Percentage
<b>gm</b>	Gram
<b>mg</b>	Miligram
<b>µg</b>	Microgram
<b>hrs</b>	Hours
<b>t</b>	Time
<b>λ<sub>max</sub></b>	Absorption maxima
<b>ml</b>	Mililiter
<b>DOH</b>	Doxycycline Hyclate
<b>GP</b>	Glycerol Phospahte
<b>HNT</b>	Halloysite nanotubes
<b>MBC</b>	Minimum bacterial concentration
<b>CDR</b>	Cumulative drug release

# Chapter 1: Introduction

## **1. Novel Drug Delivery Systems (NDDS)**

**Novel Drug Delivery Systems (NDDS)** represent a significant evolution in the field of pharmacology, designed to address the limitations of conventional drug delivery methods and enhance therapeutic efficacy. The primary objective of NDDS is to deliver drugs in a controlled, sustained, and targeted manner, thereby improving patient outcomes while minimizing side effects (Jain, 2020). Traditional drug delivery systems often suffer from issues such as poor bioavailability, rapid degradation of the drug, and non-specific distribution, which can lead to suboptimal therapeutic effects and increased adverse reactions (Kumar et al., 2019). NDDS overcome these challenges by incorporating advanced technologies and materials, enabling precise control over the release profile, targeting specific tissues or cells, and protecting the drug from premature degradation.

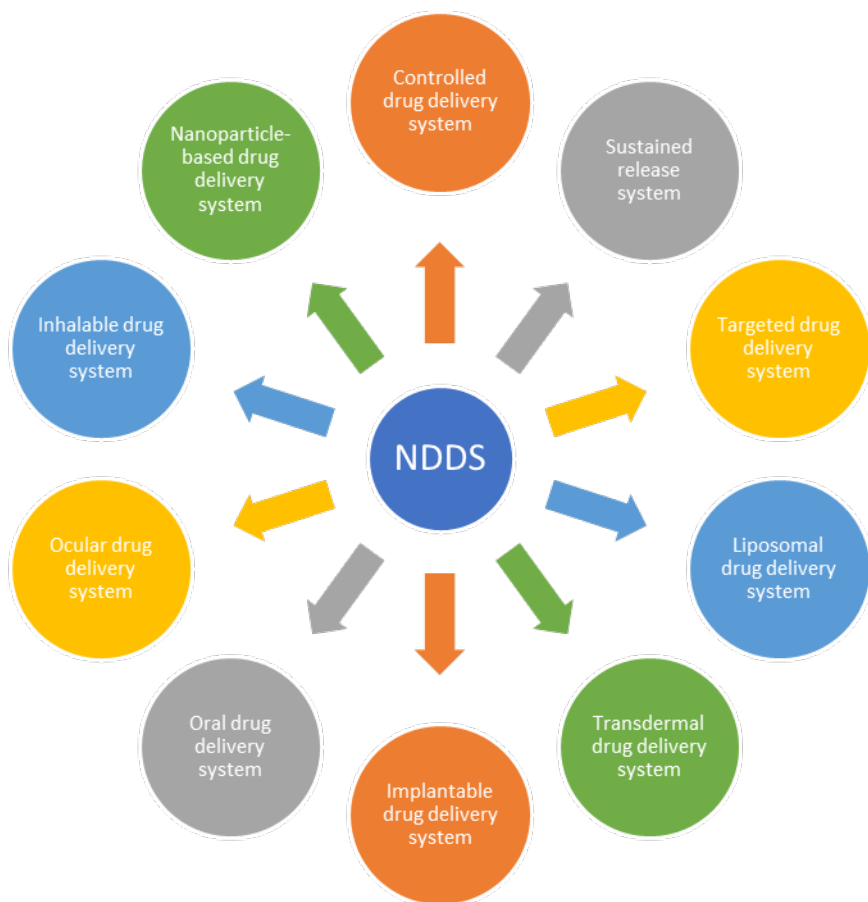


*Figure 1 Types of NDDS*

One of the key advancements in NDDS is the development of **Controlled Drug Delivery Systems (CDDS)**, which release the drug at a predetermined rate for a specified duration. CDDS can be further classified into reservoir systems, where the drug is enclosed within a polymeric membrane, and matrix systems, where the drug is uniformly dispersed within a polymer matrix (Siepmann & Peppas, 2012). These systems are particularly beneficial for chronic conditions such as diabetes, where maintaining a steady drug concentration is crucial for effective management (Huang, 2021).

Another significant type of NDDS is the **Sustained Release Systems (SRS)**, designed to gradually release the drug over an extended period. This approach is often achieved through the use of biodegradable polymers, which slowly degrade in the body, releasing the drug in a controlled manner (Fahr & Liu, 2020). SRS are commonly used in applications such as transdermal patches, which provide continuous drug delivery for pain management or hormone replacement therapy.

**Targeted Drug Delivery Systems (TDDS)** represent a major breakthrough in NDDS, focusing on delivering the drug specifically to the site of action while minimizing systemic exposure. This approach not only enhances the therapeutic effect but also reduces the risk of side effects. TDDS can be achieved through various mechanisms, including ligand-based targeting, where ligands bind to specific receptors on target cells, and nanoparticle-based systems, where drug-loaded nanoparticles are engineered to accumulate at the target site (Allen & Cullis, 2013; Wang et al., 2015). Nanoparticles, in particular, have garnered significant attention due to their ability to enhance the permeability and retention effect, making them highly effective in cancer therapy (Peer et al., 2007). However, challenges such as target specificity and potential clearance by the immune system remain significant hurdles in the widespread adoption of TDDS (Allen & Cullis, 2013).

**Liposomal Drug Delivery Systems** are another innovative type of NDDS that utilize liposomes—spherical vesicles composed of phospholipid bilayers—to encapsulate drugs. This system offers several advantages, including improved bioavailability, reduced toxicity, and the

ability to deliver both hydrophilic and hydrophobic drugs (Torchilin, 2005). Liposomal formulations have been successfully used in the treatment of various conditions, including cancer (e.g., Doxil) and fungal infections (e.g., AmBisome) (Torchilin, 2005). Despite their potential, the high cost of production and stability issues remain challenges for the widespread use of liposomal systems.

**Transdermal Drug Delivery Systems (TDDS)** offer a non-invasive alternative for drug administration, where drugs are delivered through the skin into systemic circulation. These systems are typically in the form of skin patches that release the drug over time, providing a controlled and sustained release profile (Prausnitz & Langer, 2008). Transdermal patches have been successfully used for various applications, including nicotine replacement therapy, pain management, and hormone replacement therapy. The primary advantage of TDDS is their ability to bypass the gastrointestinal tract, thus avoiding first-pass metabolism and improving bioavailability (Prausnitz & Langer, 2008).

**Implantable Drug Delivery Systems** offer another innovative approach, where devices are implanted within the body to release drugs over an extended period. These systems can be either biodegradable, where the device gradually degrades and releases the drug, or non-biodegradable, requiring surgical removal once the drug reservoir is depleted (Santini et al., 2000). Implantable systems are particularly useful for chronic conditions that require long-term drug administration, such as hormone therapy, pain management, and cancer treatment. However, the invasive nature of these systems and the potential for complications, such as infection or device failure, are significant considerations in their use (Santini et al., 2000).

**Nanoparticle-Based Drug Delivery Systems** represent a cutting-edge approach in NDDS, where nanoparticles—ranging from 1 to 100 nanometers in size—are used as carriers for drug delivery. These systems offer several advantages, including increased surface area, enhanced permeability, and the ability to bypass biological barriers (Peer et al., 2007). Nanoparticles can be engineered from various materials, including lipids, polymers, and metals, and can be

designed to release drugs in a controlled manner or target specific cells or tissues. The versatility of nanoparticle-based systems has made them a promising platform for the treatment of various diseases, including cancer, cardiovascular diseases, and neurological disorders (Peer et al., 2007). However, the potential for toxicity, immune response, and challenges in large-scale production are areas that require further research.

**Oral Controlled Release Systems** are designed to deliver drugs via the oral route with a controlled release profile. These systems include gastroretentive systems, which remain in the stomach for an extended period, and enteric-coated systems, which release the drug in the intestines to avoid degradation by stomach acid (Aulton & Taylor, 2018). Oral controlled release systems are particularly beneficial for managing chronic diseases, such as hypertension and diabetes, where maintaining a consistent drug concentration is crucial for therapeutic efficacy (Aulton & Taylor, 2018). However, factors such as variability in gastrointestinal transit time and the impact of food on drug absorption can affect the performance of these systems (Aulton & Taylor, 2018).

**Ocular Drug Delivery Systems** are specifically designed to overcome the anatomical barriers of the eye and deliver drugs effectively to ocular tissues. These systems include intraocular implants, which provide sustained release of drugs directly inside the eye, and advanced formulations of eye drops that enhance drug absorption through the cornea (Sultana et al., 2006). Ocular drug delivery systems are particularly important for treating conditions such as glaucoma, macular degeneration, and post-surgical inflammation. The primary challenge in ocular drug delivery is achieving prolonged drug retention and penetration without causing irritation or damage to the delicate tissues of the eye (Sultana et al., 2006).

Finally, **Inhalable Drug Delivery Systems** represent an important category of NDDS, particularly for the treatment of respiratory diseases. These systems are designed to deliver drugs directly to the lungs, either for local effect, as in the case of asthma or chronic obstructive pulmonary disease (COPD), or for systemic delivery, such as in the case of inhalable insulin for

diabetes (Patton & Byron, 2007). Inhalable systems offer rapid onset of action and can be highly effective for targeting diseases of the respiratory tract. However, challenges such as drug deposition in the lungs, variability in patient inhalation technique, and the need for precise dosing are critical factors that need to be addressed (Patton & Byron, 2007).

Hence, NDDS offer a promising avenue for improving drug delivery, enhancing therapeutic efficacy, and reducing side effects. As research in this field continues to advance, it is likely that new and more sophisticated systems will emerge, addressing current challenges and expanding the range of treatable conditions.

## **2. In-Situ Gel Systems in Drug Delivery**

In recent years, in-situ gels have emerged as a promising approach in the field of drug delivery systems, gaining attention for their unique ability to transform from a liquid to a gel upon exposure to physiological conditions. This transformation is typically triggered by changes in temperature, pH, or ionic concentration. In-situ gel systems offer numerous advantages, including prolonged drug release, enhanced patient compliance, and reduced systemic side effects. This review explores the various types of in-situ gel systems, their mechanisms of gelation, applications in drug delivery, and challenges associated with their development.

### **2.1. Mechanisms of Gelation in In-Situ Gel Systems**

The gelation process in in-situ gels is a critical factor that determines their effectiveness in drug delivery. Gelation can be induced through several mechanisms, including temperature-sensitive, pH-sensitive, and ion-sensitive methods.

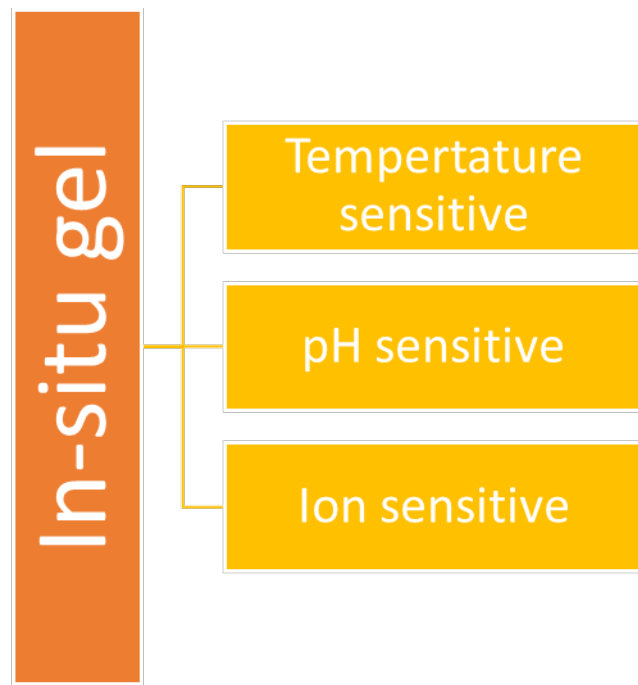


Figure 2: Types of in-situ gel

## 1. Temperature-Sensitive In-Situ Gels

Temperature-sensitive in-situ gels are designed to undergo a sol-to-gel transition upon exposure to body temperature. Polymers such as Pluronic F127 (poloxamer) and chitosan are commonly used in these systems due to their thermosensitive properties. For instance, Pluronic F127 exhibits a sol-gel transition at temperatures close to body temperature (around 37°C), making it suitable for injectable formulations (Yuan et al., 2015). The sol state allows easy administration, while the gel state ensures sustained drug release at the target site. These systems are particularly advantageous for delivering drugs to localized sites, such as in cancer therapy, where prolonged exposure to the drug is required (Vermonden et al., 2012).

## 2. pH-Sensitive In-Situ Gels

pH-sensitive in-situ gels exploit the variations in pH within the human body to trigger gelation. Polymers like poly(acrylic acid) and chitosan exhibit pH-dependent solubility and swelling behavior. For example, chitosan, which is soluble in acidic conditions, forms a gel in neutral to slightly alkaline environments (pH 6.5-7.4), making it ideal for applications in mucosal drug delivery, such as nasal or ocular delivery (Ahmed, 2015). The pH-sensitive nature of these gels ensures that the drug is released at the desired site, such as the stomach or intestines, depending on the pH of the surrounding environment (Bajpai et al., 2016).

## 3. Ion-Sensitive In-Situ Gels

Ion-sensitive in-situ gels are triggered by the presence of specific ions in the body, such as calcium or sodium ions. Alginate is a widely used polymer in these systems due to its ability to form gels in the presence of divalent cations like calcium (Lee & Mooney, 2012). When alginate is administered in its liquid form, it encounters calcium ions in the physiological environment, leading to cross-linking and gel formation. This approach is particularly useful for oral and injectable drug delivery systems, where the gel can provide a protective matrix for the encapsulated drug, allowing for controlled release over time (Sharma et al., 2018).

### **2.2. Applications of In-Situ Gel Systems**

In-situ gel systems have been explored for various drug delivery applications, ranging from ophthalmic to oral and injectable delivery systems. Their versatility and ability to provide sustained drug release have made them a popular choice in these areas.

## **1. Ophthalmic Drug Delivery**

Ophthalmic drug delivery presents unique challenges due to the rapid elimination of drugs from the ocular surface by tears and blinking. In-situ gel systems offer a solution by providing prolonged contact time with the cornea, leading to enhanced drug absorption and efficacy (Kompella & Lee, 2006). Temperature-sensitive in-situ gels, such as those based on Pluronic F127, are commonly used in ophthalmic formulations. These gels remain in a liquid state at room temperature, allowing for easy instillation into the eye, and then gel upon contact with the eye's surface (pH and temperature) (El-Kamel, 2002). The gel state ensures that the drug is retained on the ocular surface for a longer duration, reducing the frequency of administration and improving patient compliance.

## **2. Oral Drug Delivery**

Oral drug delivery remains the most preferred route of administration due to its non-invasive nature and ease of use. However, the gastrointestinal (GI) tract presents challenges such as varying pH levels, enzymatic degradation, and limited absorption windows. In-situ gel systems can address these challenges by providing a controlled release of the drug at specific sites within the GI tract. pH-sensitive in-situ gels, for example, can be designed to gel upon reaching the stomach's acidic environment or the more neutral pH of the intestines, thereby protecting the drug from degradation and ensuring targeted delivery (Mohan et al., 2020). Additionally, ion-sensitive gels like those based on alginate can form gels in the presence of calcium ions found in the GI tract, providing a protective matrix for the drug and allowing for sustained release over an extended period. Ocusert in cul-de-sac for glaucoma (pilocarpine). (Siepmann et al., 2012).

### **3. Injectable Drug Delivery**

Injectable in-situ gel systems have gained popularity for their ability to provide localized drug delivery with minimal invasiveness. These systems are particularly useful for delivering drugs to specific tissues, such as in cancer therapy, where localized and sustained drug release is crucial (Ruel-Gariépy & Leroux, 2004). Thermosensitive in-situ gels, such as those based on Pluronic F127, can be administered as a liquid at room temperature and then gel at body temperature, creating a depot at the injection site. This depot gradually releases the drug over time, maintaining therapeutic drug levels and reducing the need for frequent injections (Yuan et al., 2015). Moreover, injectable in-situ gels can be used for the delivery of biologics, such as proteins and peptides, which require protection from enzymatic degradation and controlled release (Martínez et al., 2013).

### **4. Nasal Drug Delivery**

Nasal drug delivery is an attractive route for systemic drug delivery due to the rich vascularization and high permeability of the nasal mucosa. However, the rapid clearance of drugs from the nasal cavity poses a significant challenge. In-situ gel systems can overcome this limitation by providing prolonged residence time in the nasal cavity, allowing for better absorption and sustained drug release (Vasir et al., 2005). pH-sensitive in-situ gels, such as those based on chitosan, can gel upon exposure to the slightly alkaline pH of the nasal mucosa, ensuring that the drug is retained for a longer duration and enhancing bioavailability (Wang et al., 2016). These systems are particularly beneficial for the delivery of peptides and proteins, which are prone to degradation in the GI tract and require rapid and effective absorption (Illum, 2003).

### **2.3. Challenges and Future Directions**

Despite the promising advantages of in-situ gel systems, several challenges need to be addressed to fully realize their potential in drug delivery. One of the primary challenges is the optimization of gelation conditions to ensure reproducibility and consistency in drug release. Variations in physiological conditions, such as temperature, pH, and ion concentration, can affect the gelation process and, consequently, the drug release profile (Mohan et al., 2020). Additionally, the biocompatibility and safety of the polymers used in in-situ gels must be thoroughly evaluated, as the long-term exposure to these materials could lead to adverse effects (Bajpai et al., 2016).

Another challenge is the scalability and manufacturing of in-situ gel systems. The production of these systems requires precise control over the polymer composition and gelation conditions, which can be difficult to achieve on a large scale (Sharma et al., 2018). Moreover, regulatory approval for in-situ gel systems can be challenging due to the complex nature of these formulations and the need for extensive preclinical and clinical testing to demonstrate their safety and efficacy (Ruel-Gariépy & Leroux, 2004).

Despite these challenges, the future of in-situ gel systems in drug delivery looks promising. Advances in polymer science and nanotechnology are expected to lead to the development of more sophisticated in-situ gels with improved gelation properties, biocompatibility, and drug release profiles. Furthermore, the combination of in-situ gels with other drug delivery technologies, such as nanoparticles and liposomes, could enhance their therapeutic potential and broaden their applications in the treatment of various diseases (Martínez et al., 2013). Ongoing research and development in this field will likely lead to the commercialization of novel in-situ gel systems that offer enhanced drug delivery solutions and improved patient outcomes.

In-situ gel systems represent a significant advancement in the field of drug delivery, offering a versatile and effective means of achieving sustained and localized drug release. Their ability to

undergo gelation in response to physiological triggers makes them particularly attractive for a wide range of applications, including ophthalmic, oral, injectable, and nasal drug delivery. Despite the challenges associated with their development, the continued research and innovation in this area are likely to yield new and improved in-situ gel systems that can overcome the limitations of conventional drug delivery methods. As the field of drug delivery continues to evolve, in-situ gel systems are poised to play a crucial role in the development of next-generation therapeutics.

### **3. Tooth Decay and Periodontitis: A Dual Threat to Oral Health**

Tooth decay, also known as dental caries, and periodontitis are two of the most prevalent oral health issues globally, and together they represent a significant threat to dental and overall health. Tooth decay is a process that begins when acids produced by bacteria in the mouth erode the enamel, the outermost layer of the tooth. This erosion occurs when bacteria metabolize sugars from food and beverages, producing acids that gradually demineralize the enamel (Fejerskov et al., 2015). If left untreated, tooth decay can progress through the enamel and into the dentin, the softer tissue beneath the enamel, leading to cavities. These cavities can cause pain, infection, and even tooth loss if not treated promptly. The development of tooth decay is influenced by various factors, including poor oral hygiene, frequent consumption of sugary foods and drinks, and a lack of fluoride, which helps to remineralize and protect the enamel (Pitts et al., 2017). Moreover, socioeconomic factors also play a significant role, as individuals from lower-income backgrounds may have limited access to dental care and education about proper oral hygiene practices (Petersen et al., 2005).

Periodontitis, on the other hand, is a severe gum infection that damages the soft tissue and destroys the bone that supports the teeth. It is a progression from gingivitis, the milder, reversible form of gum disease characterized by inflammation and bleeding of the gums due to plaque buildup. Periodontitis occurs when plaque spreads and grows below the gum line, where toxins produced by the bacteria in plaque irritate the gums, leading to chronic inflammation. This inflammation causes the gums to pull away from the teeth, forming pockets that can become

infected. As the immune system fights the infection, the body's response leads to the breakdown of the bone and connective tissue that hold the teeth in place, ultimately resulting in tooth loss if left untreated (Kinane et al., 2017).

The relationship between tooth decay and periodontitis is complex and bidirectional. Poor oral hygiene, a common risk factor for both conditions, leads to the accumulation of dental plaque—a sticky biofilm that harbors bacteria responsible for both caries and periodontal disease. As tooth decay progresses, it can exacerbate periodontal conditions by creating environments where bacteria can thrive, further contributing to gum inflammation and infection (Darveau, 2010). Conversely, periodontitis can also aggravate tooth decay by causing gum recession, which exposes the roots of teeth to the oral environment. Since the roots are covered by cementum rather than enamel, they are more susceptible to decay, particularly when exposed to plaque and acids from bacterial metabolism (Sbordone & Bortolaia, 2003).

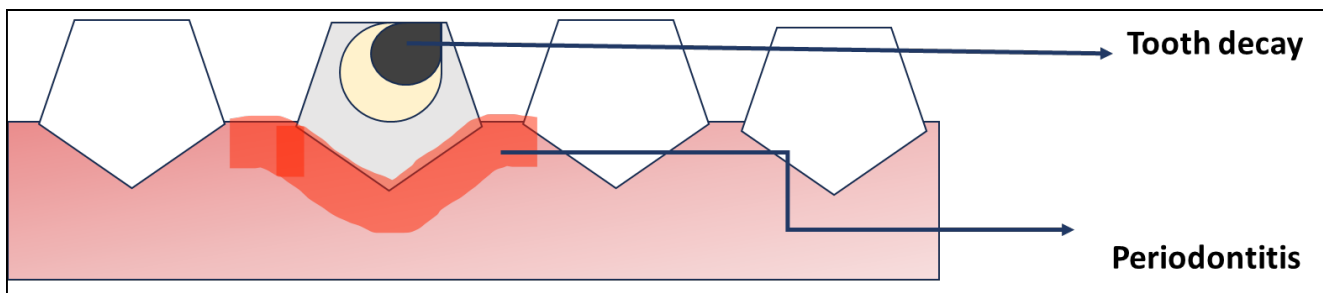


Figure 3 Tooth decay and gum swelling

In addition to local oral health consequences, both tooth decay and periodontitis have been linked to systemic health issues. Chronic periodontitis, in particular, has been associated with an increased risk of cardiovascular diseases, diabetes, and adverse pregnancy outcomes, such as preterm birth and low birth weight (Tonetti et al., 2013). The inflammation and bacterial infection that characterize periodontitis can enter the bloodstream, contributing to the systemic inflammation that underlies many chronic conditions. For instance, studies have shown that the bacteria associated with periodontitis can contribute to the formation of atherosclerotic plaques

in arteries, increasing the risk of heart attack and stroke (Sanz et al., 2020). Similarly, the chronic inflammation linked with periodontitis may interfere with insulin signaling, worsening glycemic control in individuals with diabetes (Chapple & Genco, 2013).

Preventing tooth decay and periodontitis requires a comprehensive approach that includes good oral hygiene practices, regular dental check-ups, and a balanced diet low in sugary foods and drinks. Brushing twice daily with fluoride toothpaste, flossing regularly to remove plaque from between the teeth, and visiting the dentist for professional cleanings and check-ups are essential steps in maintaining oral health (Pitts et al., 2017). Additionally, the use of fluoride, whether through drinking water, toothpaste, or professional treatments, plays a crucial role in preventing tooth decay by helping to remineralize enamel and inhibit bacterial acid production (Marinho et al., 2015). Public health measures, such as community water fluoridation and education programs about oral health, are also critical in reducing the prevalence of these conditions, particularly in underserved populations (Griffin et al., 2007).

In conclusion, tooth decay and periodontitis are interrelated oral health conditions that can have serious implications for both dental and systemic health. Understanding the risk factors and implementing preventive measures is key to managing these conditions and improving overall health outcomes. By addressing the common causes and consequences of tooth decay and periodontitis, healthcare providers can help patients maintain healthy teeth and gums throughout their lives.

#### **4. The Role of Doxycycline Hyclate in the Treatment of Tooth Decay and Periodontitis**

Doxycycline hyclate, a broad-spectrum tetracycline antibiotic, has gained prominence in the management of periodontal diseases due to its dual action as an antimicrobial agent and a modulator of host responses. In the context of tooth decay and periodontitis, doxycycline hyclate

plays a crucial role in both inhibiting the growth of pathogenic bacteria and reducing inflammation associated with periodontal tissue destruction.

Periodontitis is a chronic inflammatory disease characterized by the destruction of the supporting structures of the teeth, including the periodontal ligament and alveolar bone. This destruction is primarily driven by a dysbiosis oral microbiome, where pathogens like *Porphyromonas gingivalis* and *Aggregatibacter actinomycetemcomitans* thrive (Socransky et al., 1998). Doxycycline hydiate is particularly effective in periodontitis treatment because it inhibits the growth of these bacteria by binding to the 30S ribosomal subunit, thereby preventing protein synthesis (Walker & Winkler, 2017). Its long half-life and ability to penetrate gingival crevicular fluid make it a potent therapeutic option for maintaining subgingival antimicrobial activity (Haffajee et al., 2003).

Beyond its antimicrobial properties, doxycycline hydiate exhibits significant anti-collagenase activity, which is particularly relevant in periodontitis. Collagenases, specifically matrix metalloproteinases (MMPs), are enzymes responsible for the breakdown of collagen in the periodontal connective tissue. Elevated levels of MMPs, particularly MMP-8 and MMP-9, have been associated with the progression of periodontal disease (Golub et al., 1998). Doxycycline hydiate, at sub-antimicrobial doses, has been shown to inhibit MMPs, thus reducing collagen degradation and slowing the progression of periodontitis (Ryan et al., 2002). This therapeutic property is utilized in the form of sub-antimicrobial dose doxycycline (SDD) therapy, which is approved by the FDA for the treatment of periodontitis (Caton & Ryan, 2011).

In the management of tooth decay, or dental caries, doxycycline hydiate plays a more supportive role. While its direct effect on the carious process is limited, doxycycline can contribute to the management of caries-related infections, particularly when there is an overlap with periodontal disease or when the infection extends into the periapical tissues. Additionally, its anti-inflammatory properties may help in reducing the inflammation and secondary infection associated with severe caries (Cugini et al., 2013).

Moreover, doxycycline hydiate's use extends to the prevention of recurrent caries and periodontal disease by maintaining a balance in the oral microbiome and reducing the pathogenic bacterial load. However, the use of antibiotics like doxycycline in dental care must be carefully considered to avoid antibiotic resistance. The emergence of resistant strains due to inappropriate or prolonged use of antibiotics is a significant concern in both medical and dental fields (Preshaw, 2014). Therefore, doxycycline is often reserved for cases where mechanical debridement and other non-antibiotic therapies are insufficient, and its use is typically combined with other therapeutic interventions to optimize treatment outcomes (Pihlstrom et al., 2005).

Hence, doxycycline hydiate is a valuable tool in the management of periodontitis due to its antimicrobial and anti-collagenase properties. While its role in tooth decay is less direct, it contributes to the management of caries-related infections and inflammation. The careful and judicious use of doxycycline hydiate, particularly in combination with non-antibiotic therapies, is essential for achieving effective and sustainable outcomes in the treatment of periodontal disease and related oral health conditions.

## **5. Halloysite nanotube as drug carrier**

Halloysite nanotubes (HNTs) have emerged as a promising nanomaterial for drug delivery applications due to their unique structural and physicochemical properties. HNTs are naturally occurring aluminosilicate clay minerals that possess a tubular structure with an outer diameter of 50-70 nm, an inner diameter of 10-20 nm, and a length ranging from 200 nm to 1.5  $\mu\text{m}$  (Lvov et al., 2016). This nanotubular morphology, combined with their biocompatibility, high mechanical strength, and ease of functionalization, makes HNTs highly suitable as drug carriers for a variety of therapeutic agents.

One of the primary advantages of HNTs as drug carriers is their ability to encapsulate a wide range of drug molecules within their lumen or adsorb them onto their outer surfaces. This capacity for drug loading is facilitated by the unique structure of HNTs, where the inner lumen is positively charged and the outer surface is negatively charged. This charge differential allows for the loading of oppositely charged drug molecules, enabling controlled and sustained drug release (Joussein et al., 2005). For instance, HNTs have been successfully used to encapsulate various drugs, including anticancer agents, antibiotics, and anti-inflammatory drugs, with the release profiles being modulated by the degree of surface modification and the physicochemical properties of the drug (Li et al., 2017).

The controlled release of drugs from HNTs is a significant advantage in therapeutic applications. The release kinetics can be tailored by modifying the surface chemistry of the HNTs, coating them with polymers, or incorporating them into hydrogels. Such modifications allow for the creation of stimuli-responsive drug delivery systems where drug release can be triggered by changes in pH, temperature, or the presence of specific enzymes (Vergaro et al., 2010). This level of control is particularly beneficial in cancer therapy, where HNTs can be used to deliver chemotherapeutic agents directly to tumor sites, minimizing systemic toxicity and enhancing therapeutic efficacy (Abdullayev & Lvov, 2011). HNT have the adavantages of high specific surface area, strong adsorption capacity, good water dispersion , excellent biocompatibility, active surface chemical groups, low cost and easy access.

Furthermore, the biocompatibility and low toxicity of HNTs make them ideal candidates for in vivo drug delivery. Studies have shown that HNTs are well-tolerated by biological systems, with minimal cytotoxicity observed even at relatively high concentrations (Lecouvet et al., 2011). Additionally, HNTs exhibit excellent stability in physiological environments, ensuring that the encapsulated drugs remain protected and are released in a controlled manner over extended periods. The natural abundance and low cost of HNTs further enhance their appeal as a drug delivery platform, making them a cost-effective alternative to other nanomaterials like carbon nanotubes and mesoporous silica nanoparticles (Kamble et al., 2012).

In addition to their use as drug carriers, HNTs have been explored for a variety of biomedical applications, including tissue engineering, wound healing, and gene delivery. Their ability to be functionalized with targeting ligands also opens up possibilities for targeted drug delivery, where drugs can be delivered specifically to diseased cells, further reducing side effects and improving treatment outcomes (Lecouvet et al., 2011). The potential for HNTs to serve as multifunctional carriers that can simultaneously deliver drugs, genes, and imaging agents makes them a versatile tool in the development of next-generation therapeutic systems (Zhang et al., 2016).

In conclusion, Halloysite nanotubes offer a unique and versatile platform for drug delivery due to their structural characteristics, biocompatibility, and ease of functionalization. As research in this field continues to advance, HNTs are likely to play an increasingly important role in the development of more effective and targeted drug delivery systems, addressing some of the current challenges in pharmaceutical and biomedical applications.

## **6. In-Situ gel in periodontal diseases and tooth decay**

The phrase "periodontic disease" refers to a group of pathological disorders marked by inflammation and degradation of the dental cementum, alveolar bone, gums, and periodontal ligaments. It is a localized inflammatory response brought on by subgingival plaque and bacterial infection in a periodontal pocket. Even though bacteria are the main cause of periodontal disease, periodontitis may still develop even in the absence of microbial pathogenic factors. In order to produce nutrition for their growth, periodontal pathogens disrupt host cell membranes and extracellular matrices using their damaging byproducts and enzymes. By doing this, individuals either directly or indirectly cause harm by inciting host-mediated reactions that result in self-harm. In the initial stages of the condition, inflammation is restricted to the gingiva (known as gingivitis), but in periodontitis, it spreads to deeper tissues, resulting in bleeding, swelling, and foul breath in the gingiva. During the advanced stage of the illness, the alveolar bone starts to resorb, the periodontium's supporting collagen breaks down, and the gingival epithelium moves

along the tooth surface to create a "periodontal pocket". (Garala et al. 2013). Treatment of periodontitis include painful needle treatment or gel containing anesthesia, but this can cause numbness of mouth, cheeks, lips, and tongue, lower retention in plaque area and chances of spreading to other areas. *In-situ* gel treatment having good viscosity and mucoadhesiveness ensure better treatment of tooth decay and periodontitis(Pandit et al.2016).

With the help of in situ gel forming formulations, patients can now receive medication in a liquid dose form while yet getting a sustained release of the drug for the intended amount of time. Many polymer-based delivery systems have been created that can extend the formulation's residence time at the drug's absorption site. Water-soluble polymers that can gel after being applied to a delivery location have drawn more attention in recent years. When compared to other polymers, these so-called *in situ* gelling polymers are very beneficial because, unlike very strong gels, they are easily administered in liquid form to the drug absorption site. They enlarge to produce a robust gel at the drug absorption site, which can extend the active substance's residence period. (Garala & Joshi,2013)

## Chapter 2:Literature Review

**1. V.Khunová et.al. (2022)** conducted a study on Antibacterial Electrospun Polycaprolactone Nanofibers Reinforced by Halloysite Nanotubes for Tissue Engineering. He concluded in biomedical applications, polycaprolactone (PCL), which breaks down gradually, is used extensively. The work focuses on creating antibacterial nanofibers using halloysite nanotubes (HNTs) and PCL. Utilizing HNTs, the generated nanofibers can be used as low-cost nanocontainers to encapsulate various substances, such as DNA, medications, and enzymes. In this work, they used HNTs as a nanocarrier to transport erythromycin (ERY), a quintessential antibacterial active substance with wide antibacterial action. Nanofibers based on PCL and HNT/ERY were produced by electrospinning. The PCL nanofibers containing 7.0 wt.% HNT/ERY were surrounded by a sterile zone of inhibition, which was employed to evaluate the antibacterial activity. The morphology was seen using both TEM and SEM. The loading efficiency of HNT/ERY was evaluated, making use of thermogravimetric analysis. It was shown that the remarkable antibacterial properties of the nanofibers inhibited both Gram (-) (*Escherichia coli*) and Gram (+) (*Staphylococcus aureus*) bacteria.

Moreover, a noteworthy enhancement in mechanical properties was achieved. PCL/HNT/ERY nanofiber materials are antibacterial, nontoxic, environmentally benign, and biodegradable. They have a multitude of potential uses in biomedical sectors, such as wound healing, tissue engineering, and the prevention of bacterial infections.

**2. Hartatiek et al. (2024)** conducted a study on Investigating the Impact of Curcumin Extract Incorporation on PVA/Collagen/Chitosan/HAp Nanofiber Scaffold: Morphological, Antibacterial, Wettability, and Degradation Rate.

The aim of their work was to combine curcumin, hydroxyapatite (HAp), collagen, and chitosan to form nanofibers for bone tissue creation. Electrospinning was used to make the nanofibers, and because of this, evaluations were conducted on wettability, degradation rate, and antibacterial activity. FTIR measurement showed that all of the components were present in the nanofibers. The SEM images showed smooth, bead-free nanofibers with an average diameter of between 108 and 139 nm. The zone of inhibition against *S. aureus* and *E. coli* increased as the concentration of curcumin was tested for antibacterial activity. Water contact angle

measurements revealed a greater curcumin content and improved hydrophilicity. Finally, a positive association was seen between the immersion period and curcumin level and the deterioration rate.

These results suggested that the Artificial PVA/Collagen/Chitosan/HAp/Curcumin nanofibers have potential use in bone tissue engineering due to their beneficial properties.

**3. Y.Lvov et al.** conducted a study on Halloysite Clay Nanotubes for Loading and Sustained Release of Functional Compounds. The parameters of halloysite, an aluminosilicate tubular clay, are 50 nm in diameter, 15 nm in the inner lumen, and 600–900 nm in length. Thousands of tons of this naturally occurring, biocompatible nanomaterial is available at a low cost.

The inner lumen of halloysite can be altered to allow formulations with sustained release that can be adjusted by the tube end-stoppers for hours or days by etching to 20–30% of the tube volume and filling it with functional agents (antioxidants, anticorrosion agents, flame-retardant agents, medicines, or proteins). Clogging the tube ends with polymeric composites allows for an extra extension of the releasing period. Consequently, rubber that has been doped with the antioxidant-rich halloysite enhances its anti-aging properties for a minimum of a year. The addition of 3-5 weight percent of halloysite to polymeric materials increases their strength, and the tube's orientation ensures a gradient of properties. Halloysite nanotubes are a good mesoporous medium for catalytic nanoparticles that can be formed simply in the lumens of the tube or seeded on the surface. They have enhanced catalytic capabilities, especially at high temperatures. Research on worms and biological cells, both *in vivo* and *in vitro*, show that halloysite is harmless. Furthermore, studies are carried out to find out how well mycotoxins adsorb in animal stomachs.

**4. Clemens et al.** conducted study on Novel Antioxidant Properties of Doxycycline. Doxycycline (DOX), a broad-spectrum antibiotic and derivative of tetracycline, has multiple medical applications beyond its antibacterial properties. For example, DOX has been used to treat a number of chronically inflammatory disorders. Two potential ways that DOX stops these diseases from becoming worse are via reducing oxidative stress, which in turn reduces lipid peroxidation and inflammatory responses. Here, we looked into the hypothesis that DOX directly

scavenges reactive oxygen species (ROS) and inhibits the formation of redox-mediated malondialdehyde-acetaldehyde (MAA) protein adducts. Using a cell-free system, they demonstrated that DOX scavenges reactive oxygen species (ROS) produced during the synthesis of MAA-adducts and suppresses the creation of MAA-protein adducts. To find out if DOX scavenges any specific ROS, they examined its direct scavenging of hydrogen peroxide and superoxide. Electron paramagnetic resonance (EPR) spectroscopy was used to directly observe the scavenging of superoxide by DOX, but not hydrogen peroxide.

Moreover, they found that DOX inhibits MAA's ability to activate the redox-sensitive transcription factor Nrf2. The underestimated direct antioxidant property of DOX is highlighted by all of these findings, and this characteristic may help to explain the drug's potential for treating conditions characterized by heightened oxidative stress and chronic inflammation.

**5. Ribeiro et al. conducted study on** study of a tooth gel formulation for hygiene and oral sequelae management in irradiated patients. Numerous side effects from cervical-facial radiation therapy might occur, either systemic or localized to the mouth. These individuals' oral mucosa is severely damaged by radiation therapy, whether or not chemotherapy is used, leading to a number of problems. Dentifrices containing sodium lauryl sulfate harm the mucosa by making it dry. The goal of this effort was to create a dentifrice that would reduce xerostomia associated with a less abrasive effect. This dentifrice was meant to help with dental biofilm control, caries prevention, hygiene, and tooth sensitivity in cancer patients. Ten dentifrices' qualitative composition and physicochemical properties were examined, allowing for the creation of the suggested formulation (PF), which was examined every 180 days. Apart from demonstrating the PF's good behavior during packaging and storage, the quantitative analysis of spreadability revealed that a greater amount of propylene glycol in the PF was necessary to stop syneresis from happening after 60 days. Additionally, pH tests showed that the PF maintains dental demineralization by balancing with the pH of oral homeostasis. Recommendations state that the PF is a suitable dentifrice for individuals undergoing anticancer therapy because of its distinct composition and physicochemical feature.

**6.R.Rajan et al.** Halloysite nanotubes (HNT) as reinforcement for compatibilized blends of polypropylene (PP) and polylactic acid (PLA). Polymer blends and polyblend nanocomposites

are essential for the creation of new materials in the field of polymer science and technology. The polypropylene (PP), polylactic acid (PLA), and Halloysite nanotube (HNT) nanocomposites are one example of such a system. Another compatibilizer used to improve the interfacial contact between the polymer components is maleic anhydride-graft-polypropylene. This article details the synthesis and assessment of PP/PLA compatibilized polyblend nanocomposites in an 80:20 ratio, featuring varying HNT weight percentages between 0 and 10. The nanocomposites were assessed by differential scanning calorimetry (DSC), X-ray diffraction (XRD), transmission electron microscopy (TEM), thermogravimetric analysis, and polarized optical microscopy (POM). The FTIR data, which altered the absorption peaks that matched the hydroxyl groups attached to HNT, showed how HNT interacted with the PP/PLA combination. DSC tests of the blends and nanocomposites showed a steady rise in the crystalline quality of the composites up to 6 weight percent of HNT.

With the use of XRD and microscopic measurements such as TEM and POM, the dispersion of HNT in the polyblend is well characterized. A schematic representation of the polyblend nanocomposites is suggested based on the findings of the previously described experiments, and it is believed that 6 weight percent of HNT is the appropriate concentration for these types of polymerblends.

**7. M. Humphries et al.** conducted study Contemporary Considerations for Establishing Reference Methods for Antibacterial Susceptibility Testing. Antibacterial susceptibility testing (AST) is used to guide therapy, track resistance, and encourage the development of new antibacterial medications. Broth microdilution (BMD) has been the standard method for testing novel agents and diagnostic tests against the in vitro activity of antibacterial agents for the past fifty years. BMD requires in vitro bacterial inhibition or killing. Its shortcomings include the difficulty to precisely mimic the in vivo milieu of bacterial infections, the fact that it takes several days to finish, and its modest, difficult-to-manage variability. Moreover, newer medications (such those that target pathogenicity) whose activity cannot be determined by BMD may soon need new reference methodologies. Every new reference approach must be linked to clinical efficacy and validated by industry, regulators, and researchers worldwide. Here, we

describe the most recent reference methods for determining the in vitro antibacterial activity and go over key considerations for developing new reference methods.

**8. Sudipta Ganguly et al. (2004)** their work aimed to create a new in situ gel system combining chitosan and glyceryl monooleate (GMO) for targeted and sustained drug administration. The delivery method was composed of 0.33 M citric acid, 3% (w/v) GMO, and 3% (w/v) chitosan. A biological pH was used to generate the in-situ gel. In vitro release experiments were carried out using Sorensen's phosphate buffer (pH 7.4), and spectrophotometry or HPLC were used to assess the medicines. The impact of the cross-linker, the diffusion coefficient, and the gel's water uptake were all measured using thermogravimetric analysis (TGA). The gel's mucoadhesive capability was assessed in vitro with the EZ-Tester.

Glutaraldehyde, a cross-linker, was added, which slowed down the amount and rate of drug release. Drug-encapsulated microspheres can be used in place of free drug to prolong the in vitro release. There was a matrix diffusion-controlled mechanism for drug release from the gel. The mucoadhesive activity of chitosan was increased by three to seven times when GMO was added. Both parenteral and oral modes of prolonged drug delivery may benefit from the use of this innovative in situ gel technology.

**9. Teng-Yu Yang et al. (2015)** studied that degree of caries can be evaluated using salivary analysis. Of the salivary proteins that are known to exist, not much is known about the function of proteinase 3 (PR3), a serine protease that belongs to the chymotrypsin family, in dental caries. Children with different levels of active caries had their whole, unstimulated saliva collected, and it was examined using an enzyme-linked immunosorbent assay and a Human Protease Array Kit. When dental caries severity increased, salivary PR3 concentration was shown to be considerably lower (P<0.01); salivary pH and PR3 concentration were also found to be positively correlated ( $r=0.87$ ; P<0.01; Pearson's correlation analysis). After 12 hours of incubation, *Streptococcus mutans* UA159 growth was considerably suppressed by a PR3 concentration of 250 ng-mL<sup>-1</sup> or higher in an antibacterial test (P<0.05). The negative correlation between salivary PR3 concentration and dental caries severity and the vulnerability of *S. mutans* to PR3 suggest that PR3 is a salivary factor related to caries severity in these investigations.

**10. R . Berahman et al.** conducted study where surface-treated halloysite nanotubes (HNT) were effectively obtained. TEM, FTIR, and TGA were used to assess the grafted HNT. The silicone rubber/HNT vulcanizate nanocomposites were made with modified HNT. Rheometry, DMTA, TGA, and tensile tests were used to comprehensively study the effects of silicone rubber hardness and HNT loading on the cure characteristics, swelling behavior, dynamic mechanical, thermal, and mechanical properties of the resultant rubber compounds. The acquired results showed a correlation with the samples' microstructure as determined by SEM and XRD examinations. According to vulcanization curves, the HNT improved the rubber compounds' cure kinetics by steadily reducing the scorch and optimal cure times and gradually raising the effective torque as the HNT concentration increased. The crosslink density of the nanocomposites was increased by adding HNT to the silicone rubbers. When DMTA data were compared to unfilled silicone rubbers, they revealed limited relaxation processes in HNT-reinforced systems. This impact was especially noticeable in systems with the lowest hardness silicone rubber matrix. The filled rubbers with HNT content showed an increase in Young's modulus and tensile strength, according to the tensile data. Based on TGA data, the rubber compounds' thermal stability progressively increased as HNT loading increased in the material.

**11.G.Cavallaro et al.** conducted study on Nanohydrogel Formation within the Halloysite Lumen for Triggered and Sustained Release. A simple method for obtaining nanohydrogels inside the lumen of halloysite nanotubes (HNTs) was looked into. Hexadecyltrimethylammonium bromides and HNTs were utilized to create inorganic reverse micelles that were dissolved in chloroform. The hydrophilic cavity served as a nanoreactor to contain the production of an alginate gel that was cross-linked by calcium ions. Experiments using spectroscopy and electron imaging demonstrated the polymer's confinement within the HNT lumen and the development of a calcium-mediated network. The hybrid hydrogel's biocompatibility was demonstrated through biological testing. The HNTs' nanogel proved appropriate for drug loading and long-term release, with the possibility of chemical stimuli-induced burst release. Here, we suggest a novel approach for the creation of nanohydrogels that is based on inorganic reverse micelles and is appropriate for both biological and industrial purposes.

**12. S. Ganguly et al.** conducted study on synthesis of polydopamine-coated halloysite nanotube-based hydrogel for controlled release of a calcium channel blocker. Through the self-polymerization of dopamine (DA) on the outside of halloysite nanotubes (HNT) and gelation using alginate, a stimuli-triggered drug delivery vehicle has been created. In an alkaline solution, DA self-polymerizes after adhering to the lumen's outer surface in an aqueous medium. Alginate hydrogel has been combined with self-polymerized DA (PDA)-coated HNTs, which have undergone ionically crosslinking. Images from transmission and scanning electron microscopy suggest that the HNT surface has a PDA coating that is between 12 and 17 nm thick. The hydrogels exhibit adequate gel strength (marked difference between elastic and loss modulus) and their shear thinning nature may be observed in their rheological behavior as manufactured. The thermogravimetric analysis's thermal degradation profile suggests that the alginate is more thermally stable than it is clean. Swelling trends in aqueous medium have shown and validated PDA's role as an extra potent gelator. Two approaches have been used to achieve drug loading: post-loading and in situ loading. It has been observed that in situ loading of drug molecules has a more regulated release feature than post-loading when DA is polymerized on the HNT surface. The synthesis parameters were also changed to fine-tune this release behavior.

# Chapter 3: Aims and Objectives

### **3.Aim and Objectives**

1. Optimization of in-situ gel
2. Loading of doxycycline hyclate in halloysite nanotube.
3. Preparation of doxycycline hyclate loaded HNT *in-situ gel*.
4. Characterization of the prepared doxycycline hyclate loaded HNT *in-situ gel*.

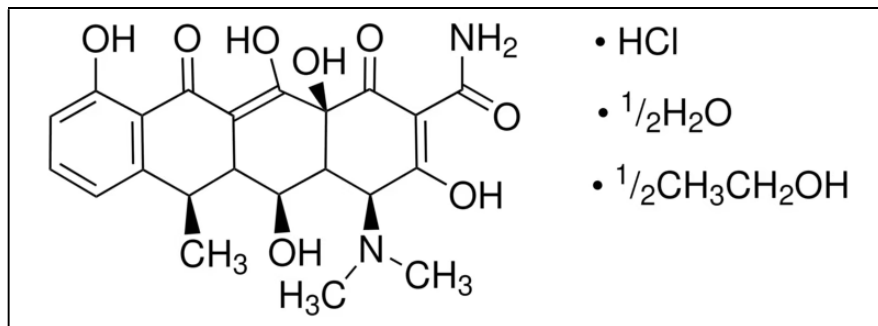
#### **3.1. Plan of Work**

- Selection of suitable chemicals, polymer and copolymer for the preparation of *in-situ gel*.
- Preparation of *in-situ gel*
- Determination of gelation time and temperature.
- Loading of different drug:HNT ratio onto prepared *in-situ gel*.
- Preformulation studies like melting point analysis UV-absorption and pH determination on prepared *in-situ gel*.
- Instrumental characterization of *in-situ gel*.
- Determination of in-vitro release kinetics, antimicrobial and antioxidant potential of *in-situ gel*.

# Chapter 4:Materials and Reagents

#### **4.1. Doxycycline hyclate**

- **Drug class:** Second generation tetracycline antibiotics.
- **Description:** A tetracycline antibiotic that dissolves in water, doxycycline hyclate kills and stops the growth of a variety of gram-positive and gram-negative bacteria. Because doxycycline hyclate inhibits collagenase and matrix metalloproteinase in the gingival crevicular fluid, it has a particular indication for adult periodontal disease. No indication of alterations or antibiotic susceptibility to opportunistic pathogens or normal periodontal flora is present.
- **Chemical formula:** C<sub>46</sub>H<sub>58</sub>Cl<sub>2</sub>N<sub>4</sub>O<sub>18</sub>
- **Chemical structure:**

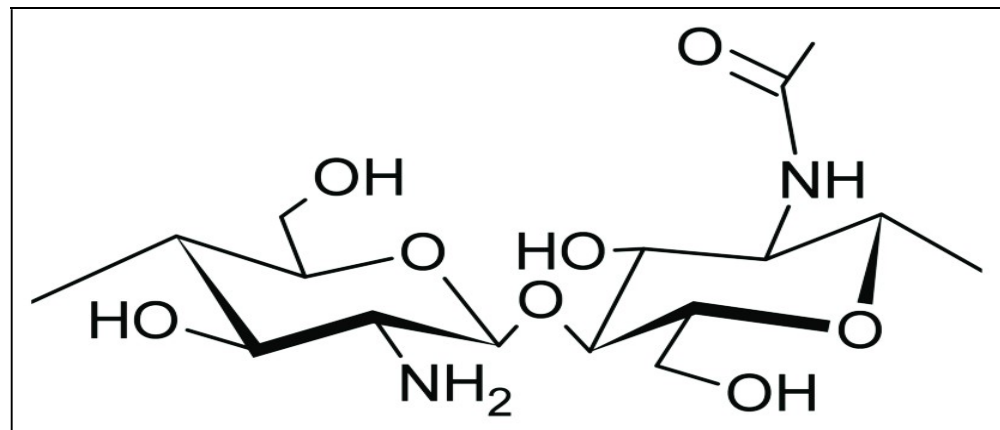


- **IUPAC name:** 6-Desoxy-5-hydroxytetracyclinehydrochloride hemihydrate hemiethanolate
- **Molecular weight:** 1025.9 g/mol
- **Melting point:** ~201 °C
- **Solubility:** This substance dissolves in water at a rate of 50 mg/ml, producing a transparent, yellow-green solution. It can take some gentle heating to completely dissolve the substance. Additionally, it is insoluble in ether or chloroform, soluble in methanol, and sparingly soluble in ethanol.

- **Mechanism of action:** Tetracyclines, such as doxycycline hydiate, have bacteriostatic properties that halt the development of bacteria by binding allosterically to the 30S prokaryotic ribosomal unit during protein synthesis. In order to halt the elongation phase and produce an ineffective cycle of protein synthesis, doxycycline hydiate inhibits the charged aminoacyl-tRNA (aa-tRNA) from adhering to the ribosomal A site. The ternary complex, which consists of aa-tRNA, GTP, and elongation factor Tu (EF-Tu), binds to the ribosome at a different rate when treated with doxycycline. The ternary complex makes an unsuccessful effort to attach the aa-tRNA to the A site. By stopping the translation of the expanding polypeptide chain, this process hinders the synthesis of vital proteins and ultimately results in the death of the bacteria.
- **Route of elimination:** The liver concentrates tetracyclines, such as doxycycline hydiate, in bile, which are then expelled in high concentrations and in a biologically active form in the urine and feces. For those with a creatinine clearance of roughly 75 mL/min, the kidneys excrete approximately 40% of doxycycline every 72 hours. For those whose creatinine clearance is less than 10 mL/min, this percentage could drop as low as 1-5% every 72 hours.
- **Adverse effect:** Compared to its tetracycline equivalents, doxycycline hydiate is a medication that is well tolerated and shows little sign of major side effects. Here are a few of the little noticed negative outcomes:
  - Bloody diarrhea
  - Leukopenia
  - Chest pain
  - Dysuria
  - Intracranial hypertension
  - Migraine
  - Hemolytic anemia

#### **4.2. Chitosan**

- **Description:** Didymella pinodes contains chitosan, a naturally occurring substance. Beta-1,4-D-glucosamine deacetylated CHITIN is a linear polysaccharide. It treats wounds and is used in HYDROGEL.
- **Synonyms:** Chicol, Flonac C, Poliglusam.
- **Chemical structure:**



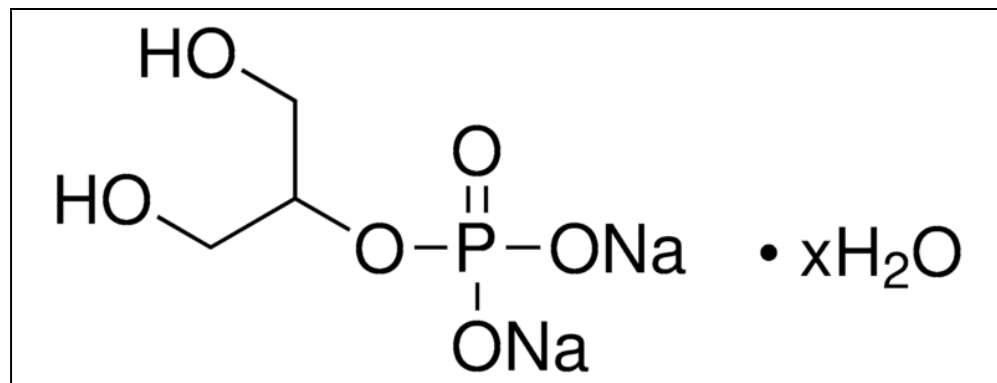
- **Molecular formula:** C<sub>56</sub>H<sub>103</sub>N<sub>9</sub>O<sub>39</sub>
- **Molecular weight:** 1526.5 g/mol
- **Physical Description:** Yellow powder
- **Chemical Classes:** Biological agents -Polysaccharides
- **Melting Point:** 102.5°C
- **Odor:** Odorless
- **Solubility:** Dilute aqueous acid (pH < 6.5).: soluble

#### **4.3. Sodium beta-glycerophosphate**

- **Description:** The disodium salt of glycerol 2-phosphate is an organic sodium salt known as sodium glycerol 2-phosphate.
- **Synonyms:** Disodium beta-glycerophosphate, Sodium 2-glycerophosphate, Sodium 1,3-dihydroxypropan-2-yl phosphate, Sodium beta-glycerophosphate

- **IUPAC name:** Disodium;1,3-dihydroxypropan-2-yl phosphate

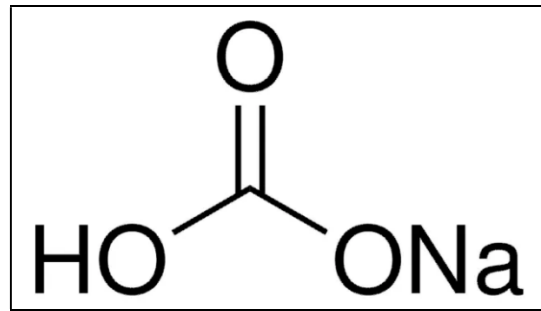
- **Chemical Structure:**



- **Molecular weight:** 216.04g/mol
- **Molecular formula:** C<sub>3</sub>H<sub>7</sub>Na<sub>2</sub>O<sub>6</sub>P
- **Physical Description:** Hydrate, white crystalline powder
- **Chemical Classes:** Organic acid, metal salts.
- **Melting point:** 102-104°C
- **Odor:** Odorless
- **Solubility:** Freely soluble in water

#### **4.4. Sodium Bicarbonate**

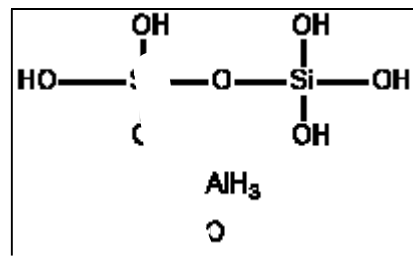
- **Description:** Sodium bicarbonate is a white, crystalline powder that is frequently used in topical cleansing solutions, systemic alkalinizers, pH buffering agents, and electrolyte replenishers.
- **Synonyms:** Baking Soda, Bicarbonate, Sodium Carbonic Acid Monosodium Salt, Hydrogen Carbonate, Sodium Soda, Baking Soda, Sodium Bicarbonate, Sodium Hydrogen Carbonate
- **Molecular Structure:**



- **Molecular weight:** 84.007 mg/mol
- **Physical description:** Colourless or white crystalline masses or crystalline powder
- **Chemical Class:** Salt, Basic
- **Colour:** White, monoclinic prisms
- **Odor:** Odorless
- **Melting point:** 50°C
- **Density:** 2.1 g/cm³
- **Taste:** Cooling, slightly alkaline taste
- **Solubility:** Soluble in water. Insoluble in ethanol

#### **4.5. Halloysite Nanotube:**

- **Description:** Halloysite has a primary hollow nanotubular structure and is a two-layered aluminosilicate. The hollow hematite nanotubes have potential use as regulated release carriers, coatings constituents, and nanocomposites.
- **Synonym:** Kaolin Clay
- **Molecular Formula:**  $\text{Al}_2\text{Si}_2\text{O}_5(\text{OH})_4$
- **Molecular Structure:**

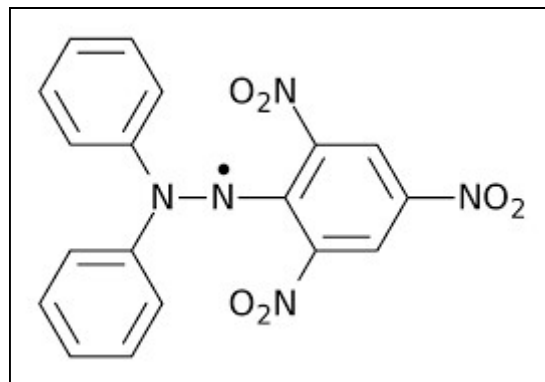


- **IUPAC:** [dihydroxy(oxoalumanyloxy)silyl]oxy-dihydroxy-oxoalumanyloxysilane

- **Form:** Crystalline, elongated mineral that can be found both hydrated and dehydrated. When it is hydrated, it is made up of curving sheets made of unit layers of kaolin.
- **Colour:** White to gray or brown solid
- **Molecular weight:** 246.19 g/mol
- **Density:** 2.53 (True specific gravity)
- **Colour:** 75-96, Hunter brightness
- **Pore Size:** 1.26-1.34 ml/g pore volume

## 4.6 DPPH radical

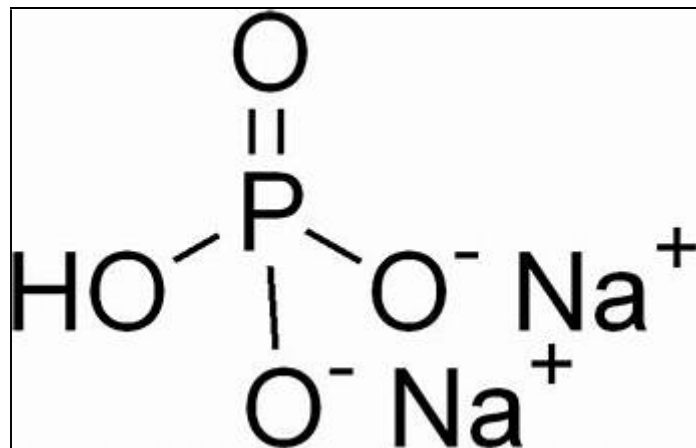
- **Description:** 1,1-diphenyl-2-picrylhydrazyl, also known as 2,2-diphenyl-1-picrylhydrazyl, is a free radical that can receive hydrogen from antioxidants. This chemical is now commonly employed in the DPPH assay to measure the antioxidant activity of fruits, medicinal herbs, and other biological substrates. Compared to the extremely reactive superoxide and hydroxyl species that are predominantly responsible for oxidative damage in biological systems, DPPH is a comparatively stable radical that does not arise spontaneously.
- **Molecular formula:** C<sub>18</sub>H<sub>12</sub>N<sub>5</sub>O<sub>6</sub><sup>+</sup>
- **Molecular Weight:** 394.3 g/mol
- **IUPAC name:** 1,1-diphenyl-2-picrylhydrazyl (DPPH)-2,2-diphenyl-1-picrylhydrazyl



- **Synonym:** 2,2-Diphenyl-1-picrylhydrazyl (free radical), 1,1-Diphenyl-2-picrylhydrazyl (free radical), 2,2-Diphenyl-1-(2,4,6-trinitrophenyl)-hydrazyl (DPPH).
- **Physical Description:** Dark violet solid

## 4.7. Disodium Phosphate

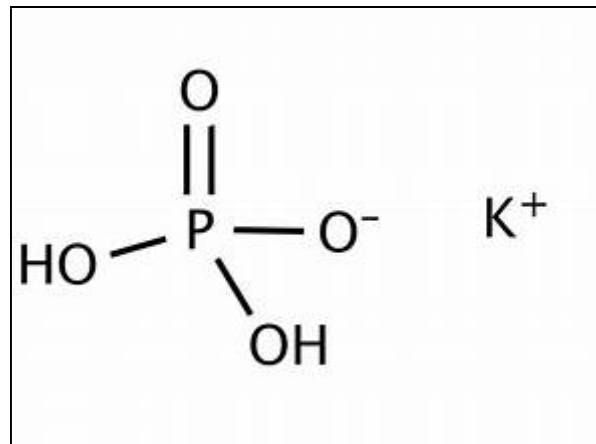
- **Description:** The crystalline solid sodium phosphate dibasic is colorless to white in appearance. water-soluble. The environment's threat is the main hazard. It is important to act quickly to prevent environmental spread. utilized for numerous purposes, including food processing, medications, fertilization, and more.
- **Molecular formula:**  $\text{Na}_2\text{HPO}_4$ ,  $\text{HO}_4\text{PNa}_2$ ,  $\text{HNa}_2\text{O}_4\text{P}$
- **Molecular weight:** 141.959 g/mol
- **IUPAC name:** Disodiumhydrogen phosphate
- **Chemical Structure:**



- **Solubility:** Soluble in water
- **Density:** 0.5-1.2 g/cm<sup>3</sup>
- **Stability:** Stable in air
- **Physical appearance:** White or colorless hygroscopic crystals or powder
- **Odor:** None
- **Taste:** Saline
- **Melting point:** 92.5 °C

## 4.8. Potassium dihydrogen phosphate

- **Description:** Potassium dihydrogen phosphate is a potassium salt in which dihydrogen phosphate(1-) is the counterion. It has a role as a fertilizer. It is a potassium salt and an inorganic phosphate.
- **Molecular weight:** 136.086 g/mol
- **Molecular formula:**  $\text{KH}_2\text{PO}_4\text{H}_2\text{KO}_4\text{P}$
- **IUPAC name:** Potassium; dihydrogen phosphate
- **Physical Description:** Dry powder, colorless and odorless crystal.
- **Melting point:** 253°C
- **Solubility:** Freely soluble in water
- **Chemical Structure:**



- **Density:** 2.34g/cu cm
- **pH:** 4.4-4.7
- **other experimental properties:** At ordinary temperatures, monopotassium phosphate is so far above its Curie point as to give piezoelectric effects in which the emf is proportional to the distorting force. There is virtually no hysteresis.

# Chapter 5: Materials and methods

## **Pre-formulation studies:**

### **1. Melting point determination:**

The capillary tubes used for the melting point study were sealed on one end by heating the end of capillary tube over spirit lamp. Doxycycline hyclate was filled inside the capillary tube, after filling some of the amount of drug the tube was gently tab to fill the tube 1-2mm. Drug filled tube was kept in melting point apparatus (SUNBIM R) inside the holder. The temperature adjuster knob was adjusted. When the drug started to melt the temperature was recorded. The time at which drug completely melted, temperature was observed and recorded. The melting point was average of the both the temperature noted above. The process was repeated for three times to obtain an optimum result.

### **2.Preparation of standard curve of Doxycycline hyclate.**

#### **2.1 Preparation of 1N phosphate buffer pH 6.8.**

Dissolve 3.468g of potassium dihydrogen orthophosphate and 8.771g of sodium hydroxide in 250 ml of distilled water. pH was recorded in suitable pH meter. To adjust the pH at 6.8 sodium chloride was added dropwise.

#### **2.2 Determination of absorption maxima.**

Determination of UV absorption maximum was done by scanning 10 mg of drug dissolved in 100 ml of PBS buffer. The range selected was 200-400 nm by using UV spectrophotometer (UV-1800, Shimadzu, Japan).

#### **2.3. Determination of Standard curve of Doxycycline hyclate.**

Primary stock solution was prepared in a 1000ml of volumetric flask by dissolving 20mg of accurately weighed doxycycline hyclate in 6.8 pH phosphate buffer and the concentration was found to be 100ppm. From this 20ml of solution was pipetted out in a 250ml volumetric flask and the volume was made upto 200ml with phosphate buffer to obtain a secondary stock of 10ppm. From the secondary stock distinct aliquots were made of different concentration like 2,4,8,10,12,14,16,18 and 20  $\mu$ g/ml which were scanned at 274.5nm (lambda max) by using UV Spectrophotometer(UV-1800,Shimadzu,Japan) with spectral bandwidth of 1 nm $\pm$ 0.3nm

wavelength accuracy. 10mm pair of quartz cells were used to record the absorbance reading. All samples were analyzed for three times to minimize the error. (Pavagada et al. 2010.)

*Table 1 Preparation of Drug solution and PBS for standard curve of DOH*

Formulation	Drug solution(ml)	PBS (ml)
F1	2	8
F2	4	6
F3	6	4
F4	8	2
F5	10	0
F6	1.2	8.8
F7	1.4	8.6
F8	1.6	8.4
F9	1.8	8.2
F10	2	8

## **2.Preparation of HNT loaded Doxycycline hydiate loaded *in-situ* gel:**

### **2.1. Preparation of HNT nanotubes for loading of drugs.**

20g of HNT was weighed and kept in a petri dish without any cover. The weighed HNT was kept in vacuum dryer at 60°C for 2 hours under full vacuum. The dried HNT powder was sealed in eppendorf and kept in desiccator.

### **2.2. Loading of HNT tube with Doxycycline hydiate.**

*Table 2 Formulation Chart of DOH loaded HNT*

Formulation	Amount of HNT (mg)	Amount of drug(mg)
F1	100	50
F2	100	100
F3	50	100

Loading of HNT was done in formulation F1, F2, and F3 according to the formulation table given above. 23 ml of distilled water was added to weighed amount of drug and HNT. The solution was stirred with glass rod and the solution was sonicated for 30 minutes. The solution was transferred in petri dish and was kept in vacuum dryer for 2 hours for 60 minutes. After drying the solution was kept in desiccator overnight.

### **2.3 Freeze drying of HNT**

The solution after overnight was transferred in a conical flask and kept in freeze dryer at -40°C for 6 hours. After freeze drying the powder was scrapped, sealed in Eppendorf and kept in desiccator.

### **2.4 Preparation of *in-situ* gel**

Two solutions were prepared solution A and B. Solution A was prepared by adding 100 mg of chitosan in 4.5 ml of 35% of HCl. Solution B was prepared by adding 25 mg of and 21 mg of sodium bicarbonate to 0.5 ml of distilled water. Both solution A and B were kept in refrigerator at 4°C. After cooling the solutions, Solution B was added to solution A on continuous stirring. Solution C of drug loaded HNT was added to A and B solution in beaker.

This solution of A, B and C in beaker was transferred to test tube and was added to water bath maintained at 37°C. The beaker was tilted every 1 min, the time when meniscus does not move formation of *in-situ* gel was confirmed.

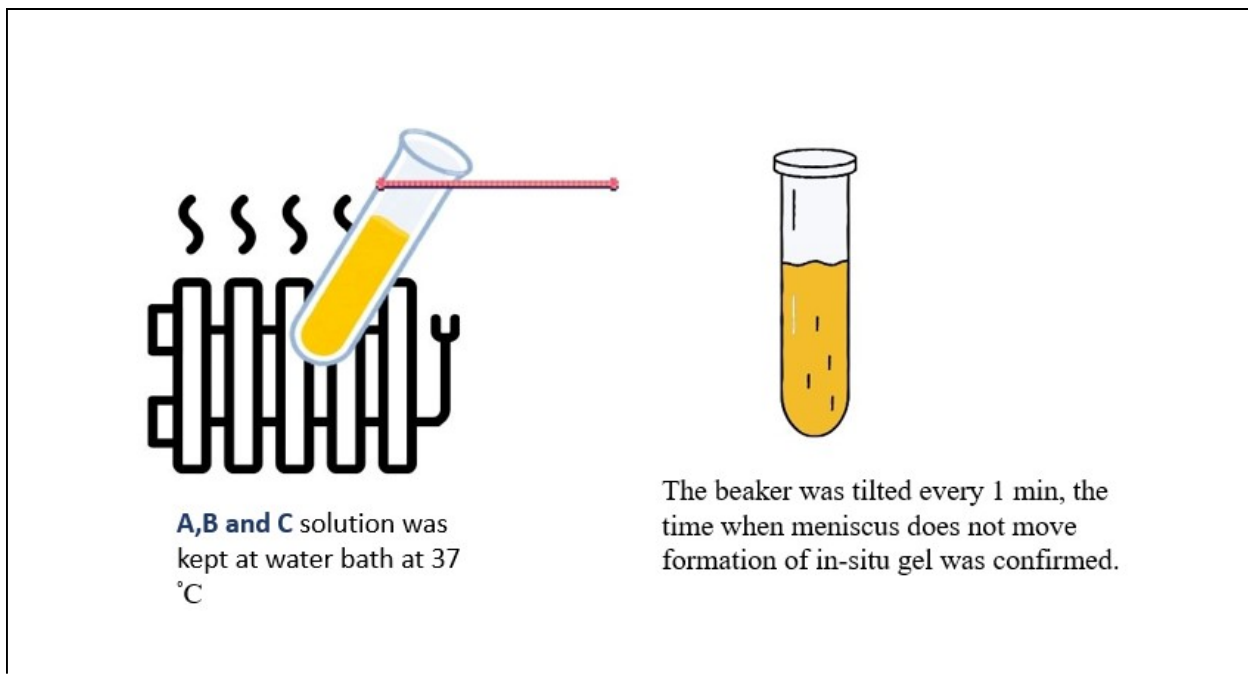
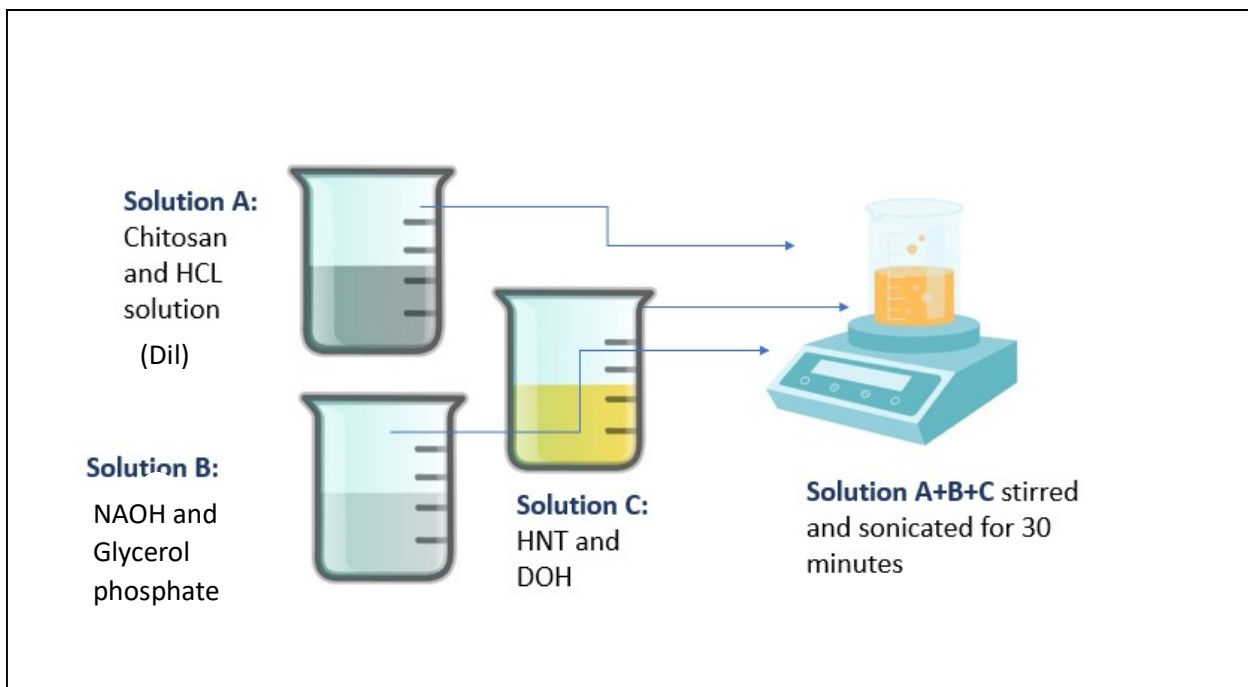


Figure 4 Preparation of DOH loaded HNT in-situ gel

### **3. pH determination of *in-situ* gel**

A pH paper was used to determine pH of an oral *in situ* gel. Saliva was collected from the mouth using a sterile swab and this was uniformly spreaded over a clean palm. Ensuring that the area is thoroughly covered but not excessively wet. Take a strip of pH paper and soak it in the saliva applied over palm. Wait for few seconds for paper to develop its color. Compare the color on the pH paper with the reference chart to determine the initial pH of saliva.

Dip the pH paper in the *in-situ* gel formulation, wait for few seconds to develop color. Blank, F1, F2 and F3 formulations were used to determine the pH. Compare the color on the pH paper with the reference chart to determine the initial pH of *in-situ* gel. (Ashlesha et al. 2015.)

## **4. Antibacterial assay**

### **4.1 Antimicrobial Susceptibility Testing**

Antibacterial susceptibility testing (AST) is used to promote the discovery of novel antibacterial drugs, monitor resistance, and direct therapy. For fifty years, innovative agents and diagnostic tests have been tested against the *in vitro* activity of antibacterial agents using broth microdilution (BMD) as the standard approach. Bacterial inhibition or death *in-vitro* is essential to BMD. It has a number of drawbacks, including the inability to accurately replicate the *in-vivo* environment of bacterial infections, the need for several days to complete, and its subtle, challenging to manage variability. Furthermore, new reference techniques may soon be required for novel drugs (such as those that target pathogenicity) whose activity cannot be assessed by BMD. Any new reference technique needs to be validated globally by regulators, industry, and researchers, and it needs to be associated with clinical efficacy. (Hartatiek et al. 2024.)

### **4.2: Disc diffusion method:**

Disc diffusion method for antimicrobial susceptibility testing was carried out according to the standard method by Bauer et al. (1966) to assess the presence of antibacterial activities of the

Doxycycline hyclate loaded HNT. 1.5% agar media was prepared and kept for autoclave at 15 psi for 30 minutes. After autoclaving agar plates were prepared. Plates were kept for blank incubation for 24 hrs. Serial dilution of drug was prepared for the concentration in microliters of 1000,800,400,200,100,50,25. Bacterial suspension of *E. coli* K-88,*L.acidophilus* NCIM 2056 and were spread on agar plate. Disc dipped in each serial dilution of drug solution were place over agar plates. Plates were labelled properly regarding strain number and dilution used in each quadrant. Plates were kept for incubation for 24 hrs. After incubation diameter was calculated and reported. (Zaidan et al. 2006)

*Table 3 Formulation table for bacterial assay*

Formulation	Amount of Drug	Amount of HNT
F1	10mg	100 mg
F2	6mg	100mg
F3	5mg	50mg

## **5.Spreadability Testing:**

For patient compliance, spreadability is a crucial aspect of dental formulation. A circle was drawn on the glass plate of 1 cm. A 50 mg of in-situ gel was weighed and was carefully placed within the pre-marked circle. Another glass plate was placed over the glass plate having in-situ gel within pre-marked circle. 50g,100g,200g of weight was permitted to settle on the top glass plate for 30 sec time intervals. It was observed that the diameter increased as a result of the gel spreading. (Harish et al. 2009.)

## **6.Swelling Index:**

In-situ gel capacity to absorb water was assessed by immersing it in PBS (pH 6.8) at 37 °C for 1, 2, 3, 4 and 5 days. The moist sample's weight, W<sub>0</sub>, was determined, and the degrees of swelling were discovered using the formula that follows:

$$\text{Swelling degree} = \frac{(W_t - W_0)}{W_0} \times 100$$

where,  $W_0$  and  $W_t$  are the weight of the freeze-dried hydrogel and the weight of the swollen hydrogel, respectively. (Jose et al. 2021)

## **7.Syringeability Test:**

When severe periodontitis was present, the administration of the medication via an injection needle straight into the periodontal pocket is a quick way to administer the in-situ gel to treat severe tooth cavity and periodontitis. According to this theory, gel compositions' syringeability was assessed with a 21 G needle.(Ashlesha et al. 2015.)

## **8.Gelation temperature:**

The gelation temperature was determined through visual inspection. An aliquot of gel containing 3 milliliters was put to a test tube and submerged in water. With consecutive 1°C temperature increases, the samples' gel-forming point was visually assessed. Gel was supposed to have formed when the formulation's meniscus stopped moving after tilting through a right angle. To ensure that the measurement was repeatable, each preparation was put to the test three times.(Ashlesha et al. 2015.)

## **9.Optical Microscopy:**

Compound light microscopy was used to study the appearance of halloysite nanotube (HNT), Drug loaded HNT(F2) and lyophilized in-gel(F2G). The purpose of performing optical microscopy is to obtain a magnified view of the substance that is placed in it so that thorough examination of substance can be carried out. A small amount of the sample of HNT, F2, F2G were taken on a glass slide to analyze the structure further under microscope.

## **10.Stability Testing:**

Effect of ambient temperature and low temperature were evaluated for *in-situ gel*. Two batches of formulation F1, F2 and F3 were prepared. One batch of samples were kept in refrigerator at 4°C and another batch of samples was kept at room temperature(25±2°C) and humidity 60%±5. The samples were stored at both low temperature condition and ambient temperature condition for a month. (Ashlesha P.Pandit et al. 2015)

## **11.Fourier Transform Infrared Spectroscopy (FTIR)**

To determine if there is a drug-polymer relation, FTIR was used. To understand this relation individual IR spectra was determined for Drug, HNT, F2 and F2G.Scanning was performed over a range of 4500-400 cm<sup>-1</sup> for a duration of 3 minute. Using attenuated total reflectance (ATIR) method the samples were passed against a high refractive index prism and infrared spectrum was measured using infrared light that was totally internally reflected in the prism. The infrared radiation interacts with the sample, causing the chemical bonds in the drug and HNT and lyophilized in-situ gel to vibrate at different frequencies. The resulting absorption spectrum is recorded and analyzed to identify the functional groups present in the sample and to provide information about the drug-HNT and lyophilized in-situ gel interaction. (Vishwanath Abasaheb Borse et al. 2019) (Dure N. Iqbal et al. 2021)

## **12.Powdered X-Ray Diffraction analysis (PXRD)**

The primary purpose of XRD analysis is to ascertain the crystallographic structure of a substance. The X-ray Diffraction analysis of in-situ gel was done by preparing the samples to be analyzed. Drug sample was in powdered, drug sample was mounted in an eppendorf tube. The blank sample and in-situ gel sample were lyophilized, not grounded in order to prevent the gel structure from breaking. All the samples drug, blank and F2G were placed in the instrument's sample stage one by one. The atoms in the sample diffract the X-ray, generating a diffraction pattern that is captured by a detector. Using suitable XRD software, the diffraction pattern was analyzed samples were scanned at range of 2θ from 5° to 90°. (Ayensu et al. 2012)(Alqurshi et al. 2017)(Tang et al. 2010)

### **13. Resazurin microtiter-plate assay**

For determination of MIC of doxycycline hydiate loaded HNT, resazurin microtiter plate assay was used. Stock solution was prepared containing 2.5mg drug loaded HNT in 5ml of distilled water. 100  $\mu$ l of stock solution (500 ppm) was added in first sample well of microplate. Serial dilutions (13 dilutions) were prepared from 250 ppm to 0.0305 ppm in 96-well plate to get another 13 sample wells. 100  $\mu$ l of nutrient broth was then transferred in 14 sample wells of microtiter plate. 10 $\mu$ l of bacteria (*E. coli* k88 and *L. acidophilus* NCIM 2056) was added in each sample well. Blank was distilled water and positive control was nutrient broth and bacteria. Nutrient broth was taken as negative control. All wells were treated with 10 $\mu$ l of resazurin dye. Upon treatment 96 well plate was incubated in incubator for 24 hours at 37°C. The color change was then assessed visually. The growth was indicated by color changes from purple to pink (or colorless). The lowest concentration at which no color change occurred was taken as the MIC value.(Elshikh et al. 2016) (Chakansin et al. 2021)

### **14. Determination of minimum bactericidal concentration (MBC) of doxycycline hydiate loaded HNT**

The wells showing complete absence of growth in the MIC assay were identified and 10 mL of each well were transferred to nutrient agar plates. The agar plates were incubated with timetemperature profiles identical to that in disc diffusion assay. The well showing the complete absence of growth on agar plates was considered as the minimum bactericidal concentration (MBC). (Krishnan et al. 2015)

### **15. Thermogravimetric analysis (TGA) and Differential thermal analysis (DTA)**

The TGA-DTA test aims to see the process that occurs by a reduction in the weight of the composite during the heating time and temperature of 0-350°C. The DTA analysis method measures changes in the sample by heating it in a particular place with a specific temperature range of 0-350°C and time so that it experiences a decrease in its mass. TGA-DTA analysis was done by preparing the sample to be analyzed. Drug, blank sample and F2G were mounted inside

an eppendorf for testing. Blank sample and F2G were lyophilized before analysis. Samples were then analyzed under TGA-DTA instrument.

## **16. Antioxidant study**

F2, F1G, F2G, F3G formulations were soaked in 6.8 pH pbs buffer for 24 hours. After 24 hours samples in phosphate buffer were centrifuged for 15 minutes at 6000 rpm. 100 $\mu$ l of each sample stock solutions were pipetted out in microplate. 2-fold dilution of each stock solutions of samples were made upto 4 serial dilution (560 $\mu$ g/ml-70 $\mu$ g/ml). Ascorbic acid was used as positive control and DPPH solution as negative control. Distilled water was used as blank. 0.1mM solution of DPPH was prepared and 150 $\mu$ l was added to sample well, negative and positive control well. 96-well microplate was kept in dark for 30 minutes. The absorbance reading was taken in triplicate to minimize the error. (Lei & Zou et al. 2023)

## **17. Field emission scanning electron microscopy (FESEM)**

Field Emission Scanning Electron Microscopy (FESEM) is a high-resolution imaging technique used to visualize the surface morphology of materials at the nanoscale. The procedure begins with the preparation of the sample involving HNT, drug loaded HNT and lyophilized gel. Samples were clean, dry, and non-conductive. Non-conductive samples were coated with a thin layer of gold, to prevent charging under the electron beam. The sample is then placed on the sample holder and introduced into the FESEM chamber, where a vacuum is maintained. A field emission gun (FEG) generates a focused electron beam that scans the surface of the sample. Secondary electrons emitted from the sample's surface are detected to produce an image with high spatial resolution. By adjusting the accelerating voltage and working distance, images with different magnifications and contrast can be obtained. The FESEM allows for detailed examination of surface features, including topography, morphology, and composition, making it invaluable in materials science, nanotechnology, and biology. (Goldstein et al. 2017)

## **18. Transmission electron microscopy (TEM)**

Transmission electron microscopy (TEM) is another widely used technique for studying the morphology and internal structure of drug loaded HNT incorporated in an *in-situ* gel. For TEM study, a small amount of samples of HNT, F2 and F2G were prepared and dissolved in suitable solvent. It is diluted and deposited on a carbon-coated copper grid with micropipette. The solvent is then allowed to evaporate, leaving behind a thin-layer of samples on the grid. The grid is then placed in the TEM instrument, which is exposed to a beam of electrons at the accelerated voltage of 200kV. The electrons interact with the sample, producing an image that reveals the internal structure of the sample, HNT, F2 and F2G at a high resolution. (Yildirim et al. 2023)

## **19. In- Vitro drug release**

In a drug release study using an *in-situ* gel formulation, the gel is prepared and loaded with the HNT containing doxycycline hydiate. The drug-loaded gel is then placed inside a dialysis membrane, which acts as a semi-permeable barrier to allow the drug to diffuse out while retaining the gel matrix. The membrane containing the gel is immersed in a beaker filled with a release medium, 6.8 pH. phosphate-buffered saline (PBS). The beaker is maintained at a constant temperature, typically 37°C, to simulate physiological conditions. This was placed over a magnetic stirrer maintained at a speed of 50-100 rpm. The study was conducted for 8 hours, and aliquots of the release medium are periodically withdrawn to measure the amount of drug released from the gel into the solution. These aliquots are then analyzed using appropriate analytical techniques, such as UV-Vis spectrophotometry, to quantify the drug concentration, enabling the determination of the drug release profile from the in situ gel formulation. (Senarat et al. 2021)

## **20. Kinetics of release**

The kinetics of drug release from a medication delivery system can be described using various mathematical models. These models consider factors such as solubility, particle size, crystallinity, and the nature of the drug-encapsulating vector. Different models include zero-order, first-order, Higuchi, Korsmeyer-Peppas, and Hixon-Crowell, each with its own equation and release rate constant. The choice of model depends on the specific drug delivery system and its release characteristics. (Dash et al. 2010)

**The formulas for the release kinetics models are:**

1. Zero-order kinetics:  $Q = K_0 t + Q_0$
2. First-order kinetics:  $Q_t = Q_0 e^{-K_f t}$
3. Higuchi model:  $Q_t = K_H \sqrt{t} + Q_0$
4. Korsmeyer-Peppas model:  $Q/Q_0 = K_K t^n$
5. Hixon-Crowell model:  $(Q_0^{1/3} - Q_t^{1/3}) = K_S t$

$Q_t$  = amount of drug released

$Q_0$  = initial amount of drug released

$K_0, K_f, K_H, K_K, K_S$  = release rate constant

# Chapter 6: Results and Discussion

## **1.Melting Point Determination:**

According to IP melting point of a substance is defined as those points of temperature at which substance begins to melt and is completely melted except as defined otherwise for certain substance. Temperature recorded of Doxycycline hyclate was  $208.6^{\circ}\text{C}$  ( $n=3$ ).~ $201^{\circ}\text{C}$  is melting point of pure Doxycycline hyclate. The reported melting point is slightly higher than ideal melting point. Confirmation of melting point indicated the purity of the product.

*Table 4 Initial and final melting point*

INTIAL TEMPERATURE ( $^{\circ}\text{C}$ )	FINAL TEMPERATURE ( $^{\circ}\text{C}$ )
200	210
202	208
202	208

## **2.Standard curve of doxycycline hyclate in 6.8 pH phosphate buffer**

The UV absorbance of doxycycline hyclate standard solution in the range of  $2-20\mu\text{g/ml}$  of drug in pH. 6.8 showed linearity at  $\lambda_{\text{max}} 274.5\text{nm}$ . The regression coefficient should be near to 1 which was obtained from the calibration curve and the corresponding absorbance is shown in the table. The line equation for the phosphate buffer solution at pH 6.8 was found to be:  $Y=0.0277X+0.0076$  ( $R^2=0.9956$ ).

*Table 5 Calibration curve of DOH*

Concentration (ppm)	Absorbance
2	$0.055\pm0.0089$
4	$0.104\pm0.0174$
6	$0.154\pm0.0121$
8	$0.218\pm0.0082$
10	$0.267\pm0.0142$
12	$0.317\pm0.0108$
14	$0.368\pm0.0168$

16	0.450±0.0132
18	0.473±0.0040
20	0.563±0.0096

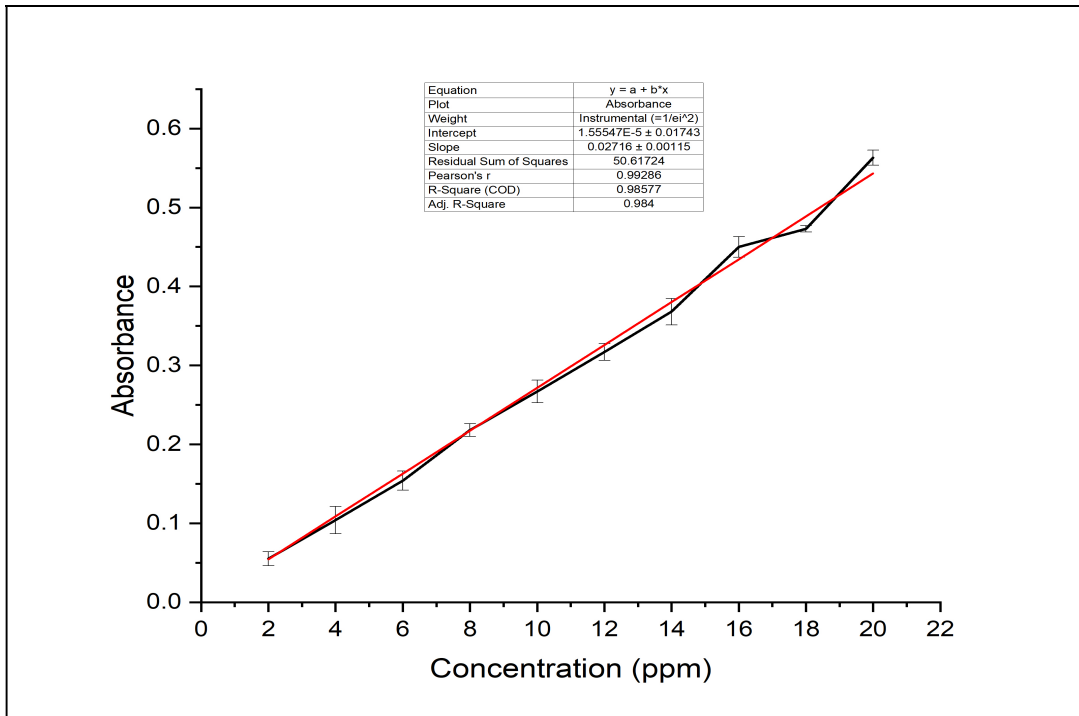


Figure 5 Calibration graph of DOH

### 3. pH determination of *in-situ* gel

The pH of the oral *in situ* gel is crucial for its stability and effectiveness. The method described here is a simple qualitative analysis. The experiment was repeated three times to ensure reproducibility and accuracy of the results of blank and F2 were found to be 7. While F1 and F2 formulations were found to have less than 7 pH. As all the formulations are under the range of saliva pH (6.2-7.6), all the formulation are suitable to be used in tooth cavity treatment. This also ensure safety, efficacy and tissue compatibility of the *in-situ* gel formulations.

It was ensured that the pH paper is not contaminated and is handled with clean hands or sterile tools. Fresh saliva was used for each measurement to ensure accuracy. The test was performed in a clean environment to avoid contamination. For more precise measurements, a pH meter should be used.

#### **4. Antibacterial assay:**

The antibacterial activity of Doxycycline hydiate was evaluated using a standard antibacterial test. This test measured the zone of inhibition formed around bacterial cultures treated with different concentrations of Doxycycline hydiate. Three representative bacterial strains were chosen: *L. acidophilus* and *L. casei* a common pathogen in biofilm formation associated tooth enamel loss and *Escherichia coli*, frequently encountered in bone and dental implant infections.

The diameter of the inhibition zone consistently increased with increasing Doxycycline hydiate concentration. Notably, the highest diameter of 2.3 cm was observed with 1000 microliters doxycycline hydiate treatment on *E. coli*, while *L. acidophilus* and *L. casei* 2.53 cm and 0.95 cm exhibited the largest zone of inhibition at 1000 microliters of doxycycline hydiate concentration.

F2 formulation having 1:1 ratio of Doxycycline hydiate showed promising zone of inhibition for all the bacterial strain chosen. Showing its better effectiveness in treating tooth related infections. An *in-situ* gel's good zone of inhibition is a positive indicator of its probable effectiveness in treating dental cavities. It implies that the gel can deliver focused, localized therapy and successfully encounter dangerous bacteria in the oral cavity.

#### **F1 Formulation:**

##### ***E. coli* K-88**

*Table 6 Zone of inhibition of F1 for E. coli K-88*

<b>Concentration (microliters)</b>	<b>Diameter (cm)</b>
1000	2.3
800	2.0

400	1.8
200	1.6
100	1.2
50	1.1
25	0.9

### *L.acidophilus* NCIM 2056

*Table 7 Zone of inhibition of F1 for L. acidophilus NCIM 2056*

Concentration (microliters)	Diameter (cm)
1000	2
800	1.8
400	1.7
200	1.6
100	1.4
50	1.23
25	1.33

### *L.casei* NCIM 2586

*Table 8 Zone of inhibition of F1 for L.casei 2586*

Concentration (microliters)	Diameter (cm)
1000	0.9
800	0.7
400	0.6
200	0.5
100	0.3
50	0.2
25	0

## **F2 Formulation:**

### **E. coli K-88**

*Table 9 Zone of inhibition of F2 E. coli K-88*

<b>Concentration (microliters)</b>	<b>Diameter (cm)</b>
1000	2.3
800	2.2
400	2.1
200	1.85
100	1.75
50	1.3
25	1.25

### **L.acidophilus NCIM 2056**

*Table 10 Zone of inhibition of F2 L. acidophilus NCIM 2056*

<b>Concentration (microliters)</b>	<b>Diameter (cm)</b>
1000	2.35
800	2.25
400	2.0
200	1.9
100	1.5
50	1.15
25	0.8

### **L.casei NCIM 2586**

*Table 11 Zone of inhibition of F2 L.casei NCIM 2586*

<b>Concentration (microliters)</b>	<b>Diameter (cm)</b>
1000	0.95
800	0.8
400	0.7
200	0.5
100	0
50	0
25	0

### **F3 Formulation:**

#### **E. coli K-88**

*Table 12 Zone of inhibition of F3 for E. coli*

<b>Concentration (microliters)</b>	<b>Diameter (cm)</b>
1000	1.95
800	1.8
400	1.6
200	1.55
100	1.2
50	1.1
25	0.85

## L.acidophilus NCIM 2056

*Table 13 Zone of inhibition of F2 L. acidophilus NCIM 2056*

Concentration (microliters)	Diameter (cm)
1000	2
800	1.95
400	1.9
200	1.75
100	1.7
50	1
25	0.9

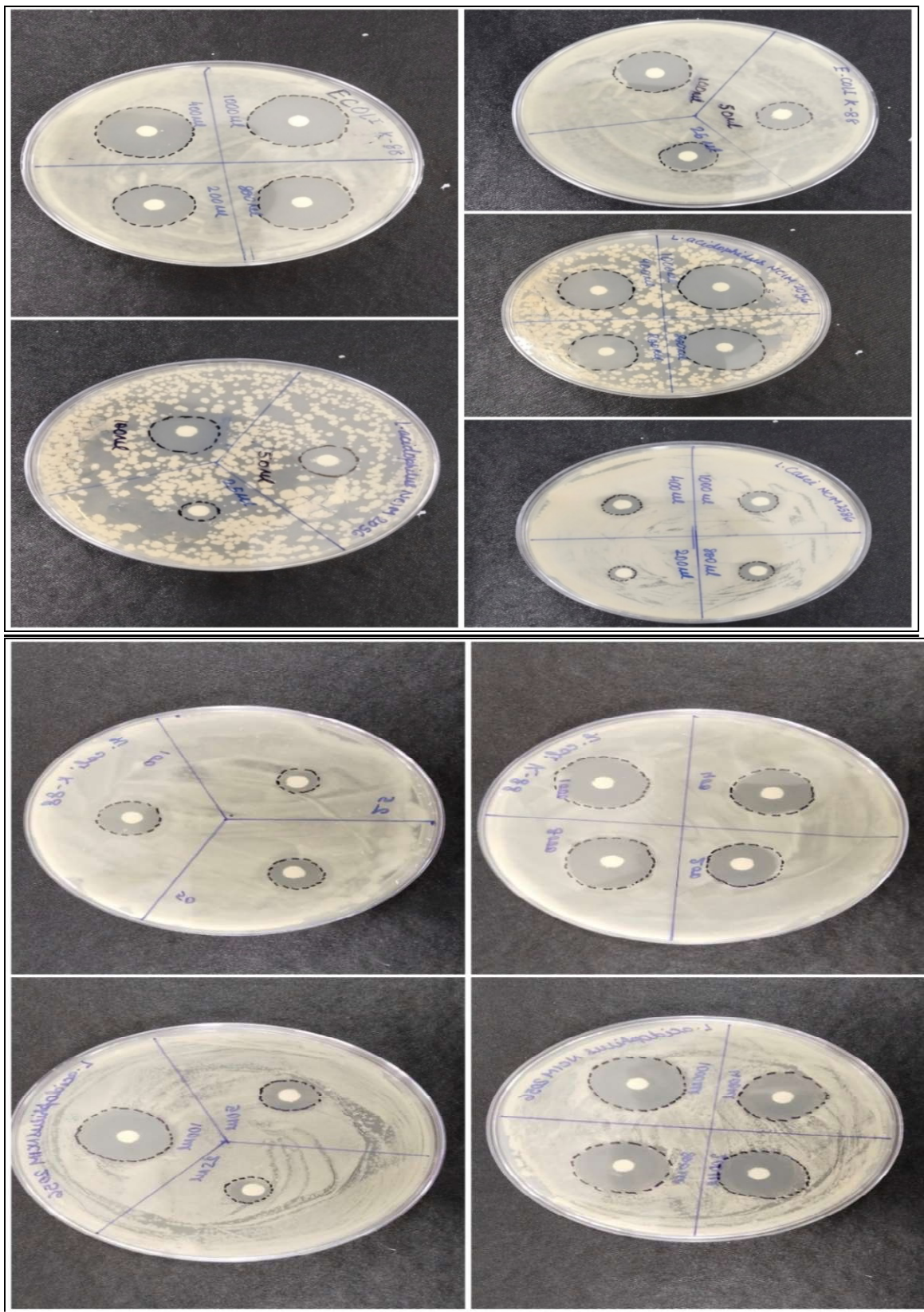


Figure 6 Zone of Inhibition of F1, F2, and F3

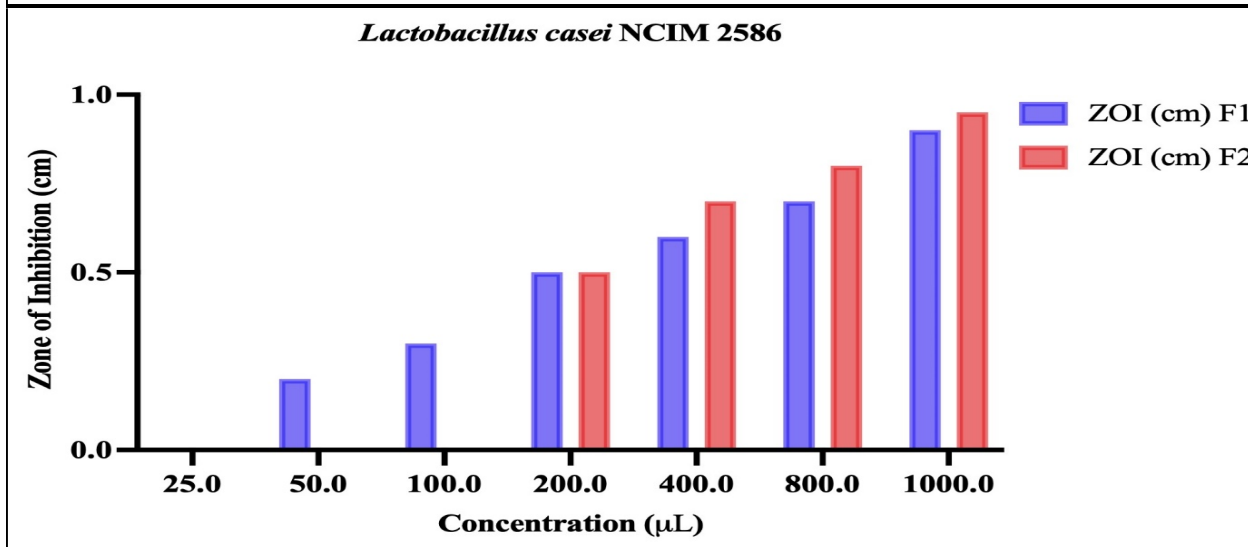
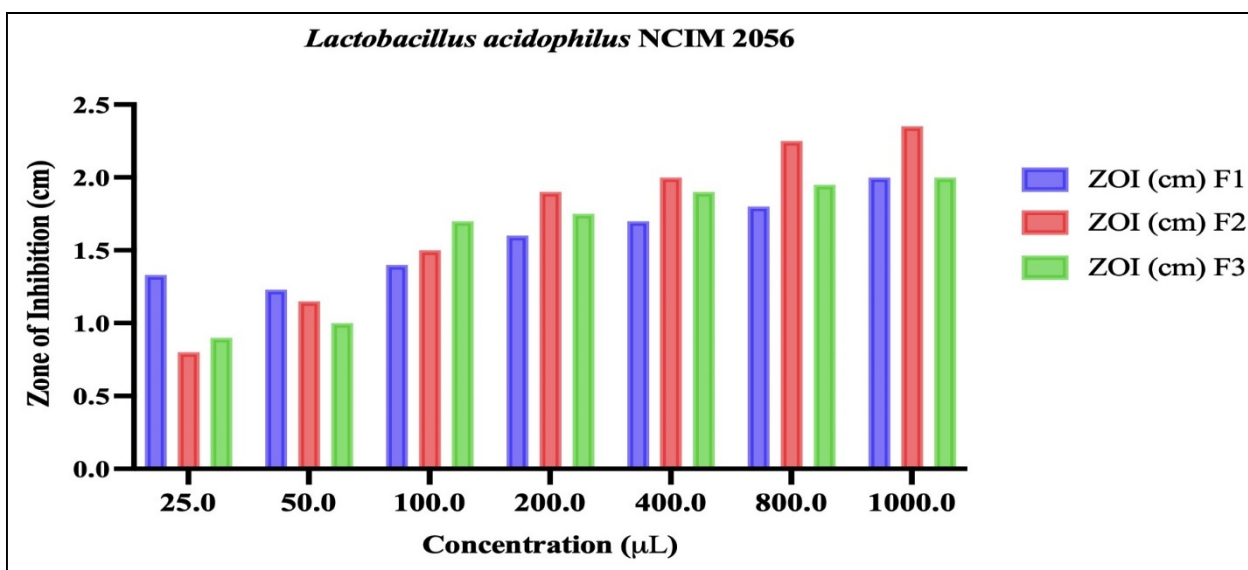
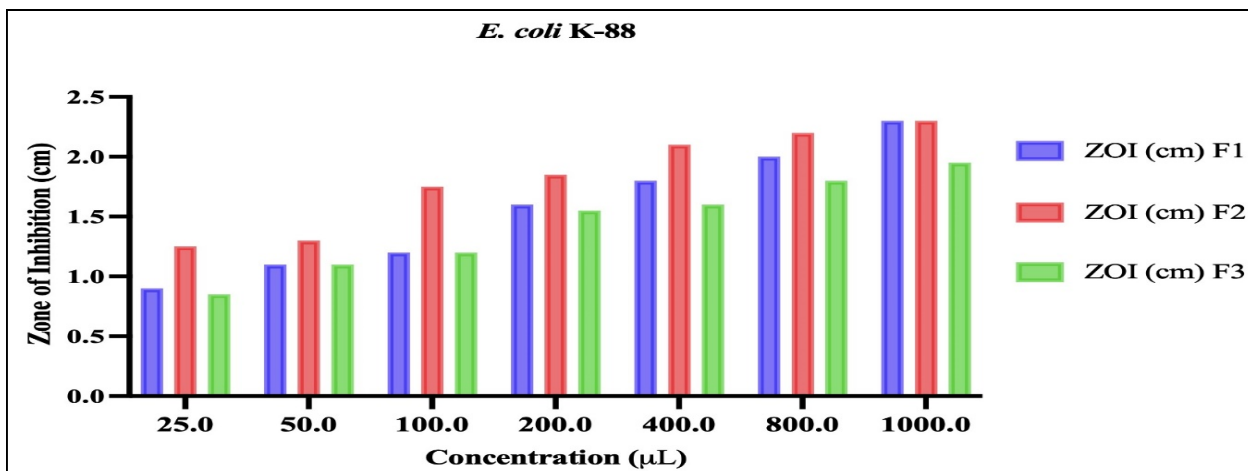


Figure 7 Graph of zone of inhibition of F1, F2, and F3

## **5.Spreadability:**

The spreadability index was determined over all samples of *the in-situ* gel including black(each formulation was tested for n=3 times for accuracy). The results indicated that the in-situ gel demonstrated a consistent spreadability index, suggesting that it spread efficiently under the given conditions.F3G showed promising spreadability followed by F2G formulation. The tooth cavities range from mm to cm depending on the level of severity. As the in-situ gel is able to show spreadability upto cm, hence showing efficient spreadability to cure dental carries.

The spreadability index values offer important information about how well the *in-situ* gel works for the intended use in the oral cavity. The gel's capacity to disperse uniformly throughout the intended area is indicated by the consistent spreadability index, which is essential for efficient drugadministration.

A high spreadability index which ensures that the treatment substance is evenly dispersed throughout the oral cavity, including difficult-to-reach locations like periodontal pockets, is beneficial.

*Table 14 Spreadability (cm) of F1, F2 and F3 samples*

<b>Formulation</b>	<b>Spreadability (cm) for 50g</b>	<b>Spreadability(cm) for 100g</b>	<b>Spreadability(cm) for 150g</b>
F1G	0.38±0.035	0.38±0.035	0.40±0
F2G	0.45±0	0.48±0.035	0.58±0.035
F3G	0.60±0.070	0.60±0.070	0.65±0.070
Gel	0.28±0.035	0.28±0.035	0.30±0

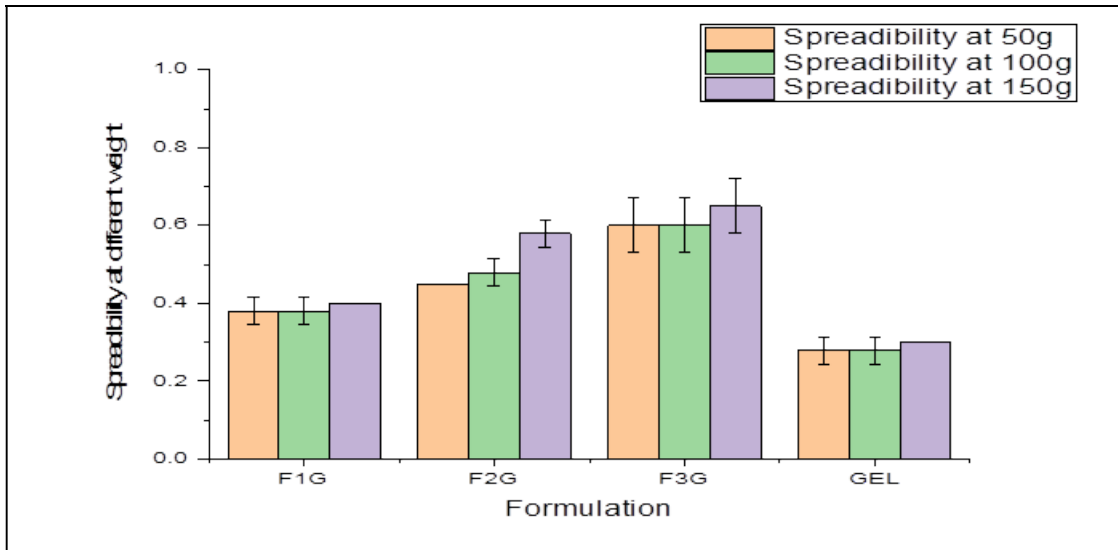


Figure 8 Graph of Spreadability of F1, F2, and F3

## **6.Swelling Index:**

The results showed that the *in-situ* gel exhibited a gradual increase in the swelling index over time then decreased and finally got constant. The swelling index values at 1, 2, 3, and 4 and 5 days were observed and it was concluded that gel started swelling on day 1 and showed sharp increase in water uptake capacity of gel, then decreased and finally became constant.

The increase in swelling index over time suggests that the *in-situ* gel is capable of absorbing fluid effectively, allowing it to swell and expand. This property is beneficial for the intended application, as it helps the gel to maintain contact with the oral cavity tissues, providing a sustained release of the active pharmaceutical ingredient. The consistent increase in the swelling index indicates that the gel's formulation is well-suited for use in the oral cavity. This is crucial for the treatment of periodontitis, as the gel must adhere to the targeted area to deliver the therapeutic agent directly to the site of infection or inflammation.

As seen that gel swelling capacity decrease and becomes constant it shows that the formulation will not cause discomfort and obstruction to oral cavity.

*Table 15 Swelling Weight of F1G, F2G and F3G sample for 1-5 days*

Formulation	Weight day 1 (mg)	Weight day 2 (mg)	Weight day 3 (mg)	Weight day 4 (mg)	Weight day 5 (mg)
<b>Blank</b>	295	340	324	261	260
<b>F1G</b>	247	284	243	243	242
<b>F2G</b>	189	309	266	252	252
<b>F3G</b>	222	249	210	169	169

*Table 16 Swelling degree of F1G, F2G and F3G samples*

Formulation	Swelling degree day 1	Swelling degree day 2	Swelling degree day 3	Swelling degree day 4	Swelling degree day 5
<b>Blank</b>	1436.5	1670.8	1587.5	1259.4	1254.2
<b>F1G</b>	1186.5	1379.1	1295.8	1165.6	1160.4
<b>F2G</b>	884.3	1509.3	1285.4	1212.5	1205.6
<b>F3G</b>	1056.3	1196.9	993.75	780.20	780.20

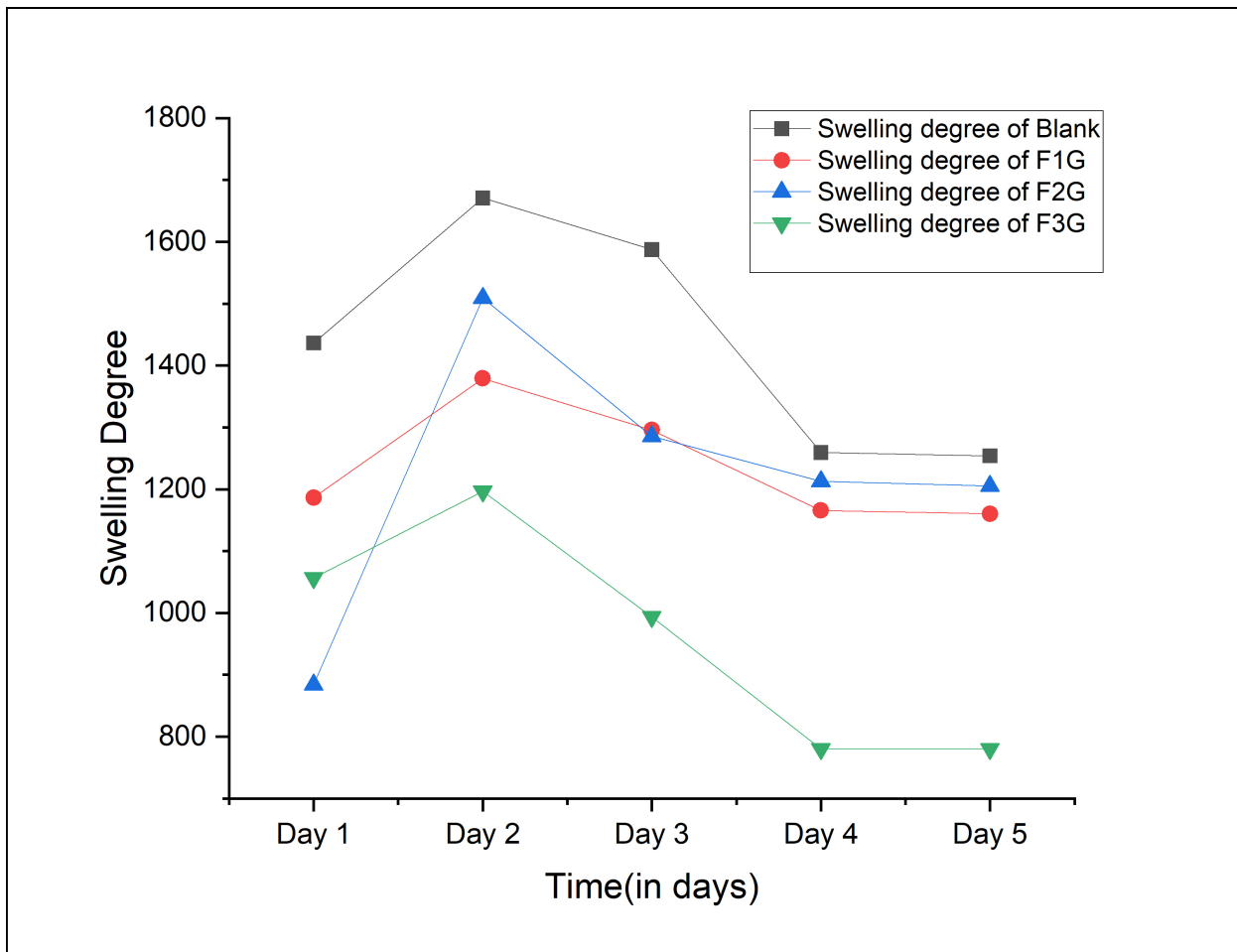
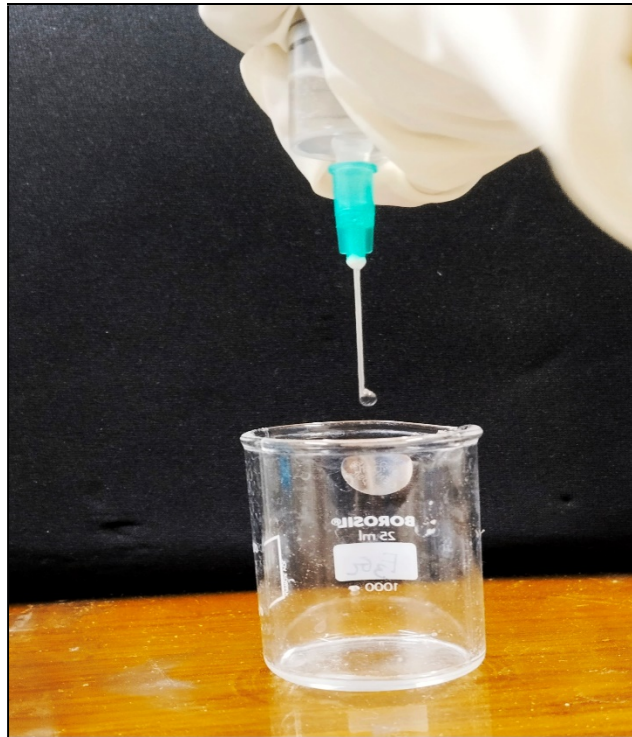


Figure 9 Graph of Swelling degree of F1, F2, and F3

## 7. Syringeability Test:

Dental gel should be liquid at storage temperature ( $25\pm2$ ) before gelling since the optimal gelation temperature range for dental gel is between  $33^{\circ}\text{C}$  and  $35^{\circ}\text{C}$ . If the liquid gel's gelation temperature is below  $33^{\circ}\text{C}$ , injection of the formulation becomes difficult and gelation occurs at room temperature. If the gelation temperature is higher than  $35^{\circ}\text{C}$ , the gel will remain liquid at physiological temperature, resulting in leaking from the periodontal pocket.

The gelation temperature of all the formulation from F1G to F2G was found to be under range of 33°C to 35°C. From Temperature 30 °C to 32°C the gel was in liquid state and they become gel with increase in temperature from 33 to 35 °C. A perfect gel was observed at the temperature 37°C.



*Figure 10 Syringability of in-situ gel*

## **8. Optical microscopy:**

Optical microscopy analysis was done at 100x magnification to observe the structure of HNT, drug loaded HNT and lyophilized *in-situ gel*. But it was difficult to observe the structure due to low magnification of trinocular microscope. The image exhibited a lump-like formation for HNT and F2 formulation. Tread-like structure was determined for the F2G formulation. Further characterization through SEM and TEM was helpful.

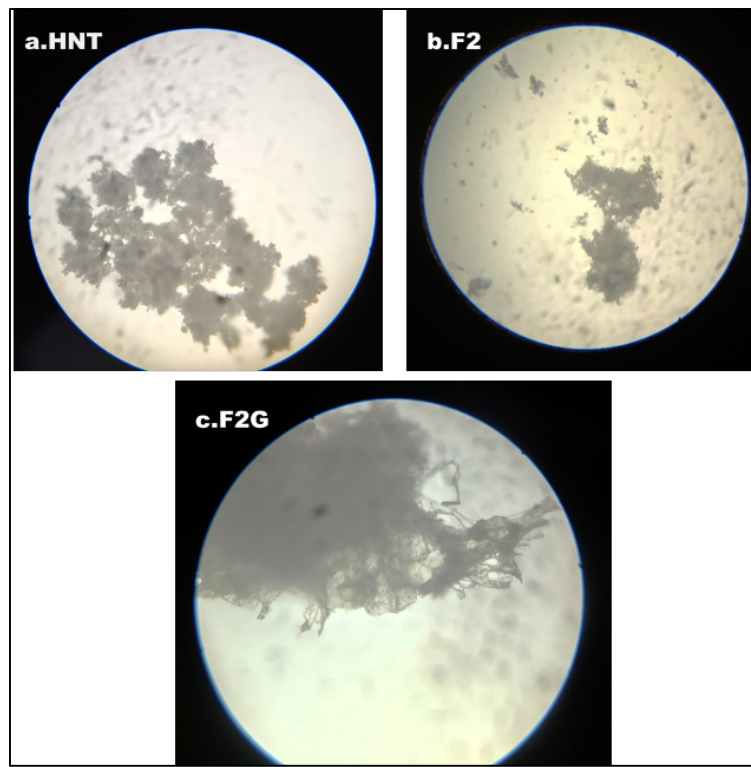


Figure 11 Optical microscopy images of the a.HNT b. F2 and c. F2G

## **9.Stability Testing:**

Stability testing for in situ gels for treating tooth cavities involves assessing the gel's performance and integrity under various conditions over a specified period. Stability testing is a crucial phase in the development of in situ gels for treating tooth cavities. This testing ensures the long-term efficacy, safety, and consistency of the gel under various environmental conditions.

The stability testing results for the in-situ gel for treating tooth cavities indicate that the gel stored at refrigerated conditions ( $4^{\circ}\text{C}$ ) remained stable, with no color change or contamination observed over the testing period. In contrast, the gel stored at room temperature ( $25\pm2^{\circ}\text{C}$ ) and humidity levels ( $60\%\pm5$ ) exhibited significant color change (reddish brown) and fungal growth. These findings suggest that the in-situ gel is sensitive to higher temperatures and humidity levels, resulting in decreased stability and potential risk of contamination. Therefore, it is recommended

to store the in-situ gel under refrigerated conditions (4°C) to maintain its quality, integrity, and safety over its shelf life.

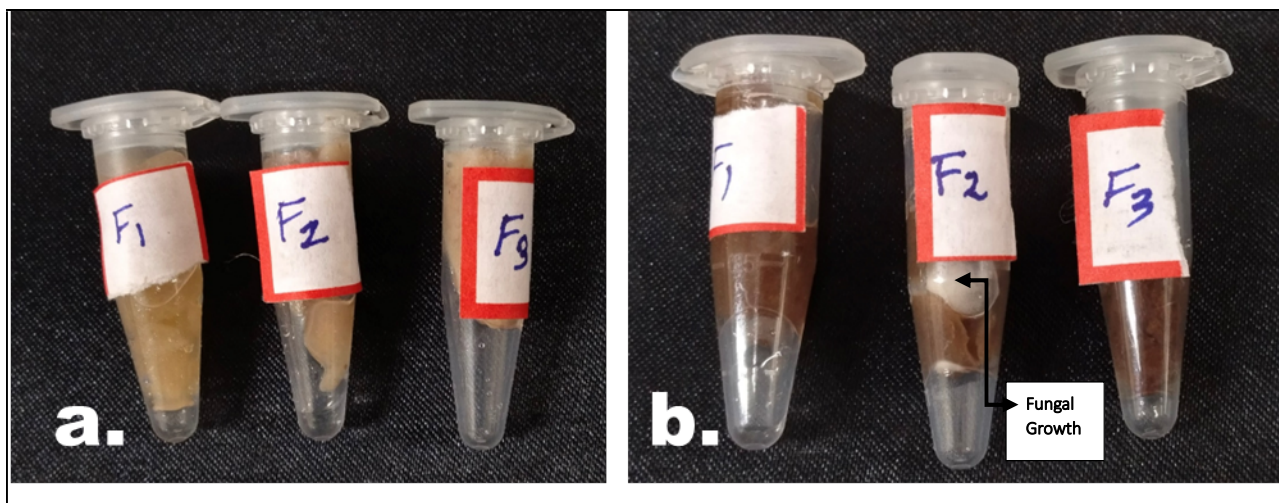


Figure 12 Stability testing of a. sample kept in refrigerated condition & b. sample kept at room temperature

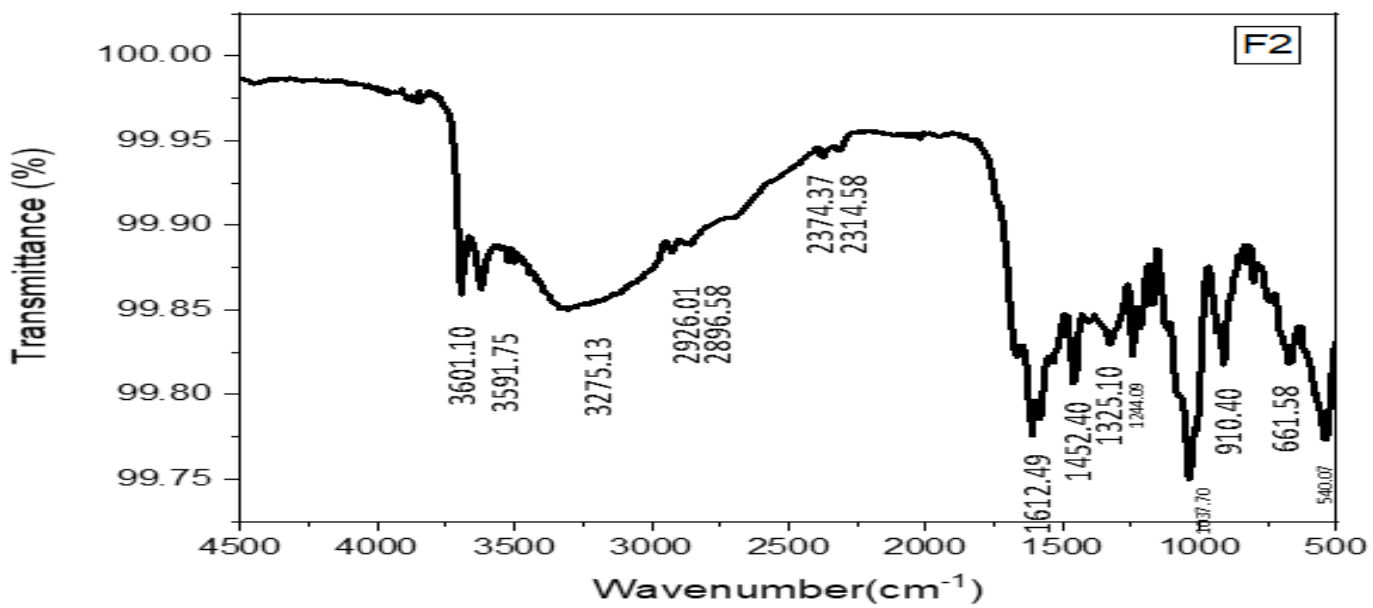
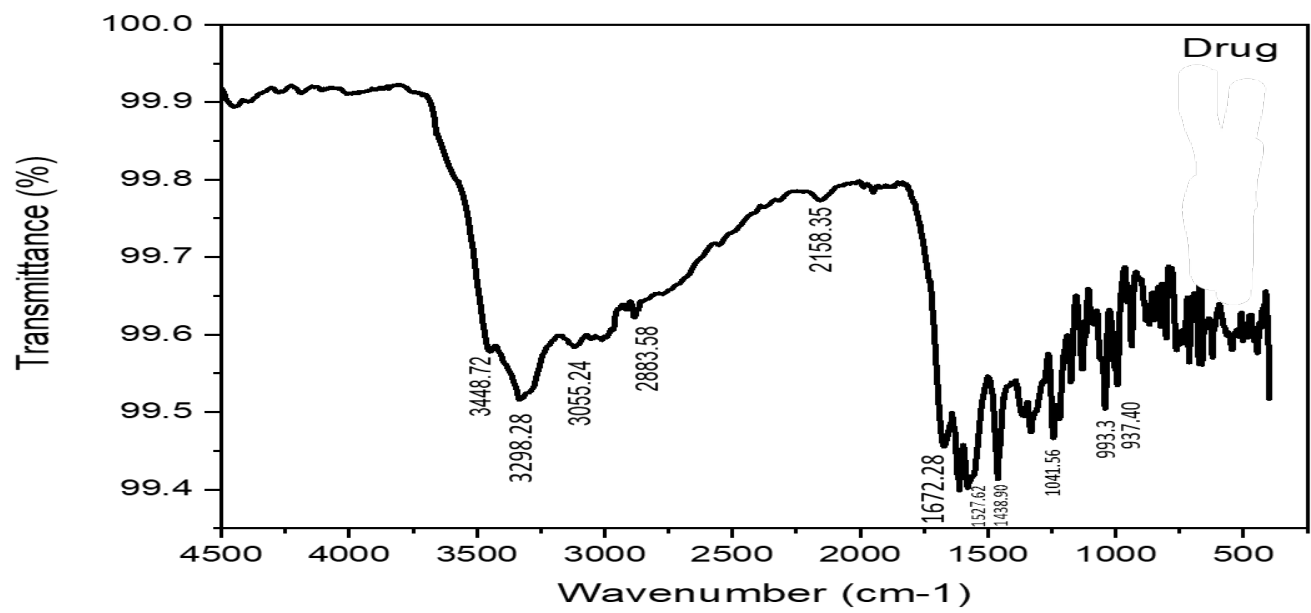
## **10. Fourier Transform Infrared Spectroscopy (FTIR)**

From the FT-IR studies, the characteristic bands for functional groups of drug Doxycycline hydralate were identified. A band was observed at 3298.28  $\text{cm}^{-1}$  which was corresponding to O-H group. A peak was observed at 1672.28  $\text{cm}^{-1}$  which denoted C=O. 1527.62  $\text{cm}^{-1}$  peak was corresponding to N-H group in doxycycline hydralate. In particular, the characteristic bands of Doxycycline hydralate at 1672.28  $\text{cm}^{-1}$  region related to the NH<sub>2</sub> group, which is known to interact with HCl, cause a decrease in transmittance intensity. The IR spectrum of drug shows a broad band between 3000 and 3500  $\text{cm}^{-1}$  of O-H str. and N-H str. at 3055.24  $\text{cm}^{-1}$ , C-H bend at 1438.90  $\text{cm}^{-1}$ , a strong signal at 1672.28  $\text{cm}^{-1}$  of C=O str, and C-O-H bend at 1438.90  $\text{cm}^{-1}$ .

HNT, the peaks at 3695.61 and 3624.25  $\text{cm}^{-1}$  are related to the Al-O-H stretching vibrations of the inner-surface hydroxyl groups and inner hydroxyl groups, respectively. Also, the peaks at the wave numbers of 752.24  $\text{cm}^{-1}$ , 1114.86  $\text{cm}^{-1}$  and 912.33  $\text{cm}^{-1}$  are assigned, respectively, to the Si-O-Al group, Si-O stretching and Al-O bending.

For sample F2, characteristic peaks were found at 3591.75 cm  $^{-1}$ , 3601.10 cm  $^{-1}$  corresponding to Al-OH stretching vibrations of halloysite nanotubes. There was a peak at 3601.10 cm  $^{-1}$  and 3591.75 cm  $^{-1}$  corresponding to the O-H stretching, which confirmed Doxycycline hydiate was loaded inside the lumen. Characteristic 2926.01 cm  $^{-1}$  and 2896.58 cm  $^{-1}$  this represents C-H stretching of Doxycycline hydiate. The peak 1612.49 cm  $^{-1}$  represents C=O stretching of amide group present in Doxycycline hydiate. The peaks at 1037.70 cm  $^{-1}$  suggest the presence of Si-O stretching vibrations, characteristic of halloysite nanotubes. Peaks at 910.40 cm  $^{-1}$  and 661.58 cm  $^{-1}$  are indicative of Al-O stretching vibrations, suggesting the presence of HNT.

For sample F2G, peaks at 2996.87 cm  $^{-1}$  may corresponds to Al-OH stretching vibrations of halloysite nanotubes or O-H stretching vibration of hydroxyl groups, possibly from chitosan. The peak at 2924.09 cm  $^{-1}$  and 2852.72 cm  $^{-1}$  are of C-H stretching vibrations, which are commonly found in organic compounds like chitosan. The peak appearing as 2924.09 and 2852.72 represents C-H stretching vibrations of drug doxycycline hydiate. Peak 1028.06 cm  $^{-1}$  represents C-O stretching vibration of doxycycline hydiate. The peak at 516.92 cm  $^{-1}$  may be due to Si-O-Si bending vibrations of halloysite nanotubes.



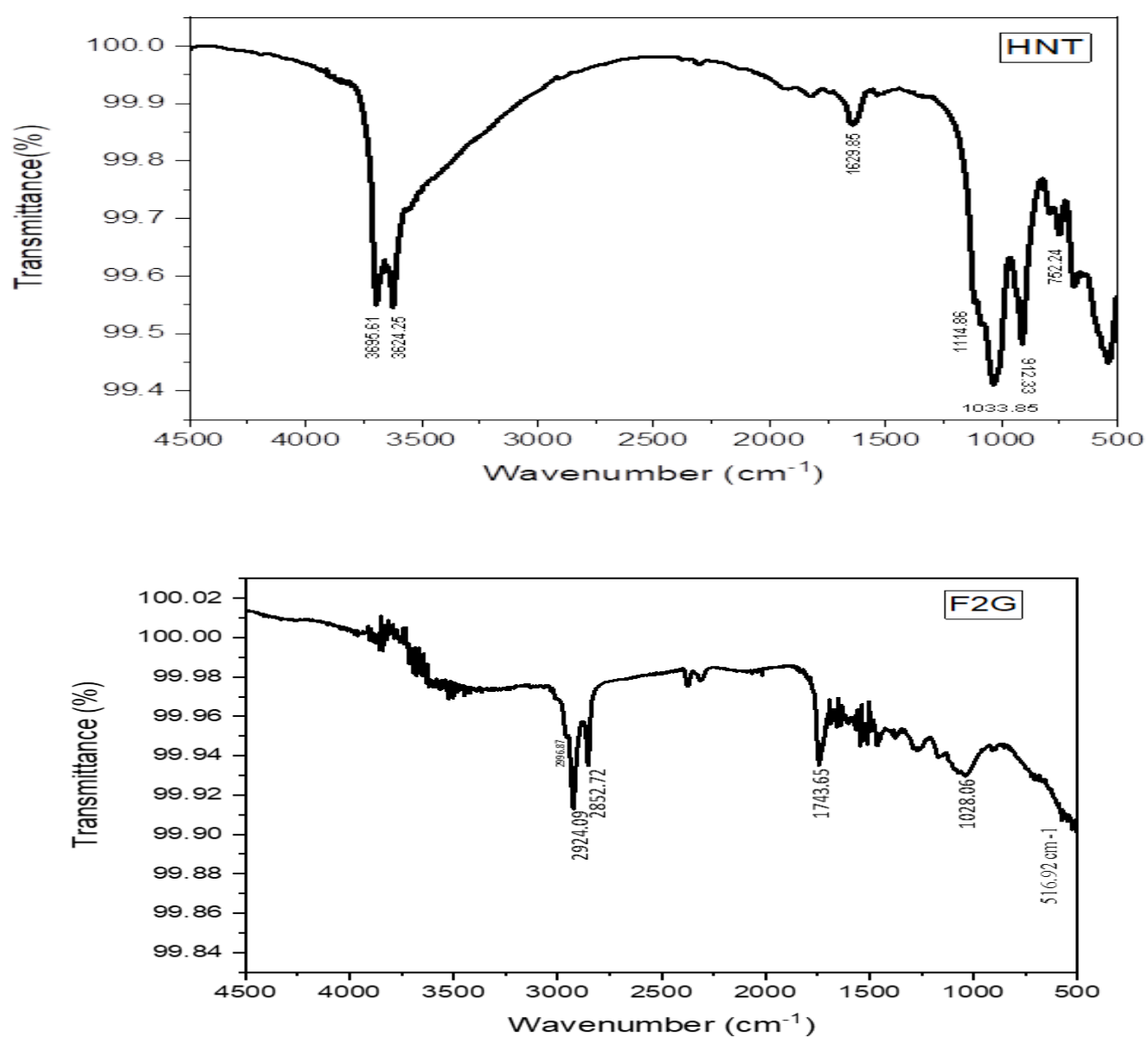


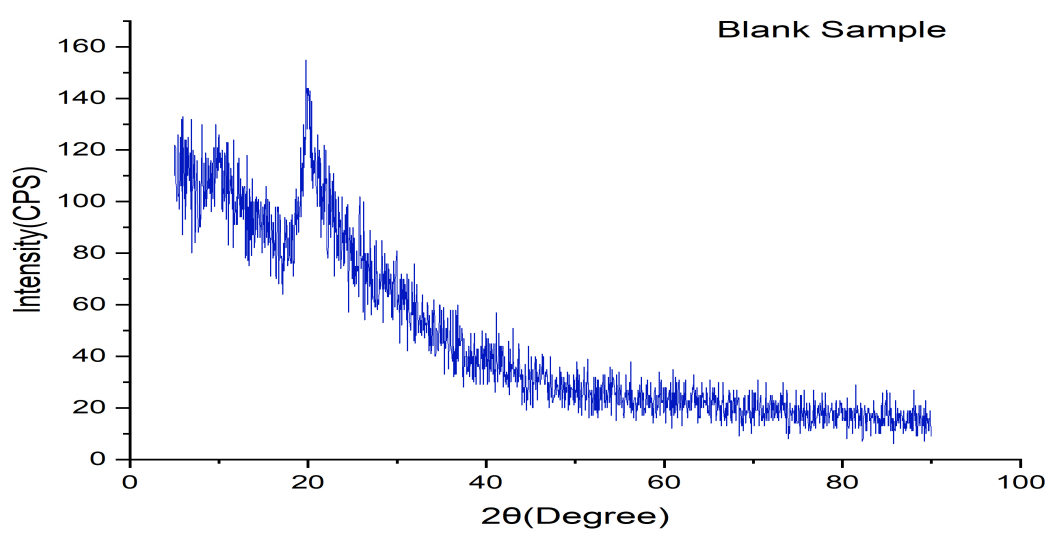
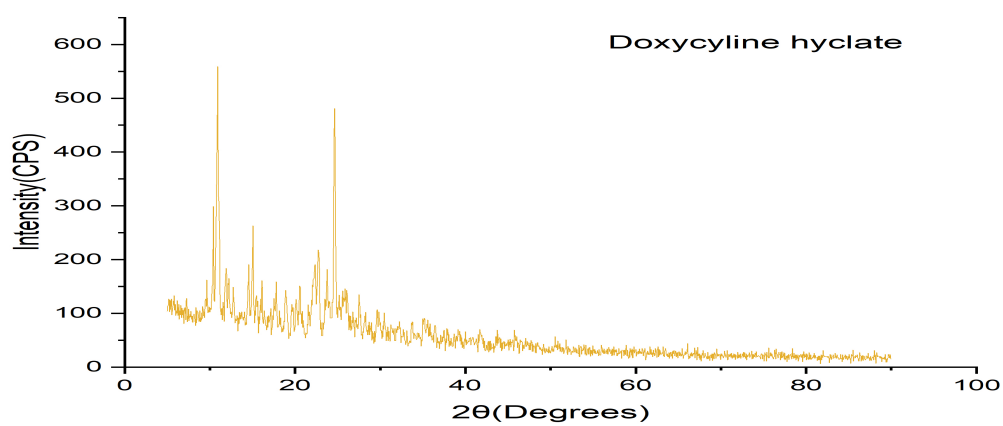
Figure 13 FTIR graph of Blank, F2, HNT and F2G

## **11. Powdered X-ray diffraction (PXRD)**

X-ray diffraction (XRD) is a powerful technique used to analyze the structure of materials at the atomic or molecular level. When applied to lyophilized gels, XRD provides valuable insights into their crystalline or amorphous nature, as well as their internal structure. By measuring the scattering of X-rays as they interact with the gel sample, we can determine the arrangement of molecules within the gel matrix, aiding in understanding its physical properties and potential applications.

For drug sample of doxycycline hydiate, peaks were observed at  $11.9^\circ, 15.05^\circ, 22.75^\circ, 27.5^\circ$  and most intense peaks were observed at  $2\theta$  of  $10.9^\circ$  and  $24.65^\circ$  showing crystalline nature of the drug. For the blank sample, peaks were observed at  $2\theta$  of  $9.65^\circ$  and  $19.75^\circ$ , which are characteristic peaks obtained from chitosan polymer. For F2G sample, peaks of  $10.15^\circ$  and  $22.7^\circ$  represent the presence of chitosan. A peak is observed around  $19.95^\circ$  which is characteristic peak of HNT nanotube. At  $10.15^\circ$  and  $24.6^\circ$  the intensity of peak has been decreased which were peaks of doxycycline hydiate showing the reduction of crystalline nature of drug. When in-situ gel was lyophilized containing drug, chitosan and HNT, decrease in number and intensity of peaks were observed. This shows that crystalline nature of drug and excipients decreased, resulting in formulation being more amorphous.

The XRD analysis indicates that the formulation containing doxycycline hydiate, chitosan, and HNT undergoes a reduction in crystallinity after lyophilization. The decrease in intensity of F2G formulation also suggests that successful loading of drug inside nanotube was done. Hence XRD analysis confirms the amorphous nature of F2G formulation due to decrease in the intensity of diffraction pattern. We can also conclude as the formulation is amorphous in nature and the drug is uniformly dispersed in matrix.



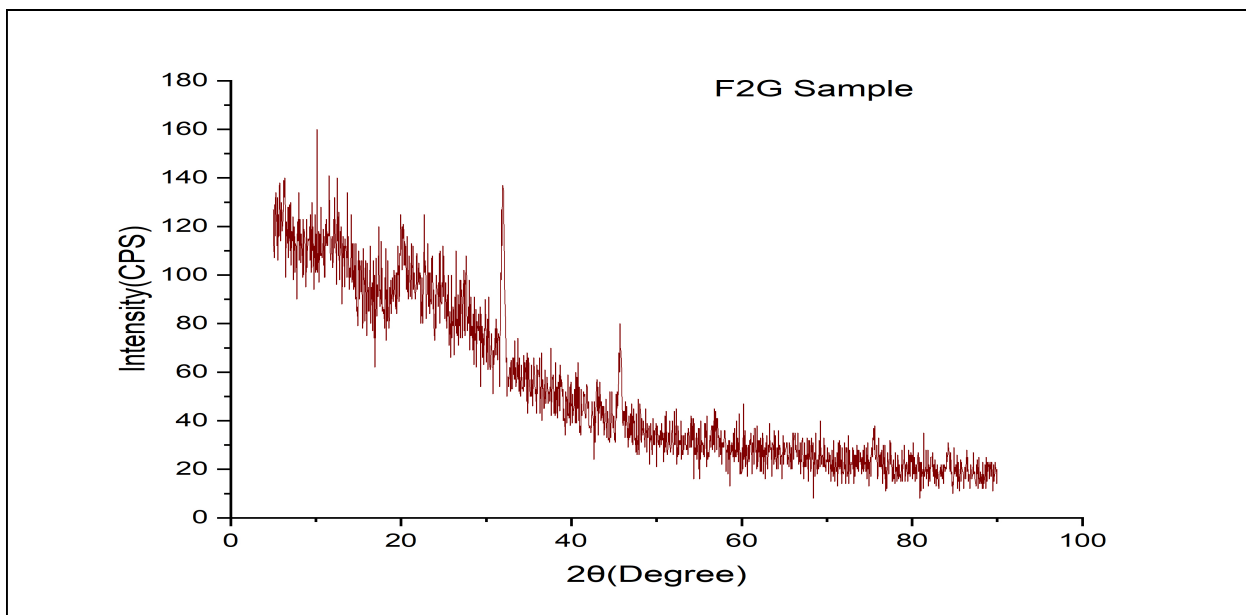


Figure 14 XRD graph of DOH, Blank, F2G

## **12. Resazurin microtiter-plate assay**

Determining the minimum inhibitory concentration (MIC) for doxycycline hydulate (DCH) loaded onto halloysite nanotubes (HNTs) is an important step in evaluating the effectiveness of this drug delivery system. For *E. coli* strain MIC reported was 0.98  $\mu\text{g}/\text{ml}$ -0.49 $\mu\text{g}/\text{ml}$ . For *L. acidophilus* reported MIC was 7.812 $\mu\text{g}/\text{ml}$ -3.91 $\mu\text{g}/\text{ml}$  for doxycycline hydulate loaded HNT. The reported minimum inhibitory concentrations (MICs) for doxycycline hydulate (DCH) loaded onto halloysite nanotubes (HNTs) indicate significant antibacterial activity against both *E. coli* and *L. acidophilus*. For the *E. coli* strain, the MIC range of 0.98  $\mu\text{g}/\text{ml}$  to 0.49  $\mu\text{g}/\text{ml}$  demonstrates a potent inhibitory effect, suggesting that DCH-loaded HNTs are highly effective at low concentrations against this Gram-negative bacterium. This low MIC range highlights the potential of the nanotube delivery system to enhance the efficacy of doxycycline, likely due to improved drug stability, sustained release, and increased local drug concentration at the site of bacterial action.

Conversely, the MIC range for *L. acidophilus*, a Gram-positive bacterium, is broader, from 7.812 $\mu\text{g}/\text{ml}$  to 3.91 $\mu\text{g}/\text{ml}$ , indicating that higher concentrations of DCH-loaded HNTs are required to achieve inhibition in some cases. This variability could be attributed to differences in

cell wall structure and drug permeability between Gram-positive and Gram-negative bacteria. The higher MIC values for *L. acidophilus* suggest that while the DCH-loaded HNTs are still effective, they may need to be administered at higher doses or optimized further to enhance delivery efficiency to this bacterial type.

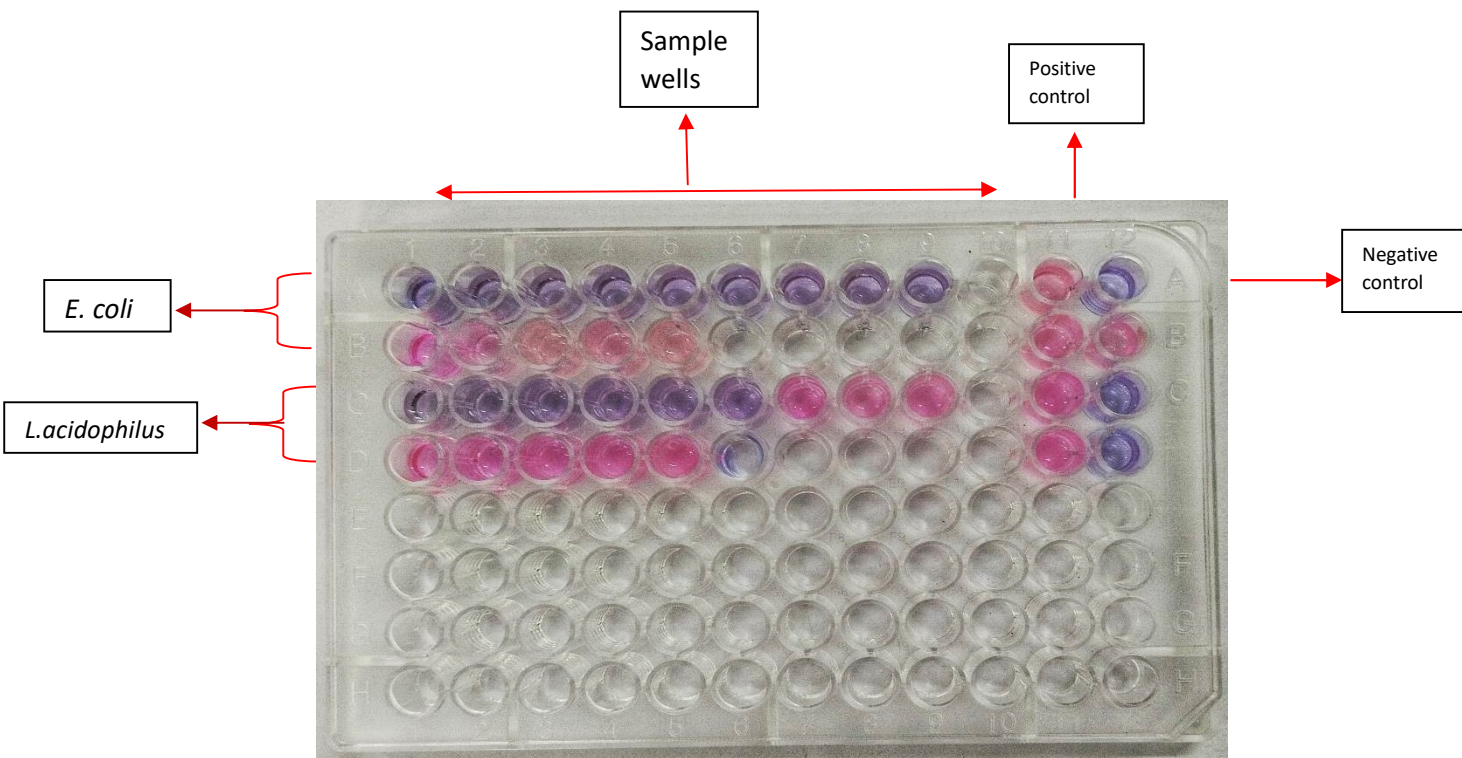


Figure 15Resazurin assay

### 13. Determination of minimum bactericidal concentration (MBC) of doxycycline hydulate loaded HNT

The determination of the minimum bactericidal concentration (MBC) of doxycycline hydulate (DCH) loaded onto halloysite nanotubes (HNTs) provides valuable insights into the bactericidal efficacy of this drug delivery system. The MBC is the lowest concentration of an antibacterial agent required to kill a particular bacterium. This measure complements the minimum inhibitory

concentration (MIC) by indicating the concentration at which bacterial cells are not only inhibited but also killed.

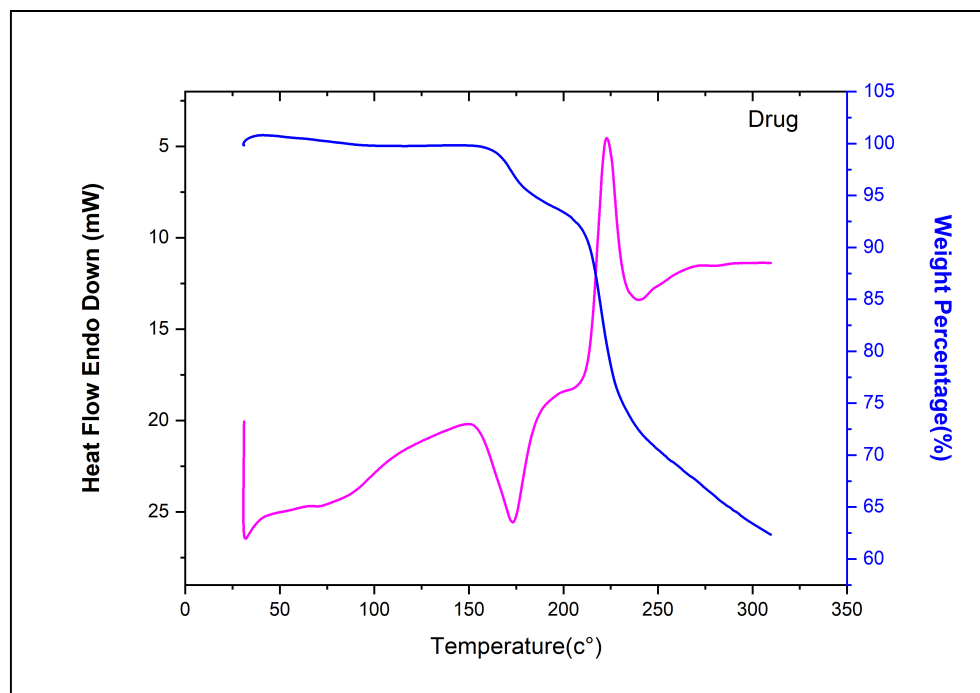
For *E. coli* MBC reported was 0.049 $\mu$ g/ml for doxycycline hydiate loaded HNT. MBC of 0.049 $\mu$ g/ml for DCH-loaded HNTs against *E. coli* indicates a highly effective bactericidal action, showcasing the advantages of using halloysite nanotubes for enhanced drug delivery.

#### **14.Thermogravimetric analysis (TGA) and Differential thermal analysis (DTA)**

Drug DOH showed one endothermic peak 172.57°C and one exothermic peak at 222.49°C for TGA. The endothermic peak for DOH was due loss of water. The exothermic peak of DOH was due to oxidative decomposition or combustion of organic compounds. The exothermic peak obtained for blank sample was 43.24°C which was probably due to breakage of cross-linking between chitosan and sodium- $\beta$  glycerol phosphate hydrate, along with breaking of hydrogen bond and release of water molecule. The TGA data obtained for F2G gave two exotherms 42.39°C and 190.08°C. First exotherm of 42.39°C might be due to breaking of crosslinking of *in situ* gel and release of water molecule. The second exotherm 190.08°C might be due to further decomposition of DOH, chitosan and sodium- $\beta$  glycerol phosphate hydrate.

DTA data obtained for drug DOH shows 99.4746804% degradation at 160.72°C and substantial 92.5188203% degradation at 206.08°C. This percentage of weight loss might be due to decomposition of drug and its further degradation with increase of heat. For blank sample two percentage loss of weight was observed, 101.177638% at 35.82°C and another of 83.2305905 at 212.91°C. The first weight loss maybe due to evaporation of water molecule from gel. And another weight loss observed might be due to degradation of chitosan and sodium- $\beta$  glycerol phosphate hydrate. DTA data received for F2G sample showed percentage weight loss of

102.188941% at 38.04°C which might be due to release of water molecule. Another percentage weight loss was observed of 98.7503717% at 213.62°C which probably was due to degradation of DOH, chitosan and sodium- $\beta$  glycerol phosphate hydrate.



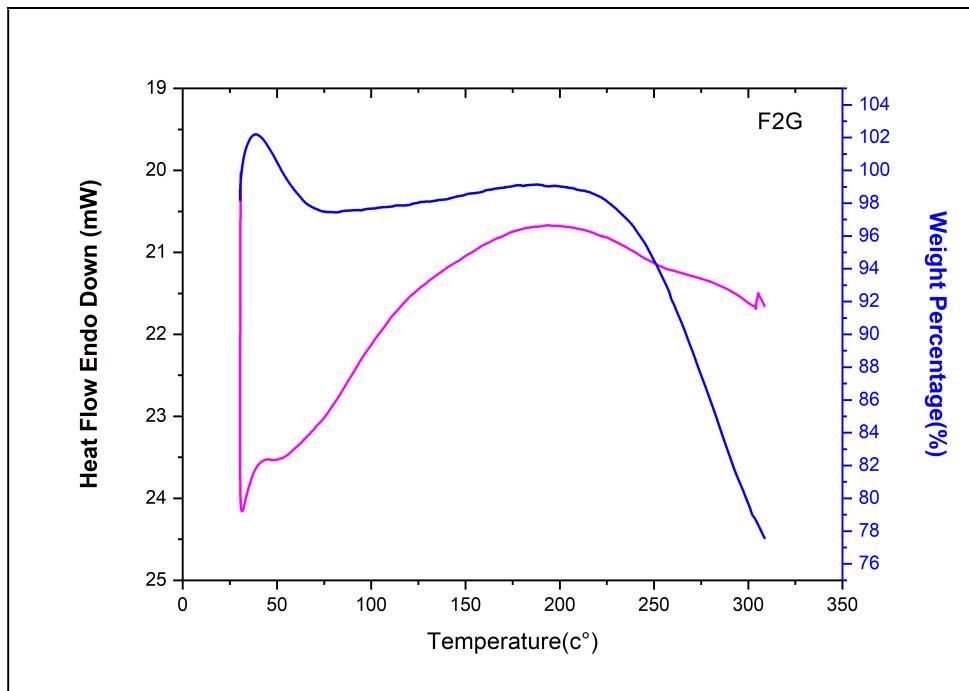
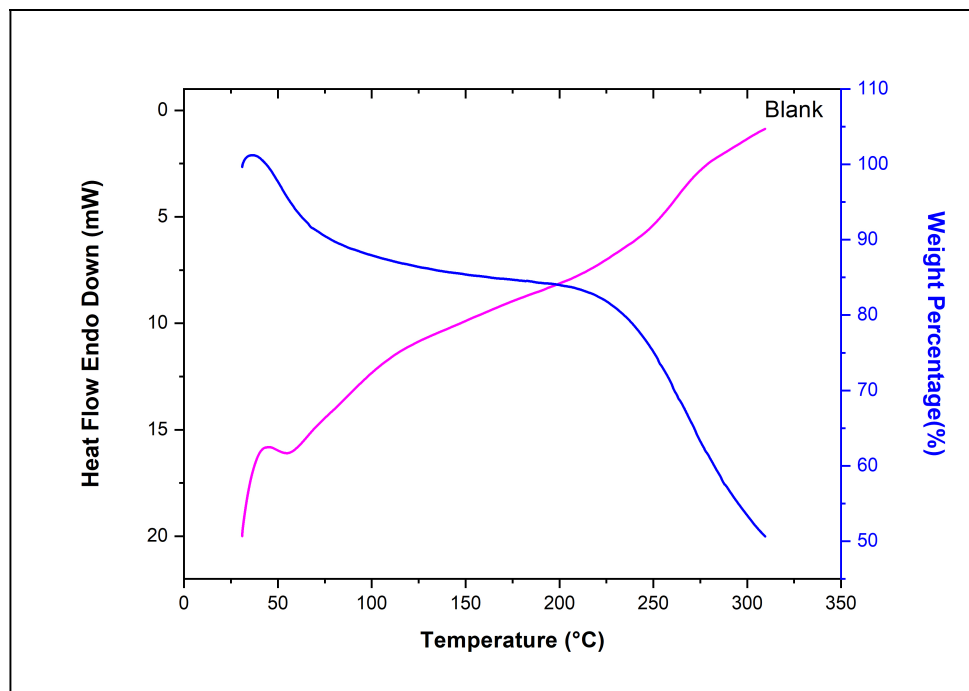


Figure 16 TGA and DTA graph of drug, Blank and F2G

## **15. Antioxidant Study**

The 2,2-diphenyl-1-picrylhydrazyl (DPPH) assay is a popular technique for determining a substance's antioxidant potential. The DPPH assay, which relies on the color change from violet to yellow as the DPPH radical is reduced by an antioxidant, is a commonly used technique for determining the antioxidant capacity of different compounds. The test is a common choice for antioxidant evaluation in research and industry because to its simplicity, speed, and sensitivity.

DOH may directly scavenge superoxide but not hydrogen peroxide. It also prevents the recognized oxidative stress product malondialdehyde-acetaldehyde (MAA)-adducts from forming. Treating chronic inflammatory diseases may benefit from DOH's reduction of oxidative stress since it lowers inflammation. Loading DOH inside HNT prevents degradation of DOH antioxidant property and enhance its potential as well promote control release.

High antioxidant potential of F2 formulation suggest it to be a potent antioxidant (180%-20.39%). Formulation F1G, F2G and F3G are having antioxidant potential between (75% - 2.20%). Chitosan and HNT allow sustain release of DOXH. But a decrease in antioxidant potential was observed for the in-situ gel due to encapsulation effect and increase viscosity due to MMW chitosan. Due to this availability and concentration of DOXH decreases which is available for antioxidant activity.

### **Formulation=F2**

*Table 17 Antioxidant % of F2 sample*

<b>Concentration(ppm)</b>	<b>Absorbance (nm)</b>	<b>Antioxidant %</b>
560	0.994967	180%
280	0.42230	78.15%
140	0.394967	73.14%
70	0.209033	38.70%
35	0.11010	20.39%

## Formulation=F1G

Table 18 Antioxidant % of F1G sample

Concentration(ppm)	Absorbance (nm)	Antioxidant%
560	0.4068	75.33%
280	0.3687	68.28%
140	0.3425	63.46%
70	0.2558	47.37%
35	0.0141	2.61%

## Formulation=F2G

Table 19 Antioxidant % of F2G sample

Concentration(ppm)	Absorbance(nm)	Antioxidant %
560	0.4028	74.59%
280	0.3416	63.26%
140	0.2261	41.87%
70	0.164266	30.42%
35	0.0119	2.20%

## Formulation=F3G

Table 20 Antioxidant % of F3G sample

Concentration(ppm)	Absorbance (nm)	Antioxidant %
560	0.458333	84.87%
280	0.324533	60.09%
140	0.227733	42.17%
70	0.199533	36.95%
35	0.061633	11.41%

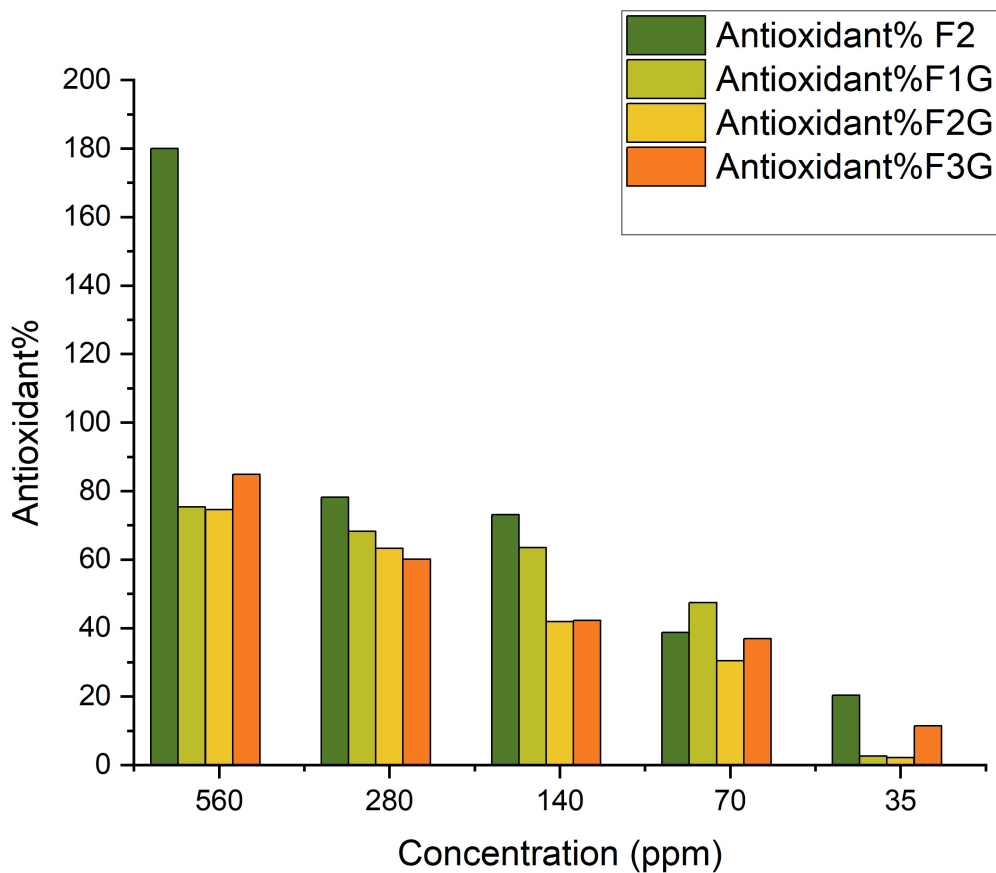
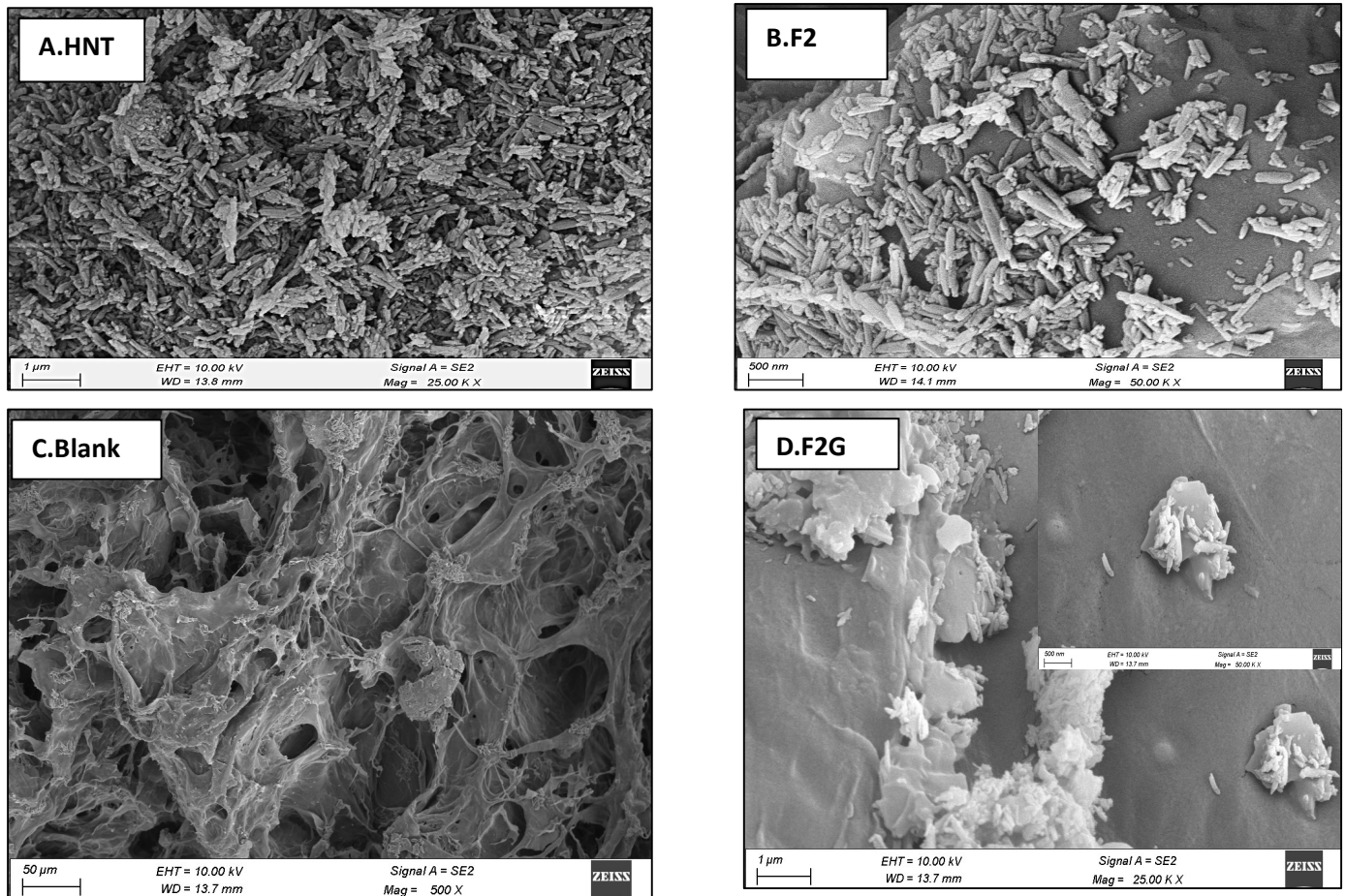


Figure 17 Graph of Antioxidant assay

## **16. Field emission scanning electron microscopy (FESEM)**

FESEM analysis was done to study the morphological structure of halloysite nanotubes, blank sample, and freeze-dried samples (F2 and F2G). Halloysite showed clear tubular shapes of the nanotubes. FESEM images in micrometer for halloysite was able to show tubular shapes of nanotubes. The FESEM images of freeze-dried samples of halloysite with DOH revealed drastic changes in the morphology of both halloysite and pure drug. Within freeze dried samples F2 dried solid mass of DOH were possibly embedded as because of smooth surface of halloysite were not seen after adhesion of drug molecules. The plate like structure for freeze dried samples

appeared. After loading of the drug solution within nanotubes, when they were dried by freeze drying, they came up with a very thin flake like appearance which we scratched to get the samples. The images of freeze-dried samples recorded as smooth surface, plate-like structures. The freeze-dried sample of blank sample appears as network-like structure, representing the gel matrix. The F2G freeze dried sample shows gel network as well as a plate-like structure which are HNT nanotubes. These nanotubes are clearly visible at nanometer range.



*Figure 18 SEM images of A. HNT, B. F2, C. Blank, and D. F2G*

## **17. Transmission electron microscopy (TEM)**

TEM analysis was studied to get more structural information of halloysite nanotubes and drug loaded into it. Hollow tubular structures of nanotubes were clearly observed having variable lengths. TEM image of the sample F2 showed that the tubular structure of halloysite nanotubes was observed clearly and also there was presence of globular structures in its inner lumen which gave evidence that the DOH had been successfully loaded into the lumen of the halloysite nanotubes. For F2G the structure of nanotube is not visible clearly, suggesting incorporation of DOH loaded HNT nanotube in gel matrix.

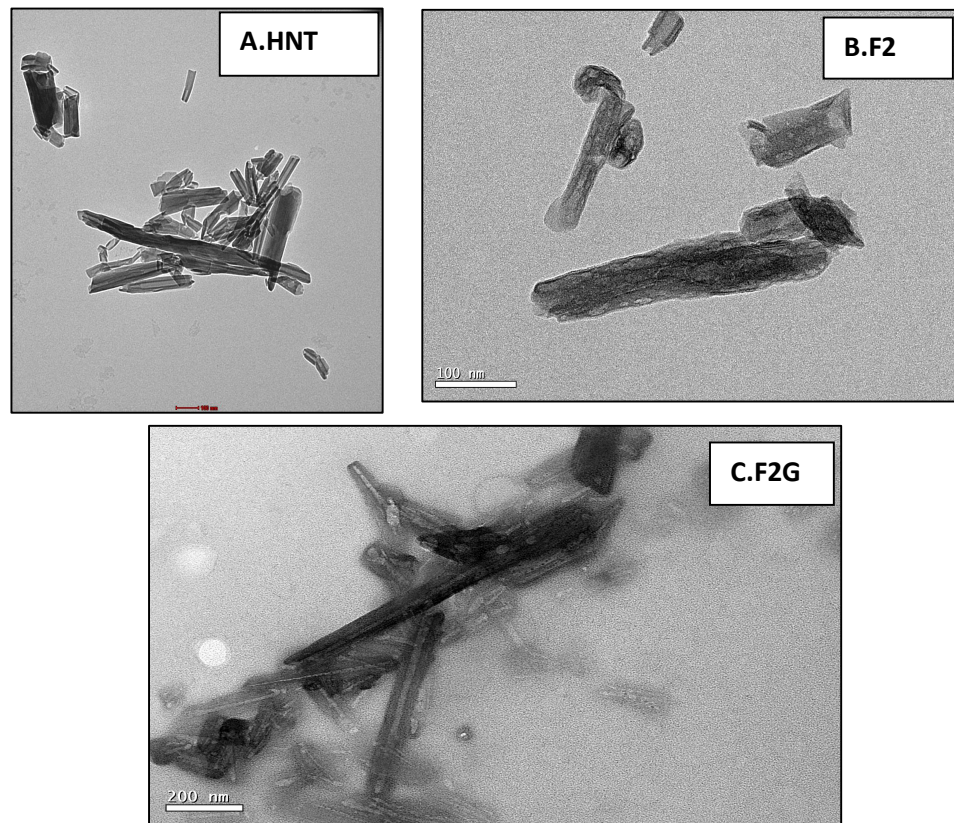


*Figure 19 TEM images of A. HNT, B. F2, C. F2G*

## 18. *In-vitro*

We carried out *in-vitro* release study for formulation F1, F2 and F3 samples. The study was conducted for 8 hours and it was observed 79.35%, 46.39% and 50.07% percentage of drug was released from F1, F2 and F3 formulation respectively. From the data collected it can be concluded that the formulation has a prolong effect as well as sustained release. The results suggest that both the concentration of HNT and the drug play a crucial role in determining the drug release profile. Formulation F1, with a lower drug content and higher HNT content, shows a more rapid and complete release compared to F2 and F3.

All three formulations demonstrate a controlled release profile, which is desirable in drug delivery systems for maintaining therapeutic levels over an extended period.

For formulations aimed at sustained release, the balance between the drug and HNT concentrations must be optimized. Formulation F1 is more suitable for a scenario where a faster release is needed, while F2 and F3 would be better suited for applications requiring a more prolonged release.

*Table 21 %CDR calculation for F1 formulation (n=3)*

Time	Absorbance	Concentration(µg)	Cumulative amount in 100 ml	Cumulative concentration in mg	Cumulative % drug release
1	0.4575	16.24187726	1624.187726	1.624187726	16.24187726
2	1.0815	38.76895307	3876.895307	3.876895307	38.76895307
3	1.266	45.42960289	4542.960289	4.542960289	45.42960289
4	1.56	56.0433213	5604.33213	5.60433213	56.0433213
5	1.6865	60.6101083	6061.01083	6.06101083	60.6101083
6	1.9115	68.73285199	6873.285199	6.873285199	68.73285199
7	2.015	72.46931408	7246.931408	7.246931408	72.46931408
8	2.2055	79.3465704	7934.65704	7.93465704	79.3465704

*Table 22 %CDR calculation for F2 formulation (n=3)*

Time	Absorbance	Concentration(µg)	Cumulative amount in 100ml	Cumulative concentration in mg	Cumulative % drug release
1	0.393	13.9133574	1391.33574	1.39133574	9.2755716
2	0.953	34.1299639	3412.99639	3.41299639	22.75330927
3	1.1085	39.74368231	3974.368231	3.974368231	26.49578821
4	1.36	48.82310469	4882.310469	4.882310469	32.54873646
5	1.4735	52.92057762	5292.057762	5.292057762	35.28038508
6	1.672	60.0866426	6008.66426	6.00866426	40.05776173
7	1.7605	63.28158845	6328.158845	6.328158845	42.18772563
8	1.935	69.58122744	6958.122744	6.958122744	46.38748496

*Table 23 %CDR calculation for F3 formulation (n=3)*

Time	Absorbance	Concentration(µg)	Cumulative amount in 100ml	Cumulative concentration in mg	Cumulative % drug release
1	0.4315	15.3032491	1530.32491	1.53032491	7.651624549
2	1.21	43.40794224	4340.794224	4.340794224	21.70397112
3	1.522	54.67148014	5467.148014	5.467148014	27.33574007
4	2.033	73.11913357	7311.913357	7.311913357	36.55956679
5	2.2145	79.67148014	7967.148014	7.967148014	39.83574007
6	2.499	89.94223827	8994.223827	8.994223827	44.97111913
7	2.5995	93.57039711	9357.039711	9.357039711	46.78519856
8	2.7815	100.1407942	10014.07942	10.01407942	50.07039711

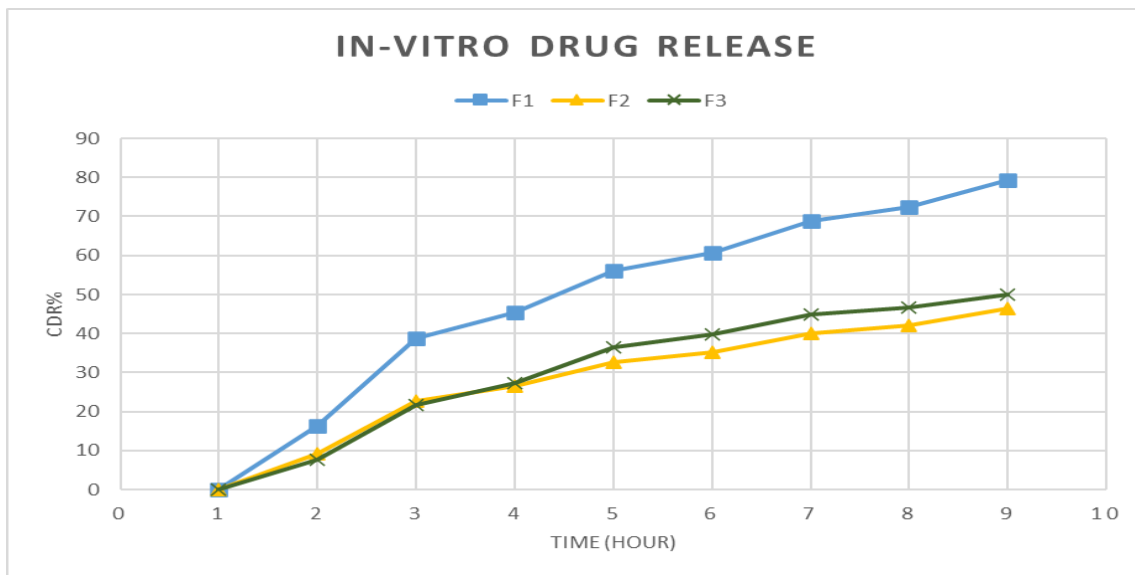


Figure 20 In-vitro drug release Graph

## 19. Drug Release

The release kinetics of the HNT-loaded doxycycline hydrate (DOH) in situ gel formulations (F1, F2, F3) were evaluated using several mathematical models: Zero Order, First Order, Hixson-Crowell, Higuchi, and Korsmeyer-Peppas. The aim was to determine the mechanism of drug release from the gel matrices.

The release data were fitted into various kinetic models to understand the drug release mechanism.

**1. Zero Order:** The  $R^2$  values for Zero Order kinetics were 0.9378, 0.9365, and 0.9263 for F1, F2, and F3, respectively. This suggests a relatively poor fit, indicating that the drug release is not concentration-independent.

**2. First Order:** The  $R^2$  values were the highest for First Order kinetics, with values of 0.9887, 0.9683, and 0.9634 for F1, F2, and F3, respectively. This indicates that the drug release is concentration-dependent, with a greater amount of drug released initially, tapering off as the concentration decreases over time.

**3.Hixson-Crowell:** The  $R^2$  values were lower for this model (0.8435, 0.8393, and 0.8226 for F1, F2, and F3, respectively), suggesting that the model does not describe the release mechanism well, which implies that the drug release is not solely governed by the dissolution of the drug particles.

**4.Higuchi:** The  $R^2$  values for Higuchi kinetics were 0.9819, 0.9805, and 0.9790 for F1, F2, and F3, respectively. This suggests that drug release is likely controlled by diffusion through the gel matrix, which is consistent with the observed sustained release profile.

**5.Korsmeyer-Peppas:** The  $R^2$  values were moderately high (0.9134, 0.9085, and 0.9000 for F1, F2, and F3, respectively). Since all the  $n$  values are between 0.5 and 1, the drug release from all three formulations follows a **non-Fickian (anomalous) diffusion mechanism**. This indicates that the release mechanism involves a combination of drug diffusion and polymer relaxation

The release of doxycycline hydiate from the HNT-loaded in situ gels follows a First Order kinetic model most closely, indicating that the release rate is concentration-dependent. The high  $R^2$  values for the Higuchi model suggest that diffusion through the gel matrix also plays a significant role in drug release.

<b>Code</b>	<b>Zero order</b>	<b>First order</b>	<b>Hixon-Crowell</b>	<b>Higuchi</b>	<b>Krosmeyer-Peppas</b>	
	$r^2$	$r^2$	$r^2$	$r^2$	$r^2n$	
<b>F1</b>	0.9378	0.9887	0.8435	0.9819	0.9134	0.601
<b>F2</b>	0.9365	0.9683	0.8393	0.9805	0.9085	0.604
<b>F3</b>	0.9263	0.9634	0.8226	0.9790	0.9000	0.669

Table 24 Calculation of Zero order kinetics

Time	CDR%F1	CDR%F2	CDR%F3
1	16.24188	9.275572	7.651625
2	38.76895	22.75331	21.70397
3	45.4296	26.49579	27.33574
4	56.04332	32.54874	36.55957
5	60.61011	35.28039	39.83574
6	68.73285	40.05776	44.97112
7	72.46931	42.18773	46.7852
8	79.34657	46.38748	50.0704

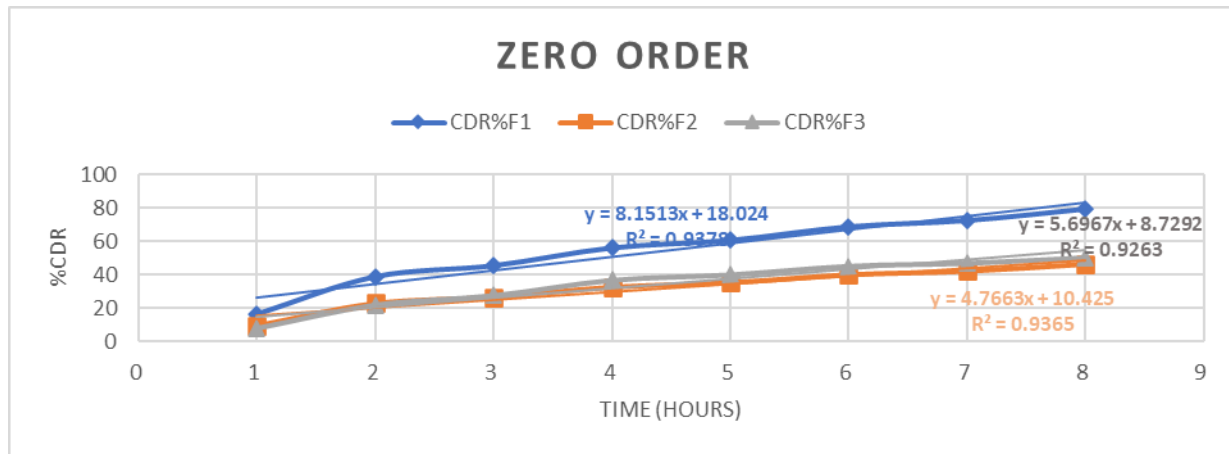


Figure 21 Zero order drug release graph

Table 25 Calculation of First order kinetics

Time (Hr)	Log %DR F1	Log %DR F2	Log %DR F3
1	1.923027	1.957724	1.965429
2	1.786972	1.88788	1.89374
3	1.736957	1.866312	1.861321
4	1.643025	1.82899	1.802366
5	1.595385	1.811036	1.779339
6	1.495088	1.777733	1.740591
7	1.439817	1.76202	1.726032
8	1.314992	1.729266	1.698358

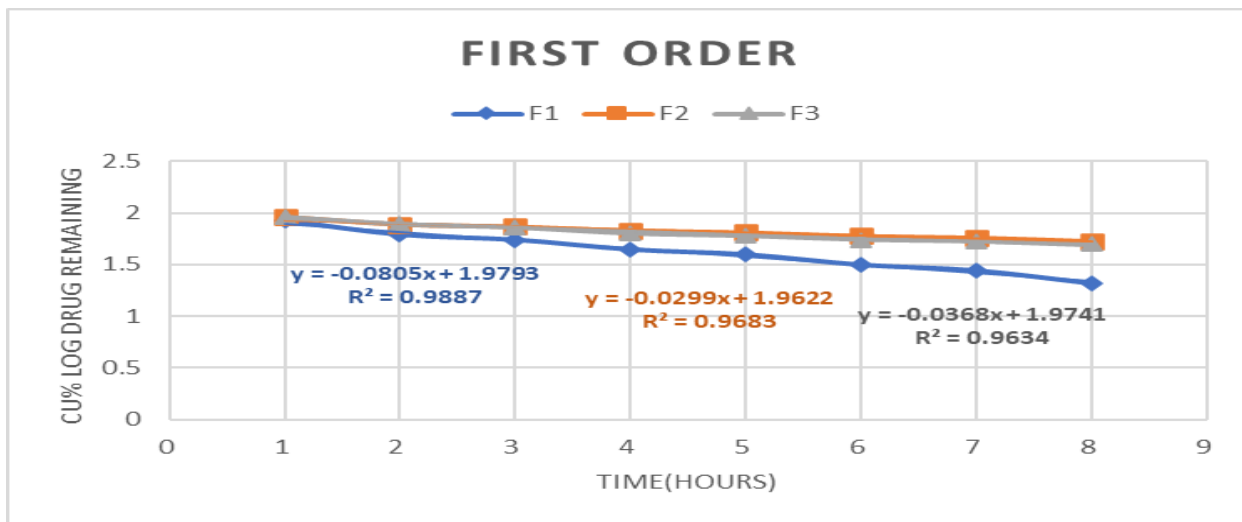


Figure 22 First order drug release graph

Table 26 Calculation of Hixon Crowell model kinetics

Time	Cube Root of %CU of F1	Cube Root of %CU of F2	Cube Root of %CU of F3
1	2.532476	2.101101	1.970537
2	3.384501	2.833663	2.789415
3	3.568176	2.981208	3.012384
4	3.826849	3.192847	3.318947
5	3.928092	3.279778	3.415264
6	4.096266	3.421597	3.556132
7	4.169187	3.481198	3.60332
8	4.297106	3.59308	3.68576

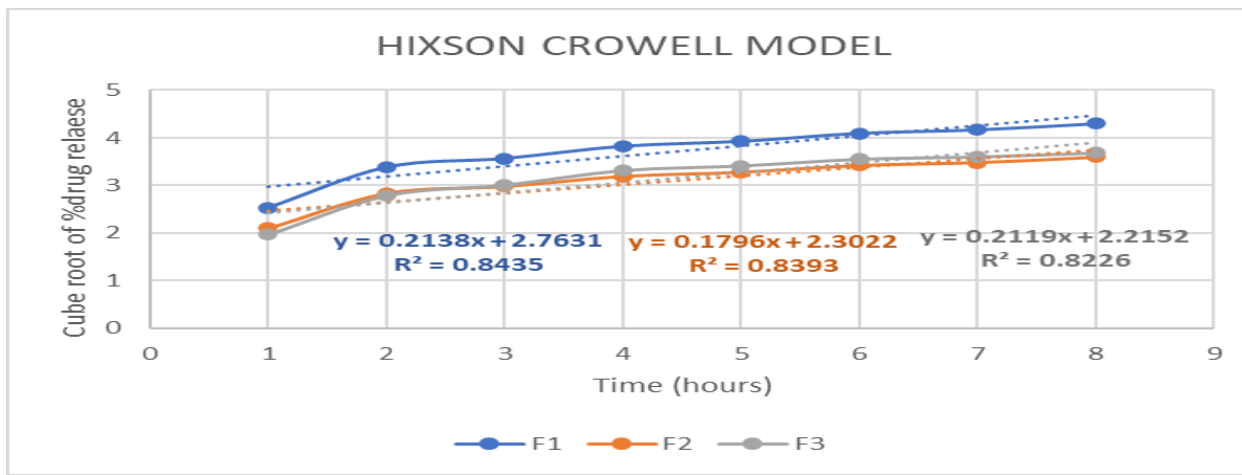


Figure 23 Hixon Crowell drug release graph

Table 27 Calculation of Higuchi model kinetics

Time	Sq.Time	%CU F1	%CU F2	%CU F3
1	1	16.24188	9.275572	7.651625
2	1.414214	38.76895	22.75331	21.70397
3	1.732051	45.4296	26.49579	27.33574
4	2	56.04332	32.54874	36.55957
5	2.236068	60.61011	35.28039	39.83574
6	2.44949	68.73285	40.05776	44.97112
7	2.645751	72.46931	42.18773	46.7852
8	2.828427	79.34657	46.38748	50.0704

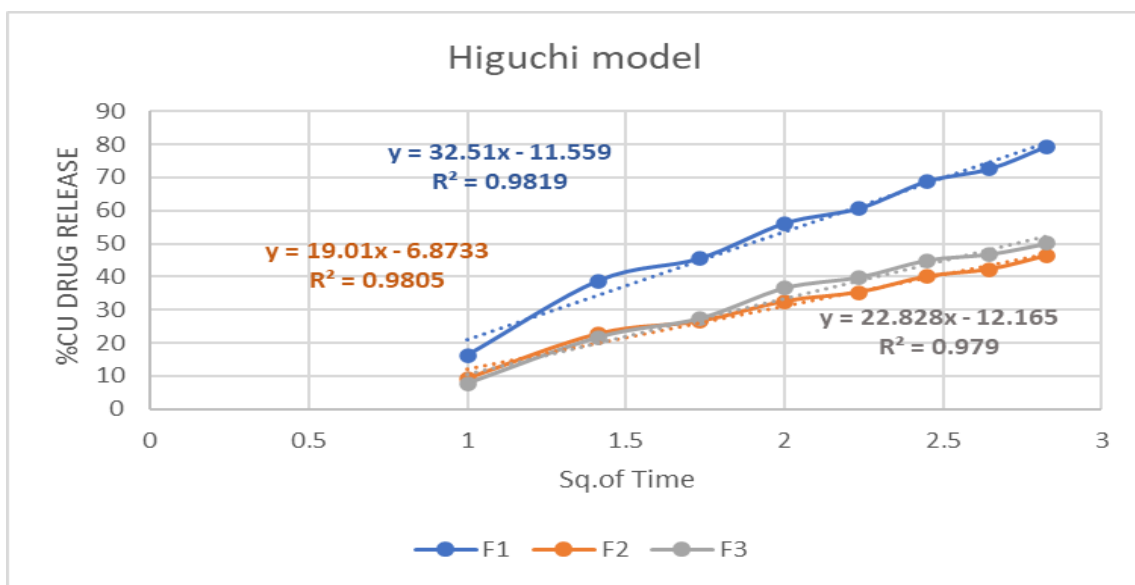


Figure 24 Higuchi model drug release graph

Table 28 Calculation of Korsmeyer Peppas kinetics

Log Time	Log % DDR F1	Log % DDR F2	Log % DDR F3
0.30103	1.210636	0.967341	0.883754
0.477121	1.588484	1.357045	1.336539
0.60206	1.657339	1.423177	1.436731
0.69897	1.748524	1.512534	1.563001
0.778151	1.782545	1.547533	1.600273
0.845098	1.837164	1.602687	1.652934
0.90309	1.860154	1.625186	1.670108
0.954243	1.899528	1.666401	1.699581

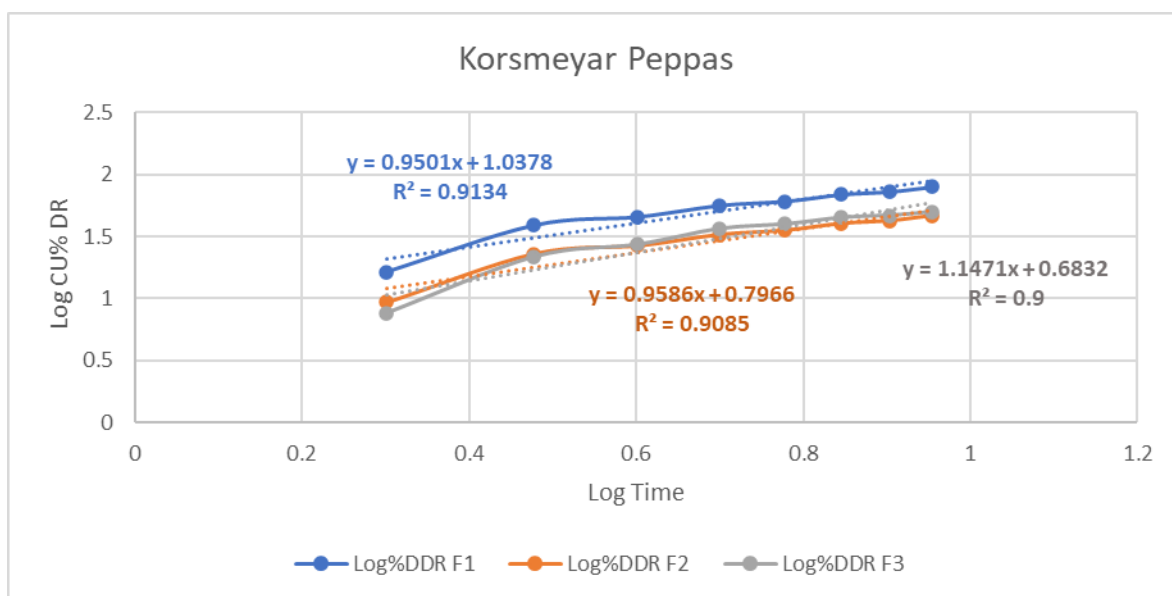


Figure 25 Korsmeyer Peppas drug release graph

## Chapter 7: Conclusion

This thesis has explored the development and characterization of HNT-loaded DOH *in-situ* gel formulations, aimed at enhancing the therapeutic efficacy and controlled release of doxycycline hyclate (DOH) for the treatment of periodontitis. The study's key objective was to investigate the influence of varying concentrations of halloysite nanotubes (HNT) and DOH on the formulation's physicochemical properties, release kinetics, and overall therapeutic potential.

The results demonstrated that the incorporation of HNT significantly improved the gel's mechanical strength and drug entrapment efficiency. The varying concentrations of HNT and DOH across the three formulations provided insight into the optimal balance required for achieving desirable release profiles. Notably, the second formulation, containing equal concentrations of HNT and DOH, exhibited the most promising characteristics in terms of sustained drug release and gel stability, making it a strong candidate for further development.

The kinetic modeling of drug release revealed that the formulations followed a non-Fickian diffusion mechanism, indicative of both diffusion and erosion processes playing a role in the drug release. This finding underscores the potential of these formulations to offer a controlled and prolonged therapeutic effect, which is crucial for the effective management of periodontitis.

Overall, this study contributes valuable knowledge to the field of novel drug delivery systems (NDDS), particularly in the context of localized drug delivery for periodontal therapy. The successful incorporation of HNT into *in situ* gels paves the way for future research and development, with the potential to translate these findings into clinically viable products. Continued exploration of the formulation parameters and *in-vivo* studies will be essential to fully realize the therapeutic potential of these gels.

In conclusion, the findings from this research not only highlight the promising role of HNT in enhancing the performance of *in-situ* gels but also provide a solid foundation for the future advancement of NDDS aimed at improving patient outcomes in the treatment of periodontitis.

## Chapter 8:References

Allen, T.M. and Cullis, P.R., 2013. Liposomal drug delivery systems: from concept to clinical applications. *Advanced drug delivery reviews*, 65(1), pp.36-48.

Aulton, M.E. and Taylor, K.M., 2007. Aulton's pharmaceutics. *The design and manufacture of medicines*, 3, pp.176-178.

Witika, B.A., Makoni, P.A., Matafwali, S.K., Chabalenge, B., Mwila, C., Kalungia, A.C., Nkanga, C.I., Bapolisi, A.M. and Walker, R.B., 2020. Biocompatibility of biomaterials for nanoencapsulation: Current approaches. *Nanomaterials*, 10(9), p.1649.

Jamrozy, M., Kudlacik-Kramarczyk, S., Drabczyk, A. and Krzan, M., 2024. Advanced Drug Carriers: A Review of Selected Protein, Polysaccharide, and Lipid Drug Delivery Platforms. *International Journal of Molecular Sciences*, 25(2), p.786.

Jain, K.K., 2020. An overview of drug delivery systems. *Drug delivery systems*, pp.1-54.

Kumar, L., Verma, S., Joshi, K., Utreja, P. and Sharma, S., 2021. Nanofiber as a novel vehicle for transdermal delivery of therapeutic agents: challenges and opportunities. *Future Journal of Pharmaceutical Sciences*, 7(1), p.175.

Patton, J.S. and Byron, P.R., 2007. Inhaling medicines: delivering drugs to the body through the lungs. *Nature reviews Drug discovery*, 6(1), pp.67-74.

Peer, D., Karp, J.M., Hong, S., Farokhzad, O.C., Margalit, R. and Langer, R., 2020. Nanocarriers as an emerging platform for cancer therapy. *Nano-enabled medical applications*, pp.61-91.

Prausnitz, M.R. and Langer, R., 2008. Transdermal drug delivery. *Nature biotechnology*, 26(11), pp.1261-1268.

Santini Jr, J.T., Cima, M.J. and Langer, R., 1999. A controlled-release microchip. *Nature*, 397(6717), pp.335-338.

Naeem, A., Yu, C., Zang, Z., Zhu, W., Deng, X. and Guan, Y., 2023. Synthesis and evaluation of rutin-hydroxypropyl  $\beta$ -cyclodextrin inclusion complexes embedded in xanthan gum-based (HPMC-g-AMPS) hydrogels for oral controlled drug delivery. *Antioxidants*, 12(3), p.552.

Bajpai, A.K., Shukla, S.K., Bhanu, S. and Kankane, S., 2008. Responsive polymers in controlled drug delivery. *Progress in Polymer Science*, 33(11), pp.1088-1118.

Chapple, I.L., Genco, R. and Working Group 2 of the Joint EFP/AAP Workshop\*, 2013. Diabetes and periodontal diseases: consensus report of the Joint EFP/AAP Workshop on Periodontitis and Systemic Diseases. *Journal of Periodontology*, 84, pp.S106-S112.

Darveau, R.P., 2010. Periodontitis: a polymicrobial disruption of host homeostasis. *Nature reviews microbiology*, 8(7), pp.481-490.- Fejerskov, O., Nyvad, B., & Kidd, E. A. M. (2015).

\*Dental caries: The disease and its clinical management\* (3rd ed.). Wiley Blackwell.

- Griffin, S.O., Jones, K. and Tomar, S.L., 2001. An economic evaluation of community water fluoridation. *Journal of public health dentistry*, 61(2), pp.78-86.
- Kinane, D.F., Stathopoulou, P.G. and Papapanou, P.N., 2017. Periodontal diseases. *Nature reviews Disease primers*, 3(1), pp.1-14.
- Marinho, V.C., Worthington, H.V., Walsh, T. and Chong, L.Y., 2015. Fluoride gels for preventing dental caries in children and adolescents. *Cochrane Database of Systematic Reviews*, (6).
- Petersen, P.E., Bourgeois, D., Ogawa, H., Estupinan-Day, S. and Ndiaye, C., 2005. The global burden of oral diseases and risks to oral health. *Bulletin of the world health organization*, 83, pp.661-669.
- Pitts, N.B., Zero, D.T., Marsh, P.D., Ekstrand, K., Weintraub, J.A., Ramos-Gomez, F., Tagami, J., Twetman, S., Tsakos, G. and Ismail, A., 2017. Dental caries. *Nature reviews Disease primers*, 3(1), pp.1-16.
- Sanz, M., Marco del Castillo, A., Jepsen, S., Gonzalez-Juanatey, J.R., D'Aiuto, F., Bouchard, P., Chapple, I., Dietrich, T., Gotsman, I., Graziani, F. and Herrera, D., 2020. Periodontitis and cardiovascular diseases: Consensus report. *Journal of clinical periodontology*, 47(3), pp.268-288.
- Sbordone, L. and Bortolaia, C., 2003. Oral microbial biofilms and plaque-related diseases: microbial communities and their role in the shift from oral health to disease. *Clinical oral investigations*, 7, pp.181-188.
- Tonetti, M.S., Jepsen, S., Jin, L. and Otomo-Corgel, J., 2017. Impact of the global burden of periodontal diseases on health, nutrition and wellbeing of mankind: A call for global action. *Journal of clinical periodontology*, 44(5), pp.456-462.
- Caton, J. and Ryan, M.E., 2011. Clinical studies on the management of periodontal diseases utilizing subantimicrobial dose doxycycline (SDD). *Pharmacological research*, 63(2), pp.114-120.
- Cugini, M. A., Haffajee, A. D., & Smith, C. (2013). The effect of scaling and root planing with doxycycline hydiate on the clinical and microbial parameters of periodontitis. *Journal of Clinical Periodontology*, 30(7), 661-666.
- Golub, L.M., Lee, H.M., Greenwald, R.A., Ryan, M.E., Sorsa, T., Salo, T. and Giannobile, W.V., 1997. A matrix metalloproteinase inhibitor reduces bone-type collagen degradation fragments and specific collagenases in gingival crevicular fluid during adult periodontitis. *Inflammation Research*, 46, pp.310-319.
- Haffajee, A.D., Socransky, S.S. and Gunsolley, J.C., 2003. Systemic anti-infective periodontal therapy. A systematic review. *Annals of periodontology*, 8(1), pp.115-181.
- Pihlstrom, B.L., Michalowicz, B.S. and Johnson, N.W., 2005. Periodontal diseases. *The lancet*, 366(9499), pp.1809-1820.

Preshaw, P.M., 2004. Antibiotics in the treatment of periodontitis. *Dental Update*, 31(8), pp.448-456.

Ryan, M.E. and Golub, L.M., 2000. Modulation of matrix metalloproteinase activities in periodontitis as a treatment strategy. *Periodontology 2000*, 24(1).

Socransky, S.S., Haffajee, A.D., Cugini, M.A., Smith, C.K.J.R. and Kent Jr, R.L., 1998. Microbial complexes in subgingival plaque. *Journal of clinical periodontology*, 25(2), pp.134-144.

Martu, M.A., Maftei, G.A., Luchian, I., Stefanescu, O.M., Scutariu, M.M. and Solomon, S.M., 2021. The effect of acknowledged and novel anti-rheumatic therapies on periodontal tissues—a narrative review. *Pharmaceuticals*, 14(12), p.1209.

Abdullayev, E. and Lvov, Y., 2013. Halloysite clay nanotubes as a ceramic “skeleton” for functional biopolymer composites with sustained drug release. *Journal of materials chemistry B*, 1(23), pp.2894-2903.

Joussein, E., Petit, S., Churchman, J., Theng, B., Righi, D. and Delvaux, B.J.C.M., 2005. Halloysite clay minerals—a review. *Clay minerals*, 40(4), pp.383-426.

Kamble, R., Ghag, M., Gaikawad, S. and Panda, B.K., 2012. Halloysite nanotubes and applications: a review. *Journal of advanced scientific research*, 3(02), pp.25-29.

Lecouvet, B., Horion, J., Dewasme, L., Bourbigot, S., & Baily, C. (2011). Halloysite nanotubes as flame retardant for intumescent poly(ethylene-co-vinyl acetate) and polypropylene. *Polymer Degradation and Stability*, 96(6), 1006-1014.

Li, X., Liu, Y., & Lvov, Y. (2017). Encapsulation of anticancer drug by halloysite nanotubes. *Journal of Materials Chemistry B*, 5(15), 2804-2812.

Abdullayev, E. and Lvov, Y., 2011. Halloysite clay nanotubes for controlled release of protective agents. *Journal of nanoscience and nanotechnology*, 11(11), pp.10007-10026.

Vergaro, V., Abdullayev, E., Lvov, Y.M., Zeitoun, A., Cingolani, R., Rinaldi, R. and Leporatti, S., 2010. Cytocompatibility and uptake of halloysite clay nanotubes. *Biomacromolecules*, 11(3), pp.820-826.

Fizir, M., Liu, W., Tang, X., Wang, F. and Benmokadem, Y., 2022. Design approaches, functionalization, and environmental and analytical applications of magnetic halloysite nanotubes: A review. *Clays and Clay Minerals*, 70(5), pp.660-694.

Garala, K., Joshi, P., Shah, M., Ramkishan, A. and Patel, J., 2013. Formulation and evaluation of periodontal in situ gel. *International journal of pharmaceutical investigation*, 3(1), p.29.

Pandit, A.P., Pol, V.V. and Kulkarni, V.S., 2016. Xyloglucan based in situ gel of lidocaine HCl for the treatment of periodontosis. *Journal of pharmaceutics*, 2016(1), p.3054321.

Yıldırım, Y., İnce, İ., Gümüştaş, B., Vardar, Ö., Yakar, N., Munjaković, H., Özdemir, G. and Emingil, G., 2023. Development of doxycycline and atorvastatin-loaded chitosan nanoparticles for local delivery in periodontal disease. *Journal of Drug Delivery Science and Technology*, 82, p.104322.

Veluri, S., Bora, D., Gupta, U.N., Sadiku, E.R., Reddy, A.B. and Jayaramudu, J., 2022. Morphological Characterization of Bio-nanocomposites. In *Polymer Based Bio-nanocomposites: Properties, Durability and Applications* (pp. 1-29). Singapore: Springer Singapore.

Ayensu, I., Mitchell, J.C. and Boateng, J.S., 2012. In vitro characterisation of chitosan based xerogels for potential buccal delivery of proteins. *Carbohydrate polymers*, 89(3), pp.935-941.

Alqurshi, A., Chan, K.L. and Royall, P.G., 2017. In-situ freeze-drying-forming amorphous solids directly within capsules: An investigation of dissolution enhancement for a poorly soluble drug. *Scientific Reports*, 7(1), pp.1-16.

Senarat, S., Lwin, W.W., Mahadlek, J. and Phaechamud, T., 2021. Doxycycline hydiate-loaded in situ forming gels composed from bleached shellac, Ethocel, and Eudragit RS for periodontal pocket delivery. *Saudi pharmaceutical journal*, 29(3), pp.252-263.

Krishnan, R., Arumugam, V. and Vasaviah, S.K., 2015. The MIC and MBC of silver nanoparticles against *Enterococcus faecalis*-a facultative anaerobe. *J Nanomed Nanotechnol*, 6(3), p.285.

Dash, S., Murthy, P.N., Nath, L. and Chowdhury, P., 2010. Kinetic modeling on drug release from controlled drug delivery systems. *Acta Pol Pharm*, 67(3), pp.217-223.

Hussain, A.I., Anwar, F., Nigam, P.S., Sarker, S.D., Moore, J.E., Rao, J.R. and Mazumdar, A., 2011. Antibacterial activity of some Lamiaceae essential oils using resazurin as an indicator of cell growth. *LWT-Food Science and Technology*, 44(4), pp.1199-1206.

Lei, X.X., Zou, C.Y., Hu, J.J., Jiang, Y.L., Zhang, X.Z., Zhao, L.M., He, T., Zhang, Q.Y., Li, Y.X., Li-Ling, J. and Xie, H.Q., 2023. Click-crosslinked in-situ hydrogel improves the therapeutic effect in wound infections through antibacterial, antioxidant and anti-inflammatory activities. *Chemical Engineering Journal*, 461, p.142092.

Heim, K.E., Tagliaferro, A.R. and Bobilya, D.J., 2002. Flavonoid antioxidants: chemistry, metabolism and structure-activity relationships. *The Journal of nutritional biochemistry*, 13(10), pp.572-584.

Borse, V.A., Gangude, A.B. and Deore, A.B., 2020. Formulation and evaluation of antibacterial topical gel of doxycycline hydiate, neem oil and tea tree oil. *Indian J. Pharm. Educ. Res*, 54(10), pp.206-212.

Pandit, A.P., Pol, V.V. and Kulkarni, V.S., 2016. Xyloglucan based in situ gel of lidocaine HCl for the treatment of periodontosis. *Journal of pharmaceutics*, 2016(1), p.3054321.

# Chapter 9: Certificate and Conferences

- International conference on recent trends in material sciences & devices 2023 ICRTMD 2023
- National workshop on ‘transformation in the pharmaceutical profession-The new age pharmacist’
- Poster presentation at NATCOMPH 2023 at NSHM knowledge campus
- National Seminar on “Role of Pharmacists in Patient Safety”
- Certificate on “Molecular dynamics simulation”
- Drug Regulatory Affairs-API & formulation (Certificate course of 3 months)
- Intellectual property rights (Certificate course)
- Clinical data management (Certificate course)



